universität wien

DIPLOMARBEIT

„Histochemische Analyse der MSC Adhäsion an Knorpeldefekten der Tibia in der Ratte.“

verfasst von

Elisabeth Richl

angestrebter akademischer Grad

Magistra der Naturwissenschaften (Mag.rer.nat.)

Wien, 2013

Studienkennzahl lt. Studienblatt:	A 442
Studienrichtung lt. Studienblatt:	Diplomstudium Anthropologie
Betreut von:	Univ.-Prof. Dr.med.vet. Reinhold Erben

Abbreviations

ACI	autologous chondrocyte implantation
ADAMTS 5	ADAM metallopeptidase with thrombospondin type 1 motif 5
ALN	aledronate
ALP	alkaline phosphatase
AMIC®	autologous matrix induced chondrogenesis
APES	3-aminopropyltrithoxy-silane
Aqua dest.	distilled water
BCIP	5-bromo-4-chloro-3-indolyl-phosphate
BFP	blue fluorescent protein
BMP2	bone morphogenetic protein
Ca	calcium
CD	dendritic cells
CFP	cyan fluorescent protein
CFU-F	colony forming unit fibroblast
Da	Dalton
DMF	dimethylformamide
ECM	extracellular matrix
EDTA	ethylenediaminetetraacetic acid
EtOH	ethanol
FBS	fetal bovine serum
GFP	green fluorescent protein
H_2O	water
HCl	hydrochloric acid
HD	homeodomain
HE	Mayer’s haematoxylin and eosin staining
HIF	hypoxia inducible factor-1α
hPLAP	human placental alkaline phosphatase
Ihh	indian hedgehog
IL	interleukin
IL1RN	interleukin-1 receptor antagonist
lacZ	reporter gene
MACI	matrix guided autologous chondrocyte implantation

MEM	Modified Eagle Medium
MeOH	methanol
Mg	magnesium
MMA	methylmethacrylate
MMP	metalloproteinase
Mn	manganese
MRI	magnetic resonance imaging
mRNA	messenger ribonucleic acid
MSC	mesenchymal stem cell
NaCl	sodium chloride
$NaIO_3$	sodium iodate
NBT	nitro blue tetrazolium chloride
NSAID	non-steroidal anti-inflammatory drugs
OA	osteoarthritis
OC	osteocalcin
ON	osteonectin
OP	osteopontin
P4	cell passage four
PBS	phosphate buffered saline
PDL	programmed death ligands
PFA	paraformaldehyde
PLLA	poly-l-lactic acid
PTHrP	asparathyroidhormone related protein
RGD	peptide (arginine-glycine-aspartic acid)
Runx2	runt-related transcription factor 2
SOCS1	suppressor of cytokine signaling 1
SOX9	transcription factor
STRO-1	cell surface protein
TGF-β	transforming growth factor-β
TNM	tetranitromethane
VEGF	vascular endothelial growth factor
X-gal	5-bromo-4-chloro-3-indolyl-β-D-galactopyranoside
YFP	yellow fluorescent protein
Zn	zinc

Contents

1. Introduction

1.1. The knee joint

The knee joint (*articularis genus*) consists of four bones, the femur, the tibia, the fibula and the patella **(Fig. 1-1)** (Schünke. et. al.; 2009). The femur and the tibia build the *art. femorotibialis* and the femur together with the patella the *art. femoropatellaris*. Both joints are coated with one articular capsule and embedded in one articular cavity. The knee belongs to the specific group of joints of freely moveable diarthroses (Faller and Schünke; 2012). Diarthrosis is a joint harboring a synovial cavity separating the involved bones. Further characteristics were the hyaline cartilage that coats the bearing areas and the articular cavity that shelters the articular capsular. The synovia within the synovial cavity does not only nourish the cartilage, it is also important in decreasing the friction between the articulated joint. Furthermore, the knee consists of menisci and articular ligaments to stabilize the freely moveable joint. The articular capsular is the prosecution of the periost and possesses an external firm fiber layer the *membrana fibrosa*. The inner *membrana synovialis* is rich in nerves and blood vessels. The outer *membrana fibrosa* is supported by several ligaments. Those ligaments are used corresponding to their functions as amplifying, conducting, or constraining ligaments. If the joint has a longer immobilization period, the fibers of the connective tissue shorten, which affects the motion ability of the whole joint. An effective regeneration of the joint needs also a reconstitution of the articular surface, as well as a *de novo* formation of the subchondral bone (Mackay, et. al.; 1998).

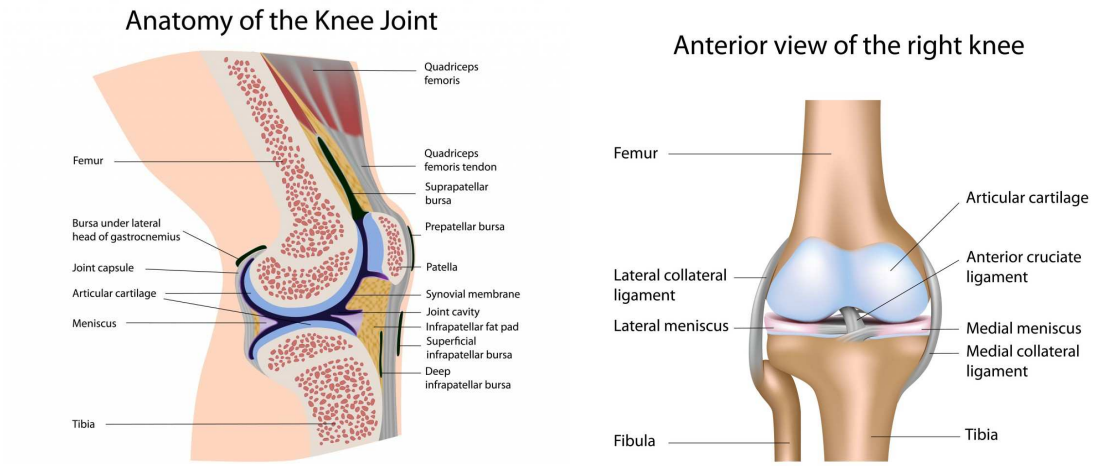

Fig. 1-1: Anatomy of the knee joint

Left a sectional view of the knee joint with the joint capsular and the articular cartilage (blue). Right the frontal view of the right knee (modified from Paul; 2012).

1.1.1. Bone

Bones consists predominantly of collagen and accumulated calcium apatite (Waldeyer; 2003). This combination makes it a compression-proof hard substance. In addition, fluorine compounds have a special significance to firm the bone material. Osteoblast and osteocytes are responsible for the formation of the bone and are in equilibrium with their counterpart the bone reducing osteoclasts. The renewing rate of bone tissue is based on the age and the health condition of the individual.

1.1.1.1. Ossification

There are two kinds of ossification, a direct (intramembranous) and an indirect (chondral and endochondral) ossification (Mutschler, et. al.; 2007). Both start from cartilage and form the trabecular bone, which later become bone lamellae. During the intramembranous ossification mesenchymal cells differentiate into osteoblasts. Osteoblasts as well as osteoclasts are essential for maintaining a constant bone volume and calcium homeostasis (Choi, et.

al.; 2011). They regulate the bone function like bone formation and resorption. One of the most important regulators of osteoblast differentiation is the bone morphogenetic protein (BMP) which is a member of the TGF-β family. BMP2 induces the factors osterix, Runx2 and a number of homeodomain (HD) proteins. These proteins are the key transcriptional factors of osteogenesis. Especially osterix is the transcriptional factor important for osteoblast and further bone formation through differentiation and proliferation. Further osterix proteins are known for their ability to regulate the osteoblast differentiation markers such as osteonectin (ON), Runx2, osteocalcin (OC), osteopontin (OP) and alkaline phosphatase (ALP). To help restoring the structure of the bone tissue, it needs to be provided with oxygen and nutrients to enhance growth, differentiation and gain back the tissue functionality (Kanczler, et. al.; 2008). This fundamental process of osseous formation, early vascular response and repair is initiated by angiogenesis through the vascular endothelial derived growth factor VEGF. VEGF stimulates chondrocyte apoptosis, angiogenesis, osteoblast migration, endochondral growth plate ossification, cartilage remodeling, and callus mineralization. Primary osteoblasts are building the basic or intercellular substance, which is not calcified, called osteoid (Mutschler, et. al.; 2007). The osteoblasts become an osteocyte through cell-cell and cell-ECM relationship (Ferrera, et. al.; 2002). Carbonate mineralization of collagen fibers finally results in the hard bone substance (Mutschler, et. al.; 2007). The chondral ossification arises from the mesenchym, which evolves the later bone derived from hyaline cartilage.

1.1.1.2. Regeneration of the bone tissue

After a bone fracture the cells of the periosteum are proliferating (Mutschler, et. al.; 2007). The cell canals as well as the reticular cells of the bone marrow are building connective tissue, called *callus*. There are two ways to regenerate the bone through direct or indirect ossification (Faller and Schünke; 2012). In both variations a trabecular bone is indicated. In the direct ossification bone develops directly out of the mesenchym. At the

indirect ossification a cartilaginous pre-skeleton arises from the mesenchym. That pre-skeleton has to ossificate into a “replacement bone”.

1.1.2. Cartilage

The cartilage differentiates out of the mesenchym (Mutschler, et. al.; 2007). At first, by augmentation of the intercellular substance the differentiated mesenchymal cells get rounded and flattened. In this phase the cells of the cartilage are called chondroblasts. Those are growing, maturating and differentiating into the later chondrocytes. Chondrocytes together with procollagen and proteoglycans build the ground substance of developing cartilage tissue. The cartilage is growing parallel to the rise of the ground substance, where the cells are dividing and drift apart simultaneously, which is called interstitial growth. The cartilage is surrounded by connective tissue (*perichondrium*), with one exception, the articular cartilage of the joint (see 1.1.2.4.). The perichondrium is rich in nerves and vessels and therefore new cartilage can grow from that tissue (appositional growth). Normally, chondrocytes are located in a cartilage cavity, which is embedded in fiber-free extracellular matrix, called *chondrone*. Because there are no blood vessels that could nourish the already differentiated cartilage, it has to support itself through diffusion, or in the case of hyaline cartilage through the synovia. There are three different kinds of cartilage, hyaline, elastic and fiber cartilage (Faller and Schünke; 2012). In their adult form all four cartilage types are free of blood vessels and are known for their compression strength, viscoelastic deformability and resisting power against shearing force and stress upon mechanical loading.

1.1.2.1. Hyaline cartilage

The hyaline cartilage looks bluish and milky in its fresh condition (Faller and Schünke; 2012). With just 45 % of collagen fibers the hyaline cartilage has the lowest percentage of fibers compared to the elastic and fiber cartilage.

Further, the collagen fibrils are masked with glycosaminoglycans which make them visible under the light microscope, because the optical reflection of the fiber is the same as it's surrounding. The hyaline cartilage covers the whole surface of the joint. It is also involved in the generation of the rips, nasal cartilage, bursa laryngeal, junction of the wind pipe and the bronchia. The epiphyseal plate consists of hyaline cartilage in times of growth. The cartilage only regenerates, if the perichondrium is still intact, which is often not the case (Mutschler, et. al.; 2007). The most important feature of the hyaline cartilage is its shock-absorbent effect that is mostly dependent on its extracellular matrix (Faller and Schünke; 2012). The matrix contains collagen fibers, macromolecules such as proteoglycans and water.

1.1.2.2. Elastic cartilage

In addition to the structure of the hyaline cartilage the elastic cartilage contains nets of elastic fibers (Faller and Schünke; 2012). It looks yellow and is situated in the auricle, parts of the larynx skeleton, epiglottis and the *tuba auditiva*. The net-like chondrocytes radiate into the perichondrium. The *chondrone* is smaller and harbors fewer cells than the hyaline cartilage (Mutschler, et. al.; 2007).

1.1.2.3. Fiber cartilage

The fiber cartilage contains a lot more collagen than the hyaline cartilage and is situated everywhere, where filaments and ligaments are stressed by pressure (Faller and Schünke; 2012). This form of cartilage is the most robust and therefore it is situated in *anulus fibrosus*, *disci* and *menisci*, where it gets highly exposed (Mutschler, et. al.; 2007). The *chondrone* is small and has fewer cells.

1.1.2.4. Articular cartilage

The articular cartilage has a smooth surface and consists of hyaline cartilage (Faller and Schünke; 2012, Mutschler, et. al.; 2007). Moreover the cartilage differs highly in its depths. On average the depth of a fully intact articular cartilage is about 2 to 3 mm in a human adult. A lack of exercise or high stress through wrong and periodically agitation, can lead to degenerative changes (arthritis) in elder people. Because of the lack of perichondrium, the ability of regeneration of the articular cartilage is weak.

The highly ordered structure and its complex interactions of matrix and chondrocytes characterize the articular cartilage (Buckwalter, et. al.; 2005). The articular cartilage has different structured zones from the superficial to the deep areas with the surrounding extracellular matrix **(Fig. 1-2)** (Goldring and Goldring; 2010). In the superficial zone the protein lubricin or proteoglycan-4 is expressed. This specific protein is important for boundary lubrication. The expression of the following proteins depends on the position within the extracellular matrix (ECM): parathyroid-hormone related protein (PTHrP), Runx2 and Indian hedgehog (Ihh). Those proteins are playing important roles for the zonal differences of the ECM concerning the function and the texture **(Fig. 1-2)**. Furthermore, it is suggested that the deeper chondrocytes adapt to low oxygen tension showed by the up-regulation of the hypoxia-inducible factor-1α (HIF-1α). Additionally, HIF-1α induces multiple genes associated with chondrocyte differentiation and cartilage anabolism.

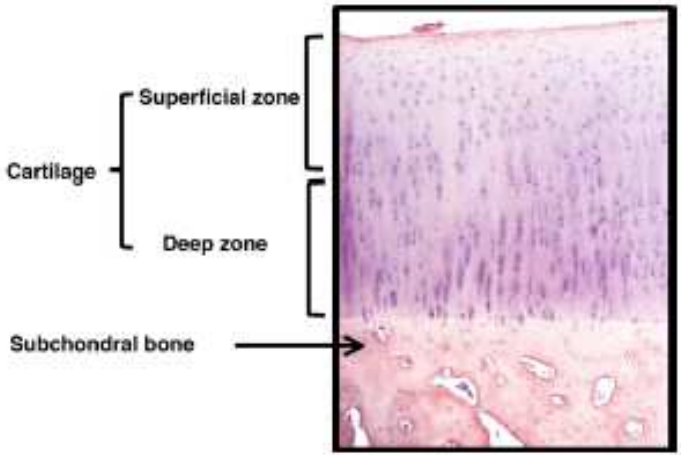

Fig. 1-2: Organization of articular cartilage

The articular cartilage consists of an upper superficial zone and a lower deep zone (modified from Kwan Tat, et. al.; 2009).

1.1.3. Menisci and ligaments of the knee

Menisci are characterized through its half-moon form and are part the knee joint **(Fig. 1-1)** (Faller and Schünke; 2012). They consist out of fiber cartilage and function as enlargement of the area of contact of the joint. They decrease the friction between the bones and serve as shock absorber. The ligaments connect muscle to the bone to make movement possible **(Fig. 1-1)**. Further, they help the muscle to work efficiently.

1.2. Arthritis

Arthritis is an inflammatory disease affecting joints. There are two types of arthritis: osteoarthritis (OA) and rheumatoid arthritis **(Fig. 1-3)**. The major symptom of rheumatoid arthritis is synovitis, the inflammation of the synovia affecting all joints (McGonagle, et. al.; 1998). Rheumatoid arthritis can be divided into subtypes, namely reactive arthritis, psoriatic arthritis and entheropathic arthritis. Those diseases are not only characterized by synovitis, but also by spinal inflammation, called spondylitis. Further, enthesitis causes the inflammation of ligaments, tendons and the insertion of

the capsule to the bone, and last but not least dactylitis, known as sausage digits. The synovitis can be triggered by many stimuli like trauma, infection, cartilage degradation and crystal formation. Furthermore, an alternative explanation is that pro-inflammatory cytokines and growth factors were released and this leads secondary to the synovitis. As a degenerative joint disease osteoarthritis is an exception. It also shows synovitis, but is not caused by joint infection like the other forms of arthritis.

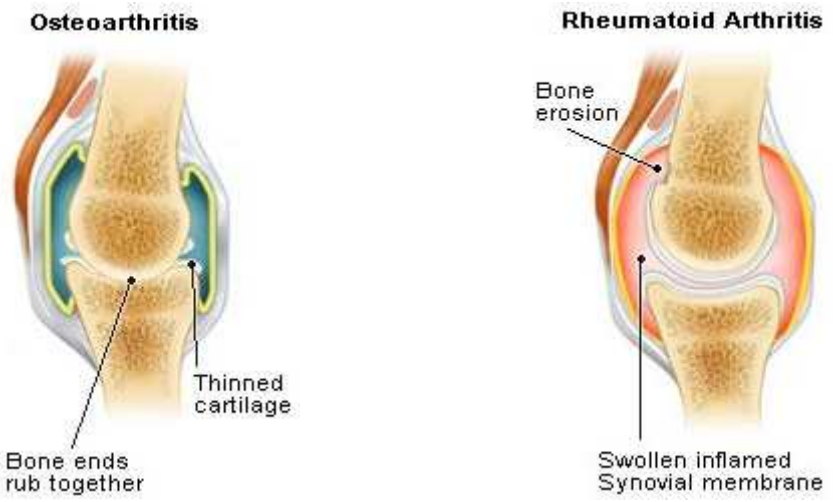

Fig 1-3: Osteoarthritic knee (left), rheumatoid arthritis (right)
In OA femur and tibia rub together resulting in thinning of the articular cartilage (modified from 3.bp.blogspot.com; 2012).
The rheumatoid arthritis shows its typical synovitis caused by a swollen and inflamed synovial membrane. In late stages also bone erosions can be observed. No contact between the bones can be noted in the rheumatoid arthritis (modified from 3.bp.blogspot.com; 2012).

1.2.1. Osteoarthritis (OA)

The name osteoarthritis derived from the Latin words ‘osteo’ meaning bone, ‘arthro’ meaning joint and ‘itis’ for inflammation (Arden, et. al., 2008). The thinning or loss of the articular cartilage of long bones over time causes a reduction of the synovial joint space where bone ends rub together **(Fig. 1-4)**. Osteoarthritis is one of the most frequent degenerative diseases that causes

joint pain and physical disability (Bond, et. al.; 2012, Conaghan, et. al.; 2008). It affects millions of men and women all over the world (Efpia-Lander Loeckx; 2012). At the age of 65 80 % of the patients show radiological signs of osteoarthritis of which 25 % also show symptoms. Currently, there is only physical, hot or cold, and medication therapy available, which contains pain killers and anti-inflammatory rheumatic medication (medicinenet; 2012).

Fig. 1-4: Osteoarthritic knee joint.

An OA knee joint shows defects in the articular cartilage, eroded menisci, bone spurs and exposed bone. The cartilage is hardly able to repair itself, which leads to a complete loss of cartilage in late stages of the disease. With the loss of cartilage and the continuing bone to bone friction, bone spurs arise and menisci erode (modified from 2.bp.blogspot.com; 2012).

In late stages OA leads to a direct bone-bone contact. This causes anatomical changes such as osteophyte formation and pain. Therefore, OA is acknowledged as a chronic disease of the whole joint. According to Arden et. al. (2008) chronic diseases are not contagious and develop gradually over time and continue to persist. The articular cartilage contains only few chondrocytes encapsulated in a water-based glycosaminoglycan matrix intensified by collagen fibers (Bulman, et. al.; 2012). This structure is rich in multilayered and complex biological material. Small defects like loss of matrix components can be repaired by hyaline cartilage (Lorenz and Richter; 2006).

There are three pathophysiological stages of osteoarthritis (Lorenz and Richter; 2006). On a molecular level the matrix molecules begin to degrade. Second, aggrecan decreases because of the increased water content and the loss of matrix molecules. In this stage chondrocytes enhance their proliferation and metabolic activity to compensate for the damage. In the last stage, the damage of the collagen network structure causes a reduction of the stiffness of the cartilage. The chondrocytes are not able to continue with their repair mechanisms, which causes a complete loss of the cartilage tissue. Subsequently, bone gets in contact with bone without any compensation of menisci and articular cartilage leading to the formation of osteophytes, a typical feature of late OA.

1.2.1.1. Risk factors

According to Conaghan et. al. (2008) the risk factors for such a common complex disorder as osteoarthritis, are numerous. They range from genetic, over constitutional to biomechanical risk factors. 40-60 % of the hand, knee and hip osteoarthritis are believed to be genetically induced. Additional, the risk factors age, female sex, high bone density and obesity can lead to OA. Last but not least there are also local, biomechanical risk factors such as joint injuries like occupational or recreational usage, joint laxity, reduction of muscle strength and joint malalignment. Some risk factors like obesity or muscle weakness are reversible or avoidable like recreational or occupational joint trauma. This is important for primary and secondary prevention. Therefore the individual risk factor differs greatly even at the joint sites.

Further, it is known that synovial inflammation is one of the symptoms and signs of OA (Kerkhof, et. al.; 2011). Synovitis is a cytokine-driven process that leads to cytokine production of the chondrocytes followed by degradation of the cartilage matrix. There are numerous genes encoding for cytokines, the outstanding ones are interleukin-1 (IL-1), IL-6 and IL-10 which are all

involved in the inflammation process. The presence of IL-1-α and -β induces the chondrocytes to decrease the synthesis of matrix components and increase the synthesis of matrix metalloproteinases. Hence, the antagonist of IL-1-α and -β named interleukin-1 receptor antagonist (IL1RN) could inhibit these effects. IL1RN plus its carrier C-T-A haplotype shows significant lower synovial fluid levels and a trend to reduce the risk of OA, but can on the other hand cause synovitis.

1.2.1.2. Changes in the articular cartilage during OA

Osteoarthritis leads to degeneration of the cartilage matrix, specifically in the characteristics of the material and the structural integrity of the surface of the articular and the hyaline cartilage (Goldring and Goldring; 2010). Further, it effects the subchondral bone, ligaments, joint capsule, periarticular muscles and synovial membrane (Murphy, et.al.; 2003). Chondrocytes are able to react on the changing environment, caused by structural changes and mechanical forces within the cartilage matrix (Goldring and Goldring; 2010). They react on changes of intrinsic and extrinsic growth factors, inflammatory mediators and cytokines. The loss of cartilage leads to pathologic progression of OA shown by the typical increase in cell proliferation and up-regulation of synthetic activity correlating with an increased production of specific ECM proteins. If the inflammation state continues, the intensified catabolic activity leads to an enhanced production of degradative proteinase genes, and hence a gradual loss of proteoglycans as well as type II collagen degradation. In humans the expression of matrix metalloproteinases (MMPs), aggrecanases, regulatory proteins, matrix proteins, transcription factors, apoptotic, and stress markers are increased. This process can cause apoptosis of chondrocytes and the degradation of ECM with the negative consequence that the cartilage is ruined.

1.2.1.3. Changes in the articular bone during OA

To be able to detect joint space narrowing by radiography a reduction of cartilage volume of 11 - 13 % is needed (Goldring and Goldring; 2010). This implicates that a significant amount of cartilage already has to be lost, in order to detect OA. Hence, OA is detected long time after the disease has been initiated. During OA 5 – 6 % cartilage loss and a joint space narrowing of 2 % can be observed per year making small changes hard to discover under the MRI. The reduction of cartilage in osteoarthritis is correlated with the narrowing joint space and the changes in the tibial joint area (Jones, et. al.; 2003). Further, there is no association between osteophytosis and the reduction of cartilage volume but an increase of tibial bone area were observed. The increase of tibial bone and osteophyte of the tibia illustrate the compensatory effects of the articular cartilage loss. Moreover, an increased turnover of subchondral bone with a specific architectural change in subchondral trabecular bone can be observed in osteoarthritic joints (Hayami, et. al.; 2003), as well as an enhanced subchondral bone sclerosis with disease progression is detected. Therefore, it is important to diagnose osteoarthritis as fast as possible to start with early interventions against bone sclerosis. Osteoclastic bone resorption had to be inhibited with a nitrogen-containing bisphosponate, alendronate (ALN), which is also used in osteoporosis prevention.

1.2.1.4. Prognosis for knee osteoarthritis

Knee osteoarthritis is very variable in its progression (Conaghan, et. al.; 2008) and there is no treatment to cure the disease. Only improvement in pain and disability is quite common, but an improvement in the damaged structure of the joint is rare once OA has been manifested. A third of the patients stay at the same level whereas another third develops a progressive symptomatic OA. Therefore, most patients with knee and hip osteoarthritis

are on pain medication (Hochberg, et. al.; 2000). The usual drugs for osteoarthritic patients are ibuprofen, tramadol and acetaminophen. Acetaminophen often fails in relieving of and should be taken cautiously by patients with existing liver diseases. However, tramadol had also shown side effects starting with nausea, drowsiness, constipation in patients with epileptic seizures. Further, some serious side effects of anti-inflammatory drugs (NSAID) can be observed. In a study among people of 65 years and older, 20 – 30 % of all hospitalizations and deaths were caused by peptic ulcer disease conducted during therapies with NSAID. Catastrophic gastrointestinal events caused by NSAID in older people are dose dependent. This shows the great importance of developing a good therapy causing no or only weak side effects. Moreover, a therapy that really cures OA is still missing, but research is focusing on promising tools such as cell-based therapies.

1.3. Cell-based therapy

A cell-based therapy with cells from adult tissues, like mesenchymal stem cells (MSC) that can differentiate into numerous connective tissue cells, opens up a field for cellular therapies without ethical considerations (Murphy J.M., et.al.; 2003). Because of the self-renewal capacity of adult stem cells, embryonic stem cells are not needed. The usage of MSC opens up a new clinical field, named regenerative medicine (Lepperdinger, et. al.; 2008). There are now treatments available for diverse diseases like inflammatory arthritis, repair of suspensory ligament tears, non-healing bone defects and fractures, bone marrow transplantation to heal disorders of bone and cartilage, to improve the tissue damage after myocardial infarction, or as gene therapy. Further, MSC have a strong ability to immunosuppressive properties that makes them ideal for an effective autologous or heterogonous transplantation (Giordano, et. al.; 2007). Moreover, MSC migrate to the injured sites, where they are needed. For example the transplantation of skeletal myoblasts or fetal cardiomyoctes is recommended to be the future

treatment after heart strokes. This active regeneration of damaged tissues is a promising key to heal degenerative diseases like osteoarthritis, with its ability to inhibit the progressive loss and enhance repair of the joint's cartilage tissue.

1.3.1. Mesenchymal stem cells (MSC)

Mesenchymal stem cells are multipotent cells that are found in the adult bone marrow (Pittenger, et. al.; 1999). Multipotent cells have the potential to differentiate into lineages of mesenchymal tissues e.g. bone, fat, cartilage, marrow stroma, and muscle **(Fig. 1-5)**. However, individual stem cells, extracted from the marrow of volunteer donors and cultivated as monolayer *in vitro*, can differentiate exclusively into osteogenic, chondrogenic and adipogenic lineages. Recent studies showed that MSC can also differentiate into neurons and astrocytes (Porcellini; 2009). Beside their ability to differentiate into several cell types, MSC also regulate the immune response by suppressing the proliferation of T- and B-lymphocytes as an immunosuppressive agent (Augello, et. al.; 2007). This ability derives from a non-major histocompartibility complex-restricted manner. Hence, MSC express CD28 that is directly involved in the regulation of the immune response and inhibits molecules that are programmed death ligands (e.g. PDL-1 and PDL-2), and an assembly of various cytokines. MSC show an immunoregulatory function *in vitro* and *in vivo* which includes alloantigen-induced dendritic cells activating CD25+, CD4+ T-cell subset differentiation.

Each cell colony derives from one colony-forming unit fibroblast (CFU-F) (Gronthos, et. al.; 1994; Weitzer; 2006) which can be identified by the antibody STRO-1. STRO-1+ cells and the CFU-F help to increase fibroblasts, smooth muscle cells and adipocytes. CFU-F have also shown osteogenic potential which originate from the STRO-1+ feature. Further, osteoprogenitors express STRO-1 which differentiate into bone cells with mineralized matrix, expressing alkaline phosphatase and osteocalcin *in vitro*.

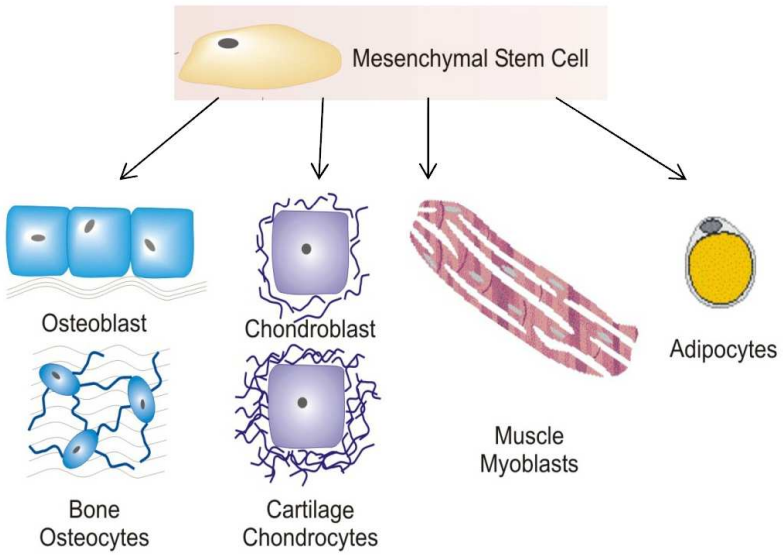

Fig. 1-5.: Differentiation potential of MSC

MSC can differentiate in primary differentiated cells as osteoblasts, chondroblasts, myoblasts and adipocytes which go on with their terminal differentiation into distinct tissue cells like osteocytes or chondrocytes (modified from Caplan and Bruder; 2001).

1.3.2. Repairing tissues with MSC

One source where mesenchymal stem cells can be isolated from, is the bone marrow (Docheva, et. al.; 2008). After the isolation of MSC, they can be expanded easily and differentiated into chondrocytes *in vitro*. Since MSC have no definitive characteristic, there are markers such as CD29.

Porcellini (2009) suggested that MSC have the possibility to repair tissues through three mechanisms. First, the reparation is led by cells with stem like abilities residing in several tissues nourished by the precursor cells in the bone marrow. Second, creating a milieu that allows the proliferation of endogenous cells and third, the stimulation of transdifferentiation and cell fusion in this newly established milieu. In MSC-based therapies there is an extensive need of cells to gain the amplified cells *in vitro* (Lepperdinger, et. al.; 2008). Therefore, the cells are expanded *in vitro*; this can lead to accumulating genetic and epigenetic changes of the cells, which in

consequence can cause a cellular transformation into cancer cells. MSC show a number of features like irreversible arrest of cell division, secretion of inflammatory cytokines, proteases and growth factors known from wound repair and resistance to apoptotic death. In this study transgenic MSC were used, because they can be easily identified through its genetic marker human placental alkaline phosphatase (hPLAP).

1.3.3. MSC adhesion

In RT-PCR analysis rat MSC had proven that type II collagen and aggrecan mRNA was expressed when culturing MSC in chondrogenic differentiation medium containing dexamethasone, ascorbate-2-phosphate, sodium pyruvate and TGF-β3 (transforming growth factor) (Agung, et. al.; 2006). If MSC are cultured in chondrogenic medium without dexamethasone, TGF-β3 collagen II and aggrecan cannot be detected. Therefore, according to Zwolanek et. al., (2013) the attachment rate of MSC is enhanced, if extracellular matrix proteins present in cartilage and bone are accessible for binding. Fibronectin, collagen I and II were capable for cell attachment in a concentration dependent and saturable manner. Further, this process can be blocked by EDTA, chelating divalent cations, or blocking the β1-subunit of integrins expressed by MSC. The later would lead to a complete inhibition of collagen I and collagen II attachment. Also the RGD peptide shows an inhibitory effect, but only for fibronectin suggesting an adhesion mediated via RGD binding integrins.

1.3.4. MSC differentiation into chondrocytes

In specialized medium human MSC differentiate under the influence of SOX-9 transfection into chondrogenic cells *in vitro* (Richardson, et. al.; 2006). Further, if cultivated on poly-l-lactic acid (PLLA) scaffolds the cells synthesize the same matrix molecules as *in vivo*.

Human MSC isolated from bone marrow have the ability to reproduce a chondrogenic phenotype and the according hypertrophic stages (Mackay, et. al.; 1998). Collagen II and aggrecan are produced by the extracellular matrix of the chondrocytes. Those proteins are structural proteins important for the precise structure and architecture of the cartilage. To induce chondrogenesis in mesenchymal stem cells the activity of the transforming growth factor-β (TGF-β), dexamethasone and thyroxine is needed. For further *in vitro* chondrogenic differentiation the synthetic glucocorticoid dexamethasone, and for steering the hypertrophy and endochondral ossification at the epiphyseal plate the protein thyroxine is responsible.

The usage of mesenchymal stem cells has the advantage of establishing a stem cell therapy without the need of embryonic stem cells (Murphy, et. al.; 2003). Its ability to differentiate into the needed tissues and the potency of self-renewal, MSC show a great opportunity to be used in an osteoarthritic therapy. To stop the loss of cartilage in the osteoarthritic joint, repair and regenerate the cartilage should be the job of introduced MSC.

1.4. Genetic markers

1.4.1. Green fluorescent protein (GFP)

GFP was first found in the jellyfish *Aquorea victoria* and is therefore a natural fluorescent protein with subsequent modifications (Sirerol-Piquer, et. al.; 2012). It is easy to trace gene expression after fusing GFP to the gene of interest not only in cell transformation and cell lineage, but also in *in vivo* real-time analysis and with electron microscopy. The calcium-activated photoprotein is the companion of GFP. The later emits at λ_{max} = 510 nm when exited with UV light or at λ_{max} = 395 nm with a minor peak at 470 nm with blue light. Further, GFP harbors all the information to synthesize its fluorophore properly. It is composed of 238 amino acids with a size of 27 kDa and contains the codon that qualifies the GFP to express itself in mammalian

cells. Variants like the cyan fluorescent protein (CFP), the blue fluorescent protein (BFP) and the yellow fluorescent protein (YFP), makes it able to detect diverse colors simultaneously. If the cells are small or the amount of GFP is low, than it is hard to detect. For example, if GFP is used in an early stage of a cell lineage, the more differentiated the cells become the more GFP gets diluted and is therefore harder to trace. Another limitation is the diminished detection level after paraffin embedding which makes it unsuitable for several applications (Odörfer, et. al.; 2008).

1.4.2. LacZ

LacZ is a reporter gene (Schmidt, et. al.; 1998) detecting the activity of a given promoter. It is frequently used in mutagenesis and mutational specificity studies (Josephy; 2000). Further, lacZ is often used in mechanistic studies, because it is easy to follow cell lineage with every transition, frame shift mutation and transversion. This characteristic gives an insight of the mutagen of the study. Therefore, it is used directly to examine the mutational specificity of the mutagen of interest, without the need of sequencing the DNA. This is possible, because lacZ carries its own genes for transfer or replication. The lacZ allele is coding for an inactive β-galactosidase, which makes it simple to trace lacZ through specific anti-β-galactosidase antibodies (Schmidt, et. al.; 2000). According to the study of Schmidt et. al. (2000) the expression of lacZ was weak and hard to trace. They tried to stain for X-gal and tested an anti-β-galactosidase antibody on cryo sections of tyrosinase-lacZ-transgenic mouse brain and could not detect a significant difference. As well as GFP also lacZ is heat labile and the enzyme gets destroyed during paraffin embedding (Odörfer, et. al.; 2008).

1.4.3. Human placental alkaline phosphatase (hPLAP)

The family of alkaline phosphatases comprises four members in humans; germ cell alkaline phosphatase, interstitial alkaline phosphatase, tissue non-specific alkaline phosphatase and the placental alkaline phosphatase (PLAP). The hPLAP has a cell surface associated with sialoprotein (Pottek, et. al.; 1997). Sialoprotein is located at the syncytiotrophoblastic membranes of the terminal placenta where hPLAP is produced. Further, it is a glycosyl-phosphatidylinositol (GPI) that attaches on a cell surface protein that marks axons, if expressed transgenically or if it is transferred into new born pups, embryos or embryonic neuronal precursors (Seijffers and Woolf; 2004). The special feature of hPLAP is its heat-stability up to 72℃ which makes it suitable for all histochemical procedures such as paraffin or MMA embedding (Odörfer, et. al.; 2008). Furthermore, the endogenous alkaline phosphatase is heat-labile, and therefore inactive. In this study hPLAP is used as genetic marker in a rat model, making it possible to follow the attachment of MSC on wild type osteochondral explants.

1.5. Aims of the study

The aim of this study is to evaluate the existing *in vitro* and *ex vivo* data of MSC adhesion, of osteochondral wild type rat tibia explants, processed with diverse serum and divalent ion concentrations. The 1mm full-thickness cartilage defect should simulate osteoarthritic damage of the cartilage. This study was established to verify the previous *in vitro* experiments, with diverse histochemical staining techniques. Further, to test which factor has the highest influence on MSC adhesion to full-thickness cartilage defects. The factors tested were 0 %, 2 %, 5 %, 10 %, 20 %, 50 %, 100 % of serum, where 0 % was used as negative control. At the various divalent ion concentrations were: 1 mM, 2.5 mM, 5 mM and 10 mM of Mg or Ca, 1 mM of Mn or Zn, 1 mM Mg with 2.5 mM Ca, 2.5 mM Mg with 1 mM Ca, 1mM Mn

with 2 mM Mg, NaCl as negative control and EDTA which chelates divalent cations.

Therefore, the first step was to establish an embedding procedure that does not refuse the epitopes to the binding sites. This is important, because the previous study showed that the β1 integrin is the main mediator of MSC attachment. Hence, MMA or paraffin would have made it hard to check this theory, because the epitopes would be harder to access and thus harder to identify. Consequently, the choice of embedding goes to Tissue-Tek®, this also meant that the sections had to be cut with a cryostat and therefore they had to be decalcified. Further, staining techniques had to be chosen to test the MSC attachment on full-thickness cartilage defects. For better identification of the donor MSC, hPLAP-tg MSC were taken. To gain a general overview of the full-thickness cartilage the sections were stained with Mayer's haematoxylin and eosin, which is the most common histochemical staining (Avwioro; 2011). For further identification of the proteoglycans and cell nuclei, two different staining methods were established the Weigert's iron haematoxylin and alcian blue and the Mayer's haematoxylin, fast green and safranin O staining. If the mentioned staining shows significant data, the hPLAP and fast red staining took place to stain the attached hPLAP-tg MSC. That would prove that those cells had attached within the full-thickness cartilage defect.

2. Materials and Methods

2.1. Material

2.1.1. MSC attachment to osteochondral explants

To receive osteochondral explants for the attachment studies tibias of wild type Fischer 344 rats were isolated after euthanasia with CO_2. The tibia and especially its plateau were carefully cleaned from surrounding soft tissue and menisci without destroying or scratching the articular cartilage surface. The whole tibia was stored in PBS until full-thickness defects were placed in the middle of the medial and the lateral compartment of the tibia plateau. Biopsy punches with 1 mm in diameter were used for generating the defects under the microscope. After abrasion the defects the tibia was broken at the epiphysis and the resulting osteochondral explant was divided into the medial and lateral compartment to receive two explants. After incubation with MEM containing 10 % FBS and 1 % Penicillin/Streptomycin the explants were used for attachment studies.

MSC were isolated from hPLAP-transgenic rats (adopted from Farrell, et. al.; 2006) and expanded *in vitro* up to P4 (passage). The cells were pre-incubated with different serum and ion concentrations and/or combinations and allowed to attach to the osteochondral explants for one hour. Adherent cells were fixed, heat-inactivated and stained for hPLAP expression. The stained osteochondral explants were used for further histochemical analysis.

2.1.2. Histochemical staining solutions

2.1.2.1. 0.001 % fast green

0.01 g fast green
1000 ml aqua dest.

2.1.2.2. 0.1 % safranin O

0.1 g safranin O
100 ml aqua dest.

2.1.2.3. 0.1 % fast red

5 g aluminium sulfate
100 ml aqua dest.
Heat aluminium sulfate solution.
0.1 g fast red
Stir until colorant is completely in solution, let it cool down and filtrate before use.

2.1.2.4. 1 % eosin

10 g eosin
1000 ml aqua dest.
Stir well and filtrate before use.

2.1.2.5. Alcian blue

1 g alcian blue
100 ml 3 % HAC (pH 2.5)

2.1.2.6. BCIP (5-bromo-4-chloro-3-indolyl-phosphate)

20 mg/ml BCIP
in 100 % DMF

2.1.2.7. Mayer’s haematoxylin

1 g haematoxylin solute in
0.2 g $NaIO_3$
50 g potash alum
1 g citric acid
1000 ml aqua dest.
Filtrate solution.

2.1.2.8. NBT (nitro blue tetrazolium chloride)

100 mg/ml NBT
in 70 % DMF

2.1.2.9. Weigert’s haematoxylin

Solution A:
1 g haematoxylin
100 ml 96 % EtOH
Mature for one week.

Solution B:

1.5 g iron(III)chloride

100 ml aqua dest

1 ml 37 % HCl

Solution A : solution B (1:1) – staining solution

2.1.3. Buffers

2.1.3.1. 1 % magnesium chloride in 100 mM tris-maleat buffer

Tris-maleat buffer

6 g maleic acid

6 g tris(hydroxymethyl)aminomethan

1 l H_2O

Adjust the pH with 1% magnesium chloride in 100 mM tris-maleat buffer to pH 9.2.

2.1.3.2. 1x PBS

8 g NaCl

0.2 g KCl

2.3 g $Na_2HPO_4+2H_2O$

0.24 g KH_2PO_4

900 ml H_2O pH 7.4

2.1.3.3. TNM buffer

100 ml 0.1 M Tris-HCl pH 9.5

5.84 g 0.1 M NaCl

1.02 g 5 mM $MgCl+6H_2O$

2.1.4. Solutions

2.1.4.1. APES (3-aminopropyltriethoxy-silane)

4 ml	APES
196 ml	acetone

2.1.4.2. 4 % PFA (paraformaldehyde)

8 g	paraformaldehyde
200 ml	aqua dest.

2.2. Methods

All methods and recipes were used according to the SOPs of the Institute of Pathophysiology of the University for Veterinary Medicine, Vienna (Erben; 2007).

2.2.1. Coating slides with APES

acetone	10 minutes
tap water	2-3 dips
acetone	5 minutes
APES/acetone solution	5 minutes
aqua dest.	2-3 dips
aqua dest.	2-3 dips

2.2.2. Cryo sectioning

The osteochondral explants were decalcified before cryo embedding. Therefore, the explants were slightly agitated in 0.5 M EDTA pH 8.0 at 4℃.

After decalcification the explants were embedded with Tissue-Tek®, shock frozen with liquid nitrogen, stored at -80℃ and de frosted overnight to -20℃ before sectioning. 11 µm thick sections were made with the “Kryostat 1720” at an average temperature of -22℃. The sections we re transferred to APES-coated slides and directly used for histochemical staining or stored at -20℃.

2.2.3. Histochemical methods

2.2.3.1. Mayer’s haematoxylin and eosin staining

Defrost cryo sections at room temperature.

wash with PBS	5 minutes
fix in 4 % PFA	5 minutes
wash in PBS	5 minutes
Mayer’s haematoxylin	5 minutes
tap water	1 minute
1 % HCl-70 % alcohol	10 seconds
running tap water	10 minutes
aqua dest.	10 seconds
1 % eosin in H_2O	5 minutes
70 % EtOH	10 seconds
90 % EtOH	2 minutes
96 % EtOH	2 minutes
isopropanol	2 minutes
isopropanol	2 minutes
xylol	5 minutes
xylol	5 minutes
mounting	Depex

2.2.3.2. Mayer’s haematoxylin, fast green and safranin O staining

Defrost cryo sections at room temperature.

wash cryo sections with PBS	5 minutes
fix in 4% PFA	5 minutes
wash in PBS	5 minutes
Mayer’s haematoxylin	5 minutes
tap water	1 minute
1 % HCl-70 % alcohol	10 seconds
running tap water	10 minutes
aqua dest.	10 seconds
0.001 % fast green	5 minutes
1 % acetic acid	8 seconds
0.1 % Safranin O	5 minutes
70 % EtOH	10 seconds
90 % EtOH	2 minutes
96 % EtOH	2 minutes
isopropanol	2 minutes
isopropanol	2 minutes
xylol	5 minutes
xylol	5 minutes
mounting	Depex

2.2.3.3. Weigert’s haematoxylin and alcian blue staining

Defrost cryo sections at room temperature.

wash cryo sections with PBS	5 minutes
fix tissue in 4% PFA	5 minutes
wash tissue in PBS	5 minutes
Weigert’s haematoxylin	5 minutes
warm tap water	wash 3 times
1 % HCl-70 % alcohol	10 seconds
warm tap water	wash 3 times
aqua dest.	1 minute
alcian blue	30 minutes
warm tap water	wash 3 times
aqua dest.	10 seconds
70 % EtOH	10 seconds
90 % EtOH	2 minutes
96 % EtOH	2 minutes
isopropanol	2 minutes
isopropanol	2 minutes
xylol	5 minutes
xylol	5 minutes
mounting	Depex

2.2.3.4. hPLAP and fast red staining

aceton/MeOH (30 %/70 %)	3 minutes at -20℃
1% $MgCl_2$ in 100 mM tris-maleat buffer 9.2 pH	In darkness overnight
place sections in 65℃ H_2O bath	35 minutes
cooling down to room temperature	20 minutes
70 µl BCIP/36 µl NBT/8 ml TNM buffer	incubate overnight in dark humid chamber
aqua dest.	5 minutes
fast red (counter stain)	5 minutes
aqua dest.	5 minutes
aqua dest.	5 minutes
30 % EtOH	5 minutes
60 % EtOH	5 minutes
80 % EtOH	5 minutes
isopropanol	5 minutes
xylol	5 minutes
mounting	Vectamount

2.2.4. Evaluation of stained sections

All in all 40 slides per two explants were made. Hence, 30 slides were coated in APES. Which were stained with three different staining protocols, 10 slides per protocol and mounted with Depex.

1) Weigert's haematoxylin and alcian blue
2) Mayer's haematoxylin and eosin
3) Mayer's haematoxylin, fast green and safranin O

The APES-free slides were taken for the hPLAP/fast red staining. Therefore, two to three slides out of ten were chosen to be stained. Those slides showed the best full-thickness cartilage defect. After the staining the slides were mounted with Vectamount.

All stained cryo sections were photographed under the microscope (Axioskop 2FS plus/FS mot) with an integrated camera (Olympus DP72). With help of the software DP2-DWS pictures were taken. White balance and rescaling was performed on the images with Adobe Photoshop.

3. Results

3.1. Preliminary studies

3.1.1. Embedding and sectioning

In this study various histochemical methods had to be adopted for the use of osteochondral explants. Rat tibia plateaus were prepared with a full-thickness cartilage defect to simulate osteoarthritis (Zwolanek, et. al.; 2013). In a previous study made by Zwolanek MSC of hPLAP-transgenic rats were allowed to attach to the explants under various conditions. To figure out a positive serum influence, and second if different concentrations of ions have an effect on MSC attachment on the full-thickness cartilage defect, the *ex vivo* attachment was validated with the ImageJ software. To give further evidence, this study should verify the previous study with diverse histochemical methods. Therefore, the explants were treated with MSC and different serum or ion concentrations. Some with full-thickness cartilage defects and some without defect to prove the concept that MSC attach better to defective cartilage like in OA.

On the full-thickness tibia plateau a 1 mm round defect was created through erasion. Therefore, if sections were made, the defect of the concerning section can vary in size. This is caused by the fact of where the sections where taken. At the beginning and at the end the defect is smaller, than in the middle of a round defect. Further, the defects were sometimes created more precisely therefore heterogeneity of the full-thickness defect performance can be visible in the results.

The right method for embedding the explants had to be established. Embedding the explants in methylmethacrylate (MMA) or paraffin would have blocked the epitopes recognized by a β1 integrin antibody, which is

according to Zwolanek D. the main mediator for the MSC attachment. Therefore, another method had to be found to embed the explants to be able to perform not only histochemical staining procedures but also immunofluorescence analysis. Thus, embedding the explants in Tissue-Tek® and making cryo sections was a suitable solution. During making cryo sections it turned out that the explants could not be cut into sections without decalcification. To overcome that problem all explants were decalcified for two weeks with 0.5 M EDTA. After two weeks the first trial run to make decalcified cryo sections had taken place, but the bones were still too hard and demure to cut. After four weeks of decalcification with 0.5 M EDTA the explants were ready to cut. On average 40 slides with three sections of two tibia plateaus were fabricated.

3.1.2. Staining procedure

Mayer's hematoxylin and eosin was used as trail staining as it serves as common staining for structural overview of tissue sections. The sections were placed onto untreated adhesive glass slides. In general, the staining worked but the loss of cryo sections during the staining procedure was too high. Hence, the slides had to be coated with 3-aminopropyltrithoxy-silane (APES) first.

At the second staining trial all sections stayed to the slide and could be analyzed under the microscope. For all future sections APES-coated slides were used and sections were arranged always in the same manner **(Fig. 3-1)** for comparison. All needed histochemical stainings could be performed without any problem of sample reduction.

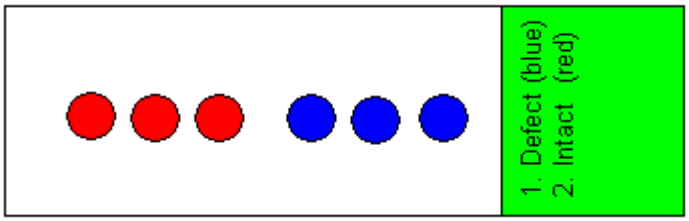

Fig. 3-1: Cryo section arrangement on the slides

The blue dots represent sections of the full-thickness cartilage defect and the red dots the intact cryo sections arranged on the glass slide after serum treatment. As the ion treatment was only performed on defective explants the blue dots represent the first and the red dots the second explant.

The second staining was the Weigert's iron haematoxylin and alcian blue staining, to get a deeper insight, if there is an increase of collagen and proteoglycan. The third, Mayer's haematoxylin/fast green/safranin O to confirm the data out of the Weigert's haematoxylin/alcian blue staining. But also to detect a difference in the increase of collagen and proteoglycan, which were visible with that staining procedure. Last but not least, the hPLAP/fast red staining took place after the positive findings of the former staining procedures to identify the attached hPLAP-tg MSC.

3.2. MSC attachment

3.2.1. MSC attachment after serum treatment

To test whether serum had an influence on the MSC attachment hPLAP-transgenic MSC were pre-incubated with increasing serum concentrations (0 %, 2 %, 5 %, 10 %, 20 %, 50 % and 100 %) prior to the attachment. To proof the concept for the *ex vivo* attachment of MSC to defective cartilage, the study was carried out by additionally performing the experiment on intact explants.

3.2.2. MSC attachment after divalent ion treatment

Divalent ion concentrations of various divalent ions (Ca, Mg, Mn, Zn, Mg/Ca, Mn/Mg, EDTA, NaCl) were tested for their ability to enhance cell attachment on full-thickness defects. All tibia plateau explants of these experiments had a full-thickness defect within their cartilage. In this case, the ability of divalent ions to enhance cell attachment was tested. Therefore, the osteochondral explants were supplemented with diverse divalent ions that were found in the bone, cartilage and synovial fluid starting with calcium and magnesium. Those are important ions for calcification of the bone. Further, Zn and Mn were tested too.

3.3. Results MSC attachment after serum concentration

3.3.1. Mayer‘s haematoxylin/eosin

Mayer’s haematoxylin is commonly used as a nuclear counter stain for illustrating the glycogen, mucicarmine and amyloid (Avwioro; 2011). If sections were stained with Mayer’s haematoxylin and eosin (HE staining), the nuclear chromatin would show coloration from blue to purple (Kieman; 2008). Further, collagens, cytoplasm and keratin were stained in pink colors. The HE staining is a very common staining, and is often used as structural overview staining and to identify cancer cells (Kurita, et. al.; 2008). It counts as gold standard within the surgical field. Therefore, the first staining of the sections was the HE staining to show a structural overview of the explants with **(Fig. 3-2)** and without defect **(Fig. 3-3)**, and if cells can be found within the full-thickness cartilage defect.

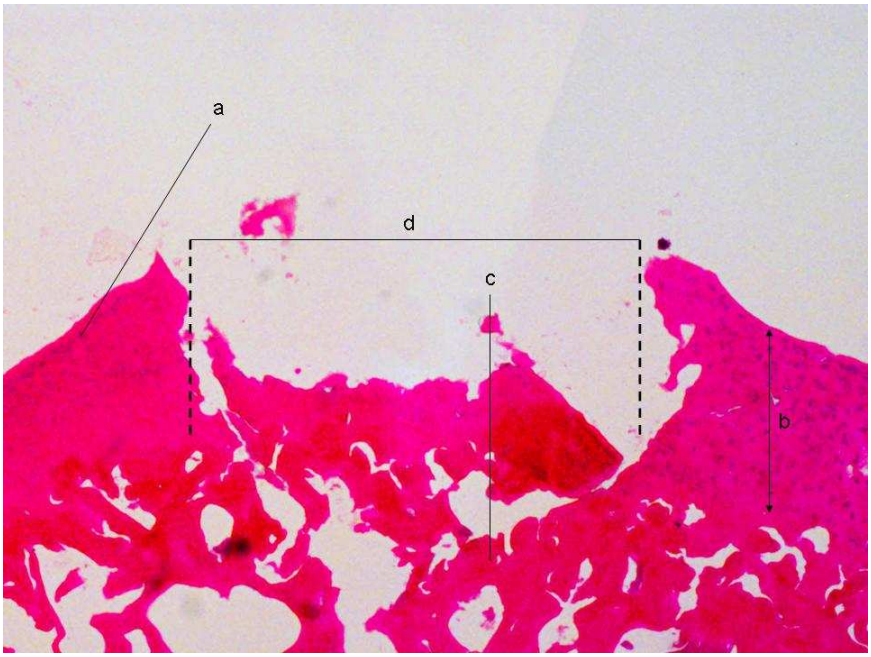

Fig. 3-2: Histological appearance of a full-thickness cartilage defect of the rat tibia plateau.

Cryosections of osteochondral explants with a full-thickness cartilage defect were stained with Mayer's haematoxylin and eosin for histological analysis. Cell nuclei were stained in brown (a), and cartilage in red (b). The subchondral bone in purple (c), as well as the defect of the cartilage of the tibia plateau (d, dashed line), were visible. 5 % serum concentration. Magnification: 10-fold.

The osteochondral explant in **Fig. 3-2** showed a clear full-thickness cartilage defect until the subchondral bone. In contrast, intact explants showed a totally intact cartilage surface with underneath subchondral bone **(Fig. 3-3)**. Only few nuclei could be found in the cartilage, as there were only few chondrocytes embedded within the cartilage's extracellular matrix.

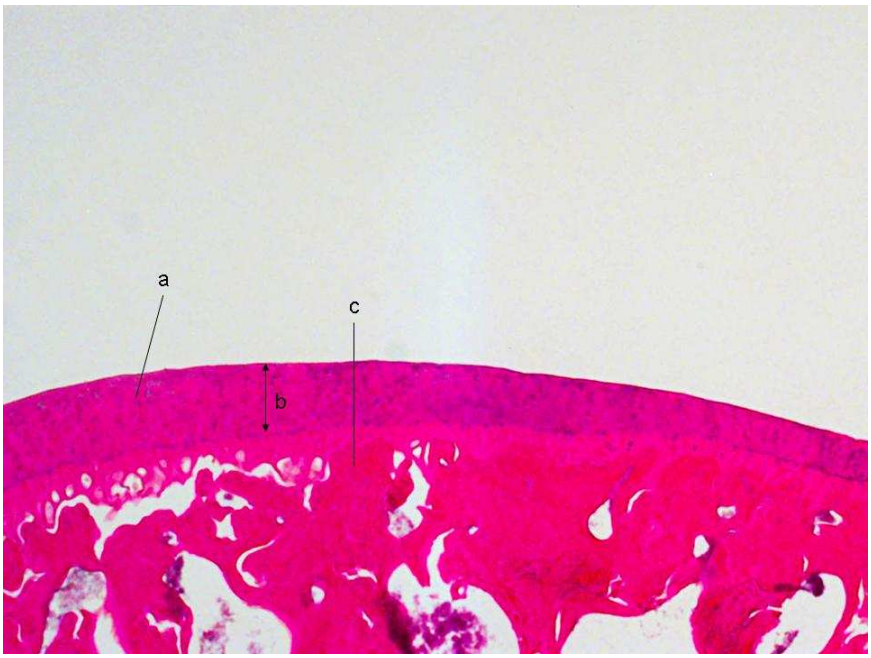

Fig. 3-3: Histological appearance of intact cartilage of the rat tibia plateau. Cryosections of osteochondral explants intact cartilage were stained with Mayer's haematoxylin and eosin for histological analysis. Cell nuclei were stained in brown (a), and cartilage in red (b). The subchondral bone in purple (c). 20 % serum concentration. Magnification: 10-fold.

In *ex vivo* attachment studies increasing serum concentrations had a positive effect on the MSC attachment (unpublished data). At low serum concentrations no differences between intact and defective cartilage and no significant increase in the MSC attachment could be observed **(Fig. 3-4)**. The more serum MSC got pre-incubated with, the more attachment of MSC to defective osteochondral explants was observed compared to intact explants **(Fig. 3-5)**. The increasing number of nuclei visible within the defect could further demonstrate this fact. At 100 % serum the highest density of nuclei in the upper layer of the defective cartilage could be seen indicating attachment of MSC predominantly within the defective area **(Fig. 3-6)**. Those results resembled the prior obtained data from *in vitro* and *ex vivo* attachment studies.

Comparing the sections of defective explants with each other the heterogeneity of full-thickness defect performance got visible. Some of the

defects were abrased very precisely some of them showed remaining cartilage tissue mainly within the middle of the defect. The different sizes of the defect depended on the area where the section was taken; if the defective area was quite small the section was located more at the beginning or the end of the defect. Nevertheless, the influence of serum on the attachment of MSC to defective cartilage was visible and comparable among all sections.

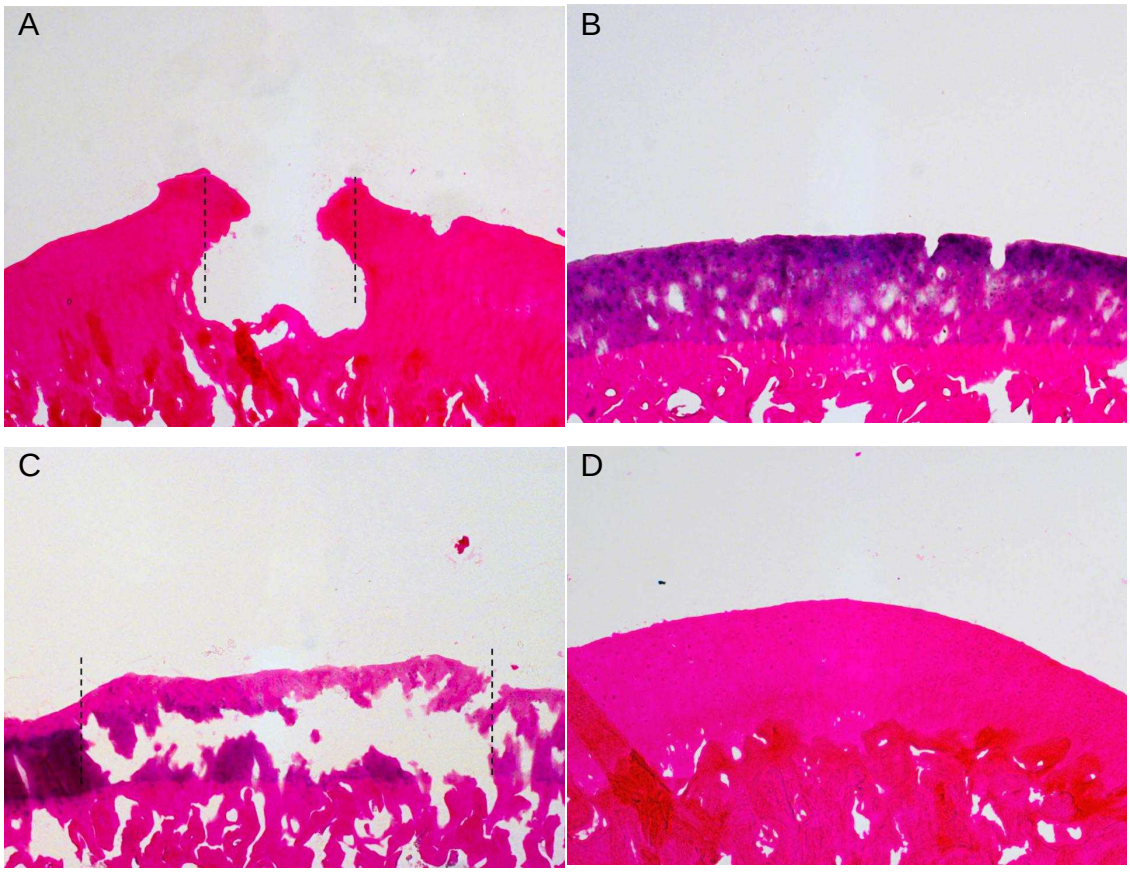

Fig. 3-4: Histological appearance of rat tibia plateaus after MSC attachment with different serum concentrations starting from 0 % to 2 %.

Cells were allowed to attach to the cartilage surface of rat tibia plateaus supplemented with 0 % (A and B) and 2 % serum (C and D). C demonstrated the heterogeneity of the experiment and the performance of full-thickness defects. Further, some tibia plateaus showed a higher concentration of cells in the margin areas of the defect (B and C). Magnification: 10-fold.

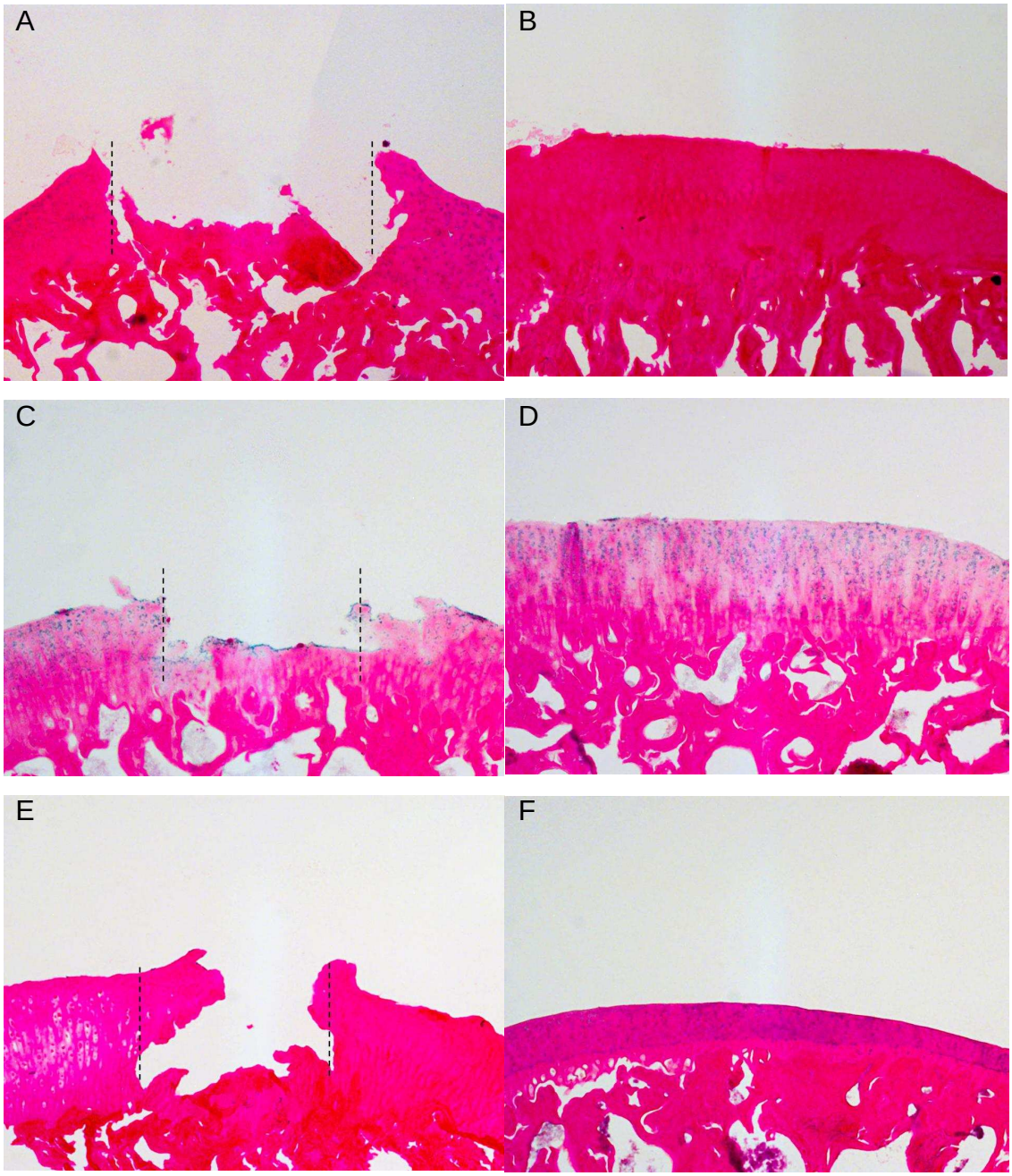

Fig. 3-5: Histological appearance of rat tibia plateaus after MSC attachment with different serum concentrations starting from 5 % to 20 %.

Cells were allowed to attach to the cartilage surface of rat tibia plateaus supplemented with 5 % (A and B), 10 % (C and D) and 20 % serum (E and F). At 10 % and 20 % serum (C and E) the surface appeared darker, which indicated that more cells had attached within the defect. Magnification: 10-fold.

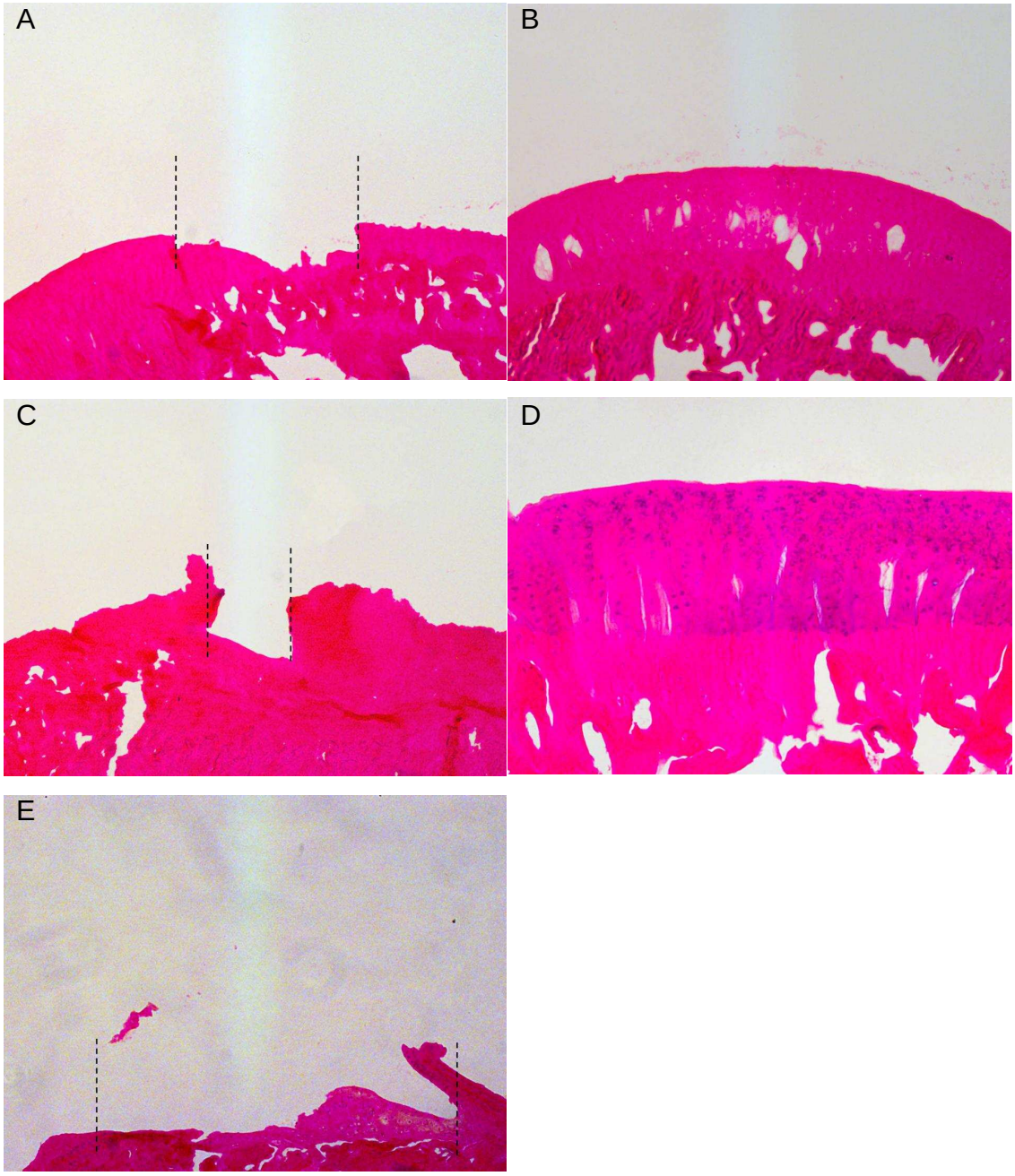

Fig. 3-6: Histological appearance of rat tibia plateaus after MSC attachment with 100 % serum concentrations.

Cells were allowed to attach to the cartilage surface of rat tibia plateaus supplemented with 50 % (A and B) and 100 % serum (C, D and E).The highest density of cell nuclei could be found in the upper layer of the full-thickness cartilage in C, D, and E, in both tibia plateaus with and without defect. Moreover the defect area showed a higher density of chondrocytes and cell nuclei (C). Magnification: 10-fold.

3.3.2. Weigert‘s iron haematoxylin/alcian blue

Weigert’s iron haematoxylin is also used as a nuclear counter stain (Avwioro; 2011). Especially, in combination with other stains that demonstrates collagen, muscles and connective tissue. Therefore, alcian blue was taken as co-staining. Alcian blue generated a distinctive blue staining of proteoglycans and collagen components predominantly found in cartilage (Gruber, et. al.; 2001). During OA a loss of proteoglycans and collagen II occurred. Weigert’s iron haematoxylin/alcian blue staining showed the amount of proteoglycans and collagen of the full-thickness cartilage with **(Fig. 3-7)** and without defect **(Fig. 3-8)** after MSC attachment with increasing serum concentrations.

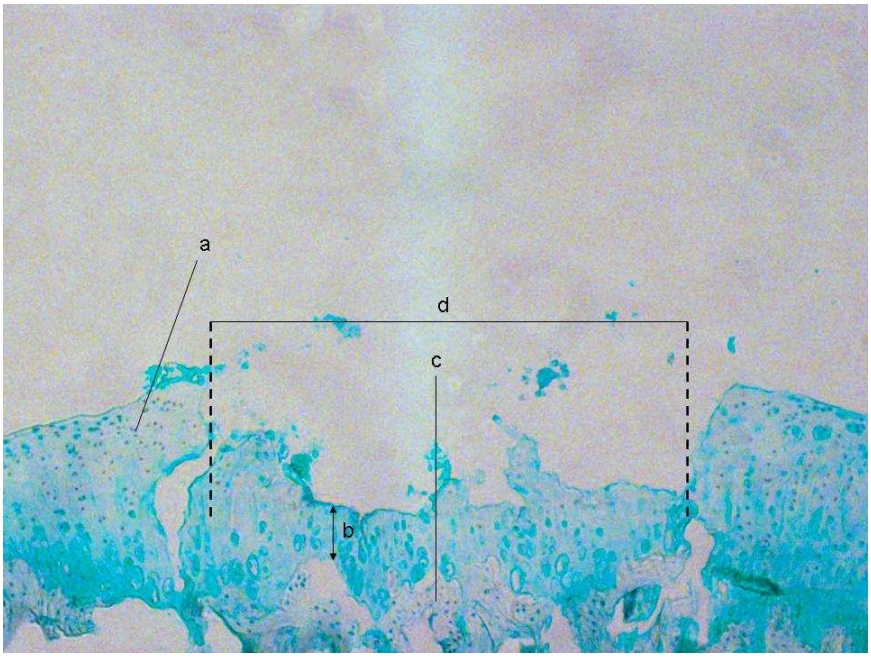

Fig. 3-7: Histological appearance of a full-thickness cartilage defect of the rat tibia plateau.

Cryosections of osteochondral explants with a full-thickness cartilage defect were stained with Weigert’s iron haematoxylin and alcian blue for histological analysis. Cell nuclei were stained in brown (a), and cartilage in blue (b). The subchondral bone (c), as well as the defect of the cartilage of the tibia plateau (d, dashed line), were visible. Magnification: 10-fold.

The osteochondral explants of **Fig. 3-7** and **Fig. 3-8** showed a clear difference between the Mayer’s haematoxylin and eosin staining. In the

Weigert's haematoxylin and alcian blue staining a more detailed picture of the structures in the cartilage was now visible, the deeper blue areas showed a higher concentration of collagen and proteoglycans, than the lighter blue areas. Compared with the Mayer's haematoxylin and eosin staining, where the cell nuclei were sticking out more clearly. Between the defective full-thickness cartilage **(Fig. 3-7)** and the intact cartilage **(Fig. 3-8)**, a higher concentration of collagen and proteoglycans could be observed in the middle of the defective area.

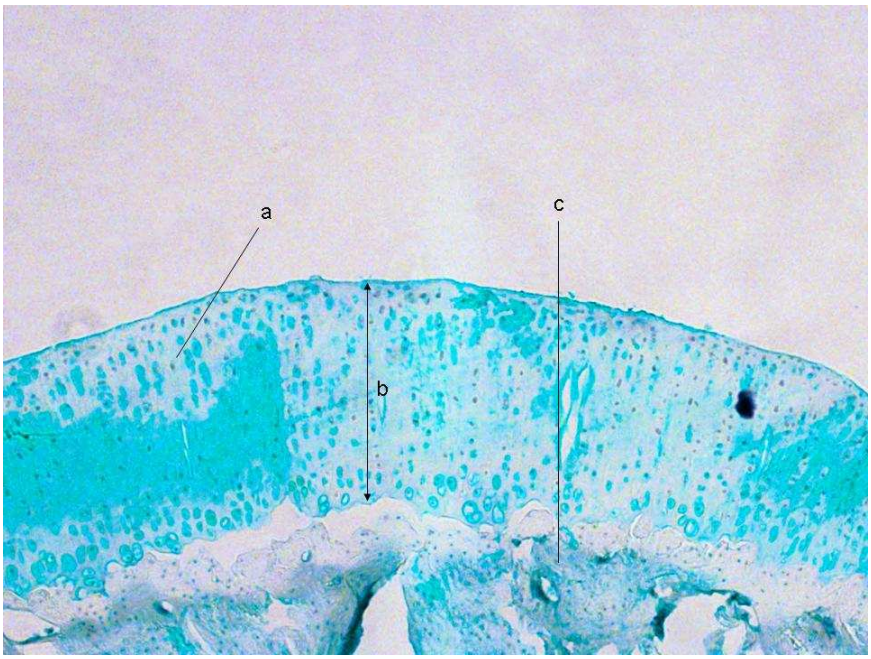

Fig. 3-8: Histological appearance of a full-thickness cartilage of the rat tibia plateau.

Cryosections of osteochondral explants with a full-thickness cartilage defect were stained with Weigert's iron haematoxylin and alcian blue for histological analysis. Cell nuclei were stained in brown (a), cartilage in blue (b), and the subchondral bone (c). Magnification: 10-fold.

Like in the Mayer's haematoxylin and eosin staining **(Fig. 3-4** to **Fig. 3-6)** the number of cell nuclei increased with the enhanced serum concentration. At 20 % serum concentration there was also an increase of cell nuclei visible in the intact areas **(Fig. 3-5)**. This process is also true for the increase of collagen and proteogylcan visible in **Fig. 3-9** to **Fig. 3-11**. Further, a rise in

collagen and proteoglycans could be seen. The deeper blue surface of the defective area at 20 % to 100 % serum reflected the higher levels of collagen and proteoglycans. The osteochondral explants supplemented with 0 % serum served as negative control for a better comparability between the serum concentration experiments. If there would be an increase of cell nuclei, collagen and proteoglycans in the 0 % serum samples, serum could not be the significant factor in cell attachment. This was not observed.

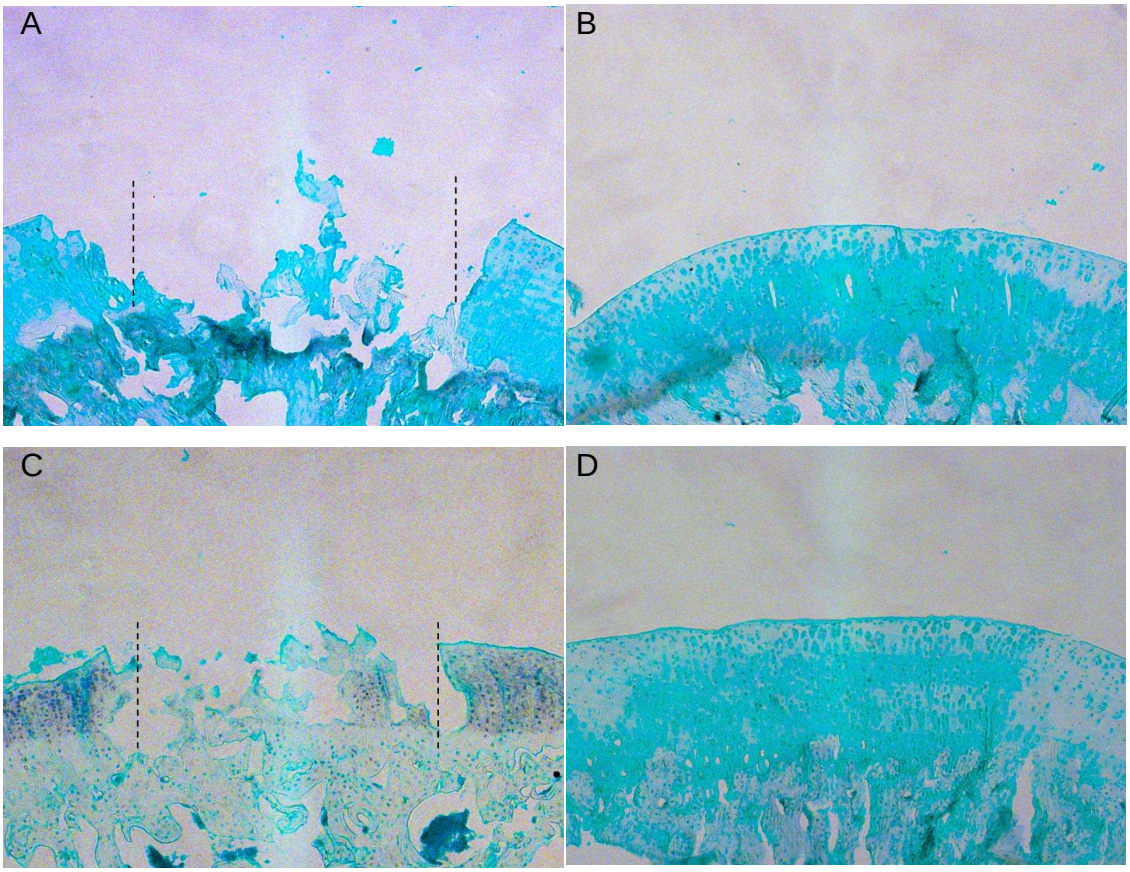

Fig. 3-9: Histological appearance of rat tibia plateaus after MSC attachment with different serum concentrations starting from 0 % to 2 %.

Cells were allowed to attach to the cartilage surface of rat tibia plateaus supplemented with 0 % (A and B) or 2 % serum (C and D). The more serum was supplemented the better cells attached to full-thickness cartilage defects (A and C) compared to the attachment to the intact cartilage surface (B and D). Magnification: 10-fold.

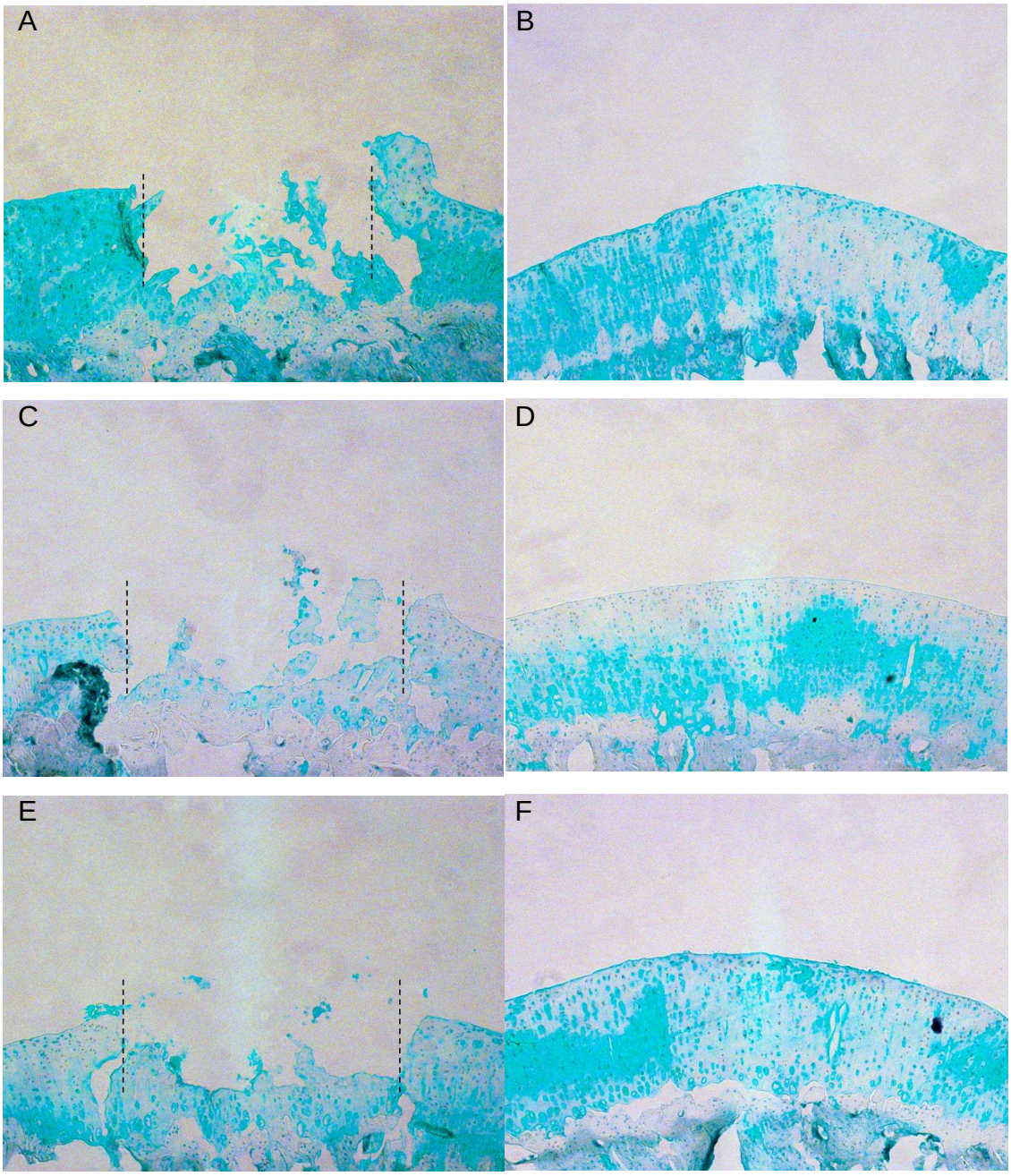

Fig. 3-10: Histological appearance of rat tibia plateaus after MSC attachment with different serum concentrations starting from 5 % to 20 %.

Cells were allowed to attach to the cartilage surface of rat tibia plateaus supplemented with 5 % (A and B) 10 % (C and D) or 20 % serum (E and F). Enhancing the serum concentration triggered the cell attachment even on the intact condylus of the tibia plateau shown in (F) in comparison to (B) and (D). Magnification: 10-fold.

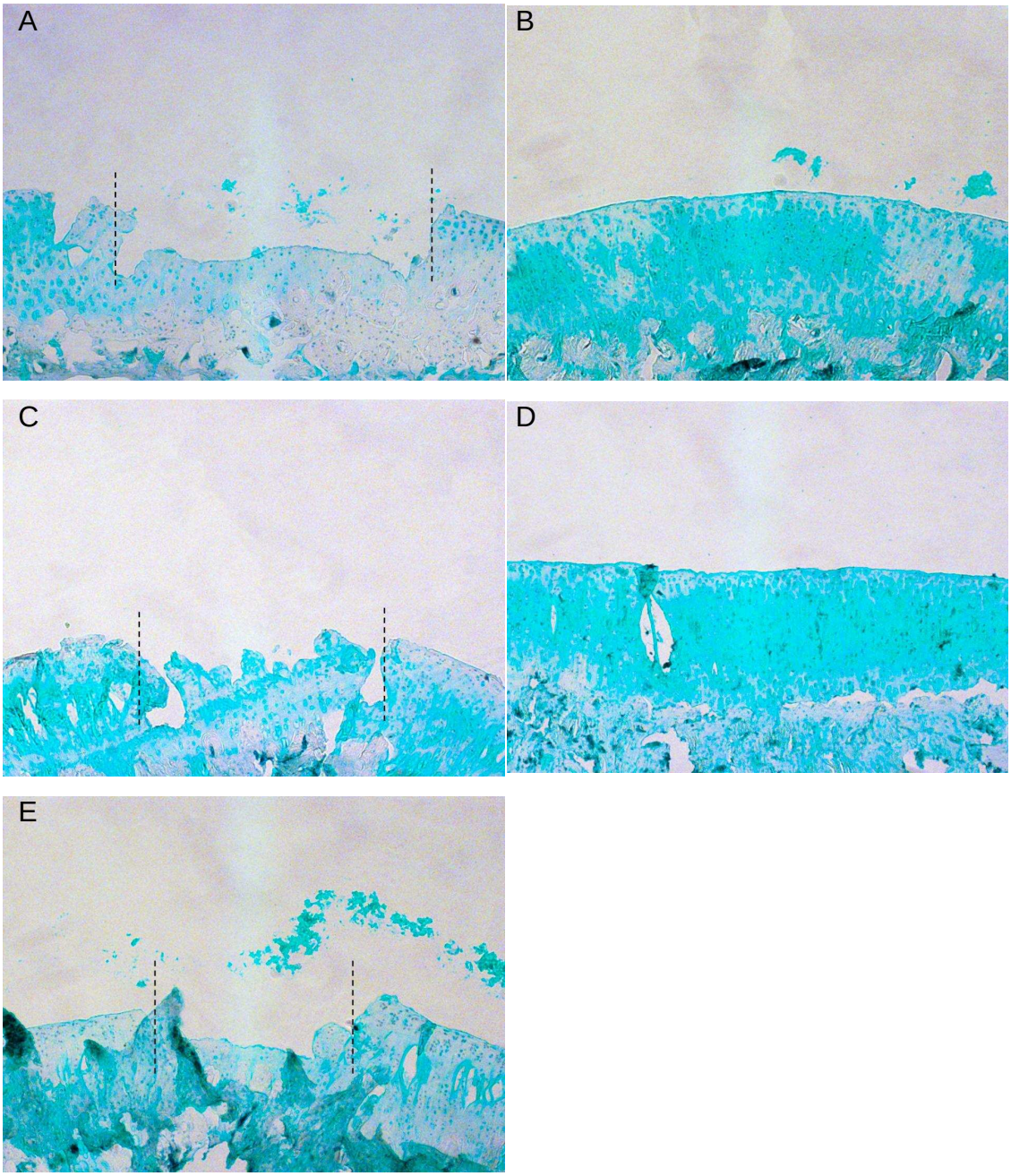

Fig. 3-11: Histological appearance of rat tibia plateaus after MSC attachment with 50 % and 100 % serum concentrations.

Cells were allowed to attach to the cartilage surface of rat tibia plateaus supplemented with 50 % (A and B) to 100 % serum (C, D and E).The highest density of cell nuclei could be found in the upper layer of the full-thickness cartilage in both tibia plateaus with (C and E) and without defect (D). Furthermore, the density of cell nuclei was also increased in the defect. Magnification: 10-fold.

3.3.3. Mayer‘s haematoxylin/fast green/ safranin O

Mayer’s haematoxylin is, as mentioned, used as a nuclear counter stain particularly in a three color staining procedure. The fast green and safranin O staining are very common in the histological analysis of OA (Sagar, et. al.; 2013, Veje, et. al.; 2003). Fast green stained collagens in blue, whereas safranin O stained glycosaminoglycans in orange of osteochondral explants with **(Fig. 3-12)** and without defect **(Fig. 3-13)** after attachment of serum-incubated MSC.

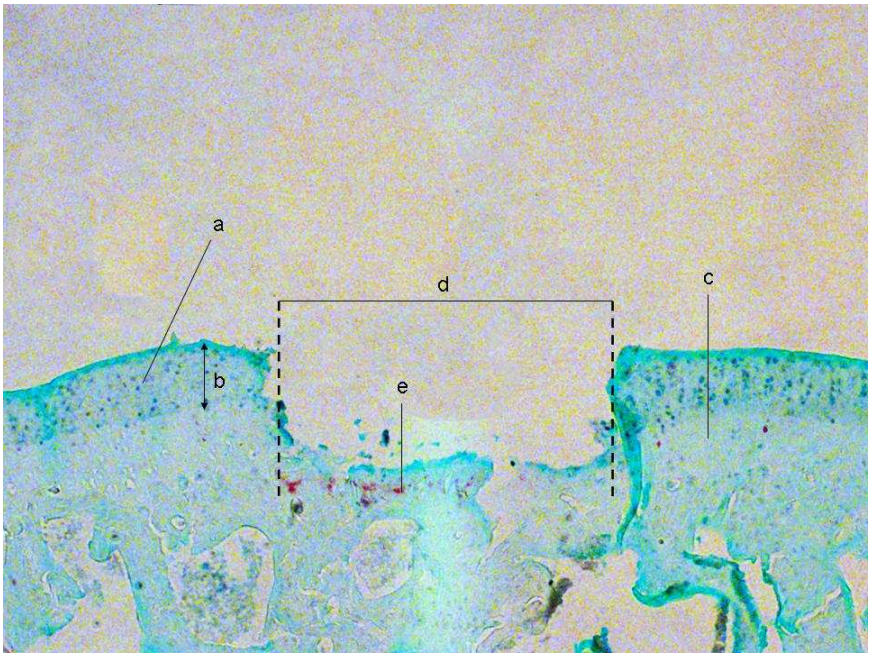

Fig. 3-12: Histological appearance of a full-thickness cartilage defect of the rat tibia plateau.

Cryosections of osteochondral explants with a full-thickness cartilage defect were stained with Mayer’s haematoxylin, fast green and safranin O for histological analysis. Cell nuclei were stained in brown (a), and cartilage, collagen in green (b). The subchondral bone in green (c), as well as the defect of the cartilage of the tibia plateau (d, dashed line), are visible. Cartilage and glycosaminoglycans in orange (e). 10 % serum concentration. Magnification: 10-fold.

To give an overview of the structures of the osteochondral explants **Fig. 3-12** demonstrated the full-thickness cartilage defect until the subchondral bone. On the contrary, **Fig 3-13** showed an intact full-thickness cartilage of the tibia plateau.

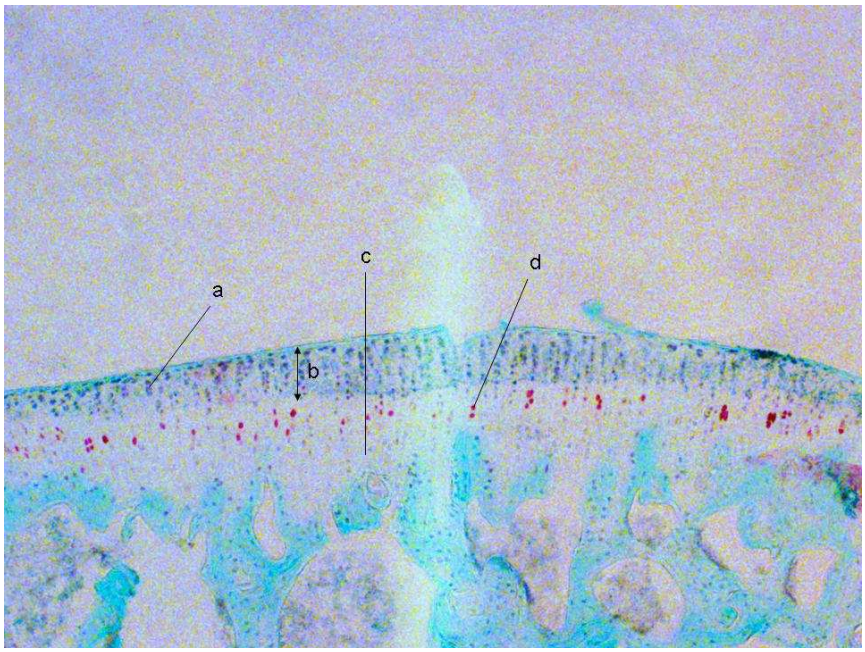

Fig. 3-13: Histological appearance of a full-thickness cartilage of the rat tibia plateau.

Cryosections of osteochondral explants with a full-thickness cartilage defect were stained with Mayer's haematoxylin, fast green and safranin O for histological analysis. Cell nuclei were stained in brown (a), and cartilage, collagen in green (b). The subchondral bone in green (c), cartilage and glycosaminoglycans in orange (d). 10 % serum concentration. Magnification: 10-fold.

The Mayer's haematoxylin, fast green and safranin O staining was more specific than the Weigert's haematoxylin and alcian blue staining. Because, with the Weigert's haematoxylin and alcian blue staining collagens and proteoglycans were stained in the same color blue. Therefore, an increase of collagen or proteoglycan could be observed **(Fig. 3-14** to **Fig. 3-16)**.

Performing Mayer's hematoxylin/fast green/safranin O staining for defective and intact explants with attached MSC at increasing serum concentrations **(Fig. 3-14** to **3-16)** gave insights of differences of glycosaminoglycan and

collagen levels. At low levels **(Fig. 3-14** and **Fig. 3-15)** from 0 % to 5 % serum, no increase of collagen or proteoglycan could be observed. From 10 % to 100 % there was an increase of collagen going hand in hand with the increase of the serum concentration **(Fig. 3-15** to **Fig. 3-16)**. The increase of proteoglycan was not that strong than the increase of collagen. Except at 100 % serum **(Fig. 3-16)**, where the increase of proteoglycan was as strong as the increase of collagen.

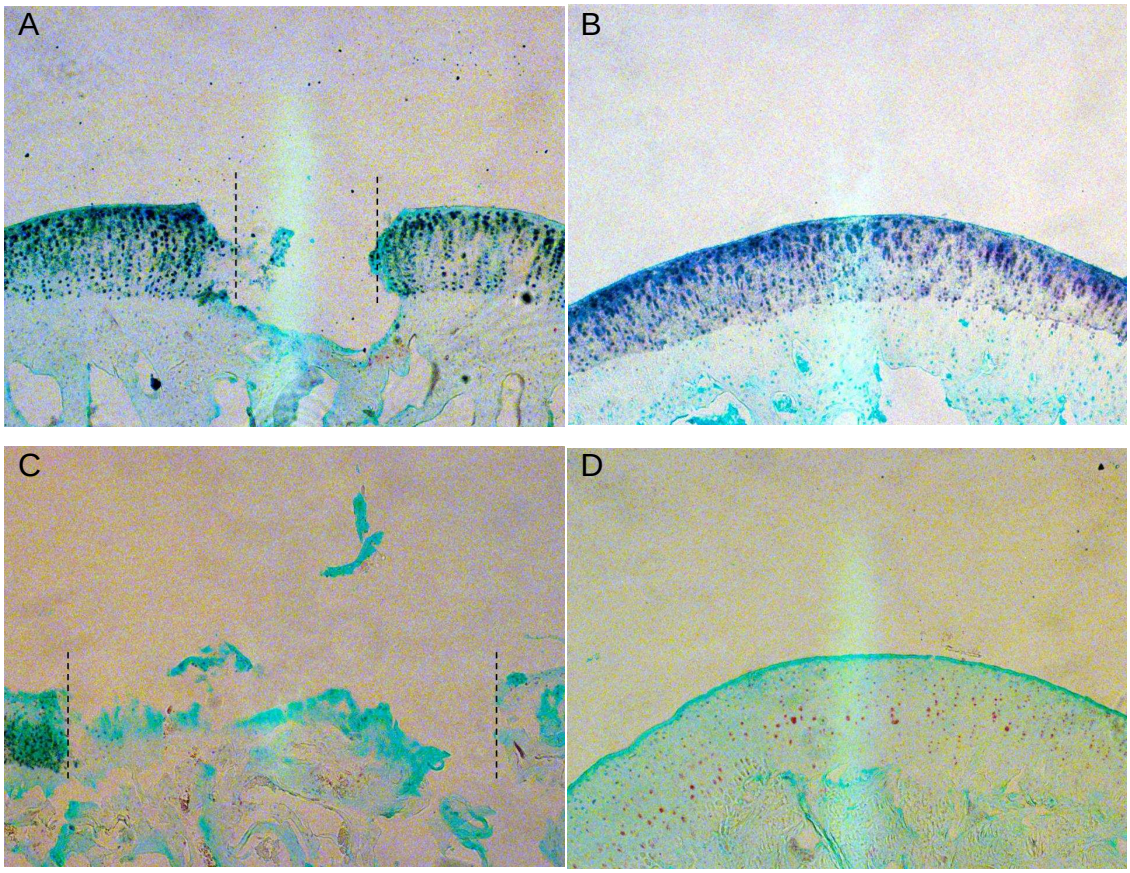

Fig. 3-14: Histological appearance of rat tibia plateaus after MSC attachment with different serum concentrations starting from 0 % to 2 %.

Cells were allowed to attach to the cartilage surface of rat tibia plateaus supplemented with 0 % (A and B) or 2 % serum (C and D). Within the low serum group, the density of chondrocytes and cartilage was depressed. This also effected the attachment of cells, which was on a base level with 0 % and 2 % serum (A and C). Magnification: 10-fold.

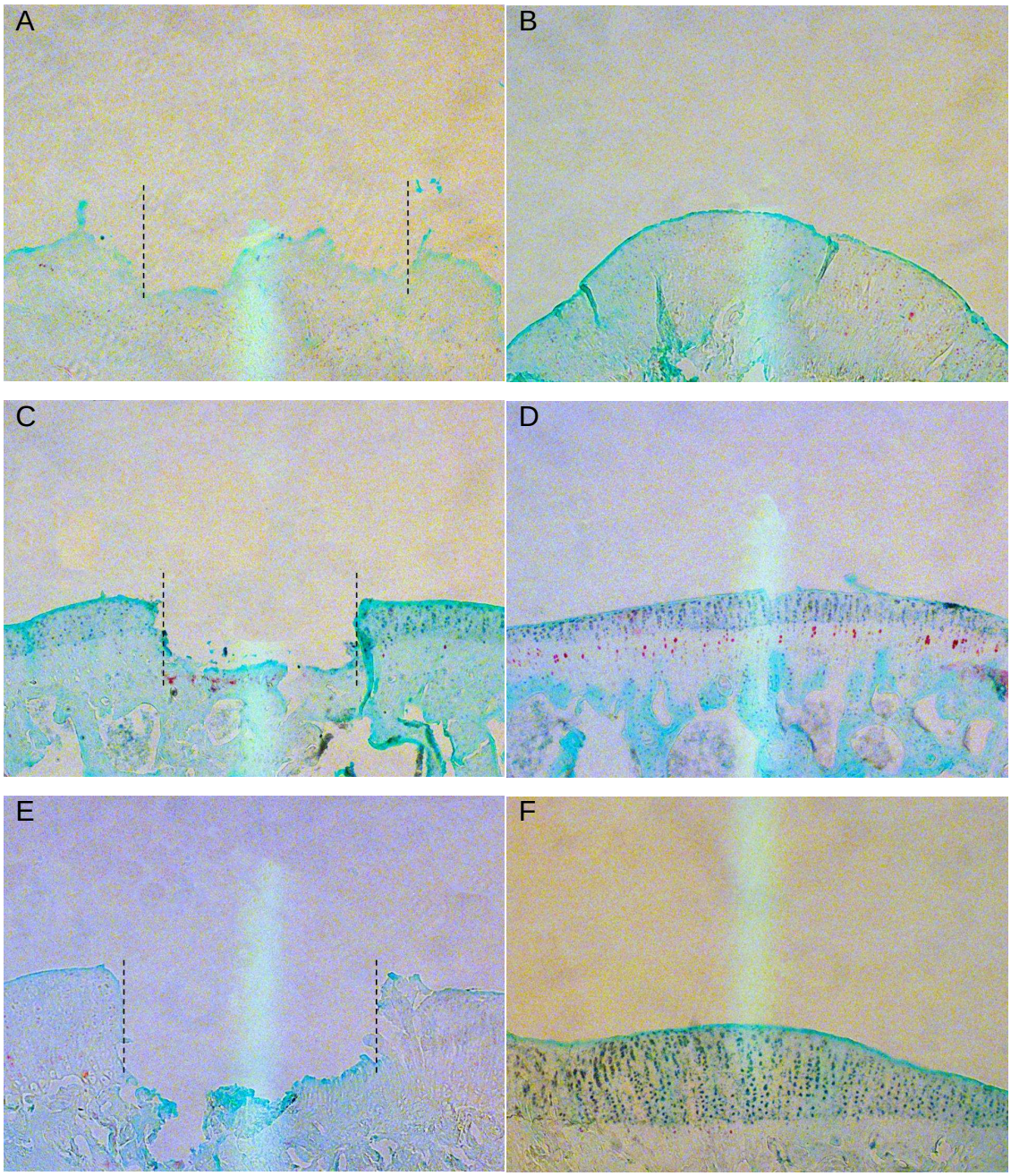

Fig. 3-15: Histological appearance of rat tibia plateaus after MSC attachment with different serum concentrations starting from 5 % to 20 %.

Cells were allowed to attach to the cartilage surface of rat tibia plateaus supplemented with 5 % (A and B), 10 % (C and D), or 20 % serum (E and F). Increasing the serum concentration effected the cell attachment not only in the defect areas, but also on the intact full-thickness cartilage (E and F). Magnification: 10-fold.

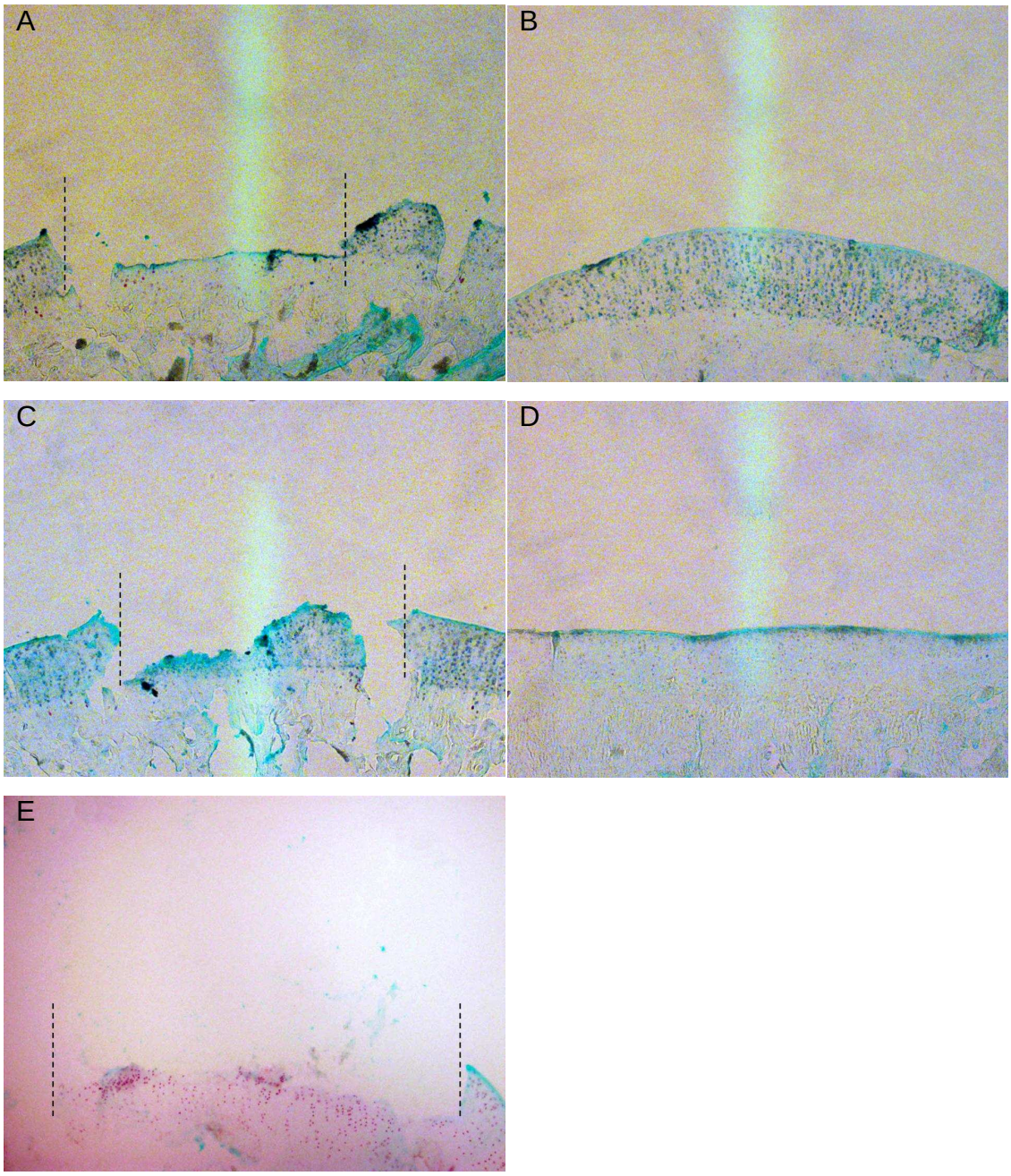

Fig. 3-16: Histological appearance of rat tibia plateaus after MSC attachment with 50 % and 100 % serum concentrations.

Cells were allowed to attach to the cartilage surface of rat tibia plateaus supplemented with 50 % (A, B) and 100 % serum (C, D and E). The darker surface within and without defect indicated a higher concentration of chondrocytes and cell nuclei (A, B, C, D and E). A significant increase of proteoglycan within the full-thickness cartilage defect was observed (E). Magnification: 10-fold.

3.3.4. hPLAP/fast red

The tibia plateaus were allowed to attach to hPLAP-transgenic MSC pre-incubated with diverse serum concentrations. After the staining procedures with Mayer's haematoxylin and eosin, Weigert's iron haematoxylin/alcian blue and Mayer's hematoxylin/fast green and safranin O were positive for an enhancement in glycosaminoglycans, collagens and nuclei within and without the full-thickness cartilage defects, hPLAP/fast red staining was performed. This staining should prove that hPLAP cells had attached within and next to the defect. Fast red was used as counter stain, staining nonspecifically every tissue and cell present in the section **(Fig. 3-17** and **3-18)**. In contrast, hPLAP specifically stained hPLAP-transgenic cells attached to the explants' surface blue **(Fig. 3-19** and **3-20)**.

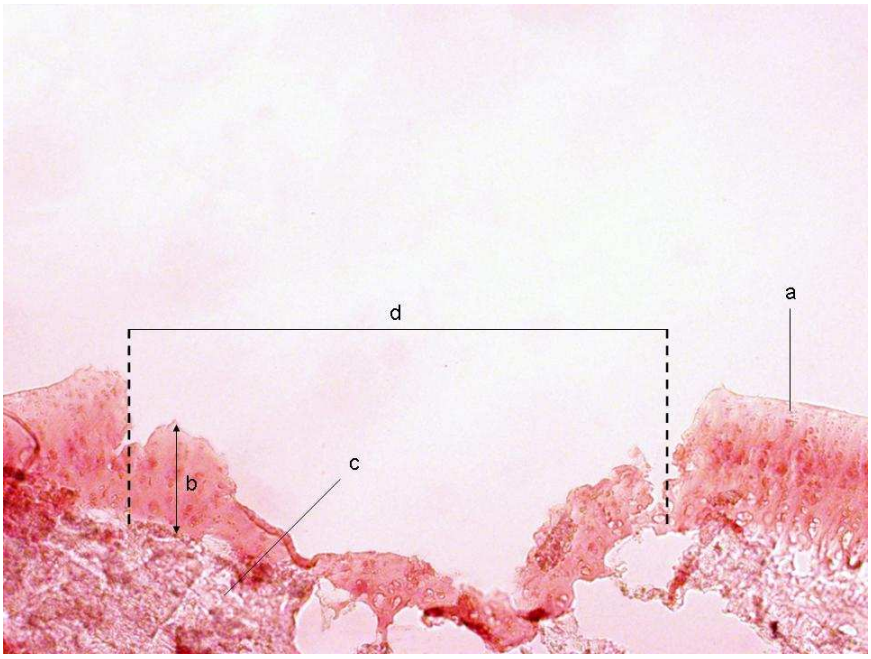

Fig. 3-17: Histological appearance of a full-thickness cartilage defect of the rat tibia plateau.

Cryosections of osteochondral explants with a full-thickness cartilage defect were stained with hPLAP and fast red for histological analysis. Cell nuclei were stained in brown (a), cartilage, with chondrocytes (b). The subchondral bone in red (c), as well as the defect of the cartilage of the tibia plateau (d, dashed line), are visible. 0 % serum. Magnification: 10-fold.

Fig. 3-17 and **Fig. 3-18** were osteochondral explants at 0 % serum level. Therefore, no attachment was observed. This was important, because 0 % served negative control of the experiment. No attachment at this rate meant that the experiment worked properly. The tibia plateau showed the full-thickness cartilage defect until the subchondral bone **(Fig. 3-17)** or the intact cartilage of the osteochondral explant **(Fig. 3-18)**. Further, the cartilage with its typical structure of osteocytes could be observed.

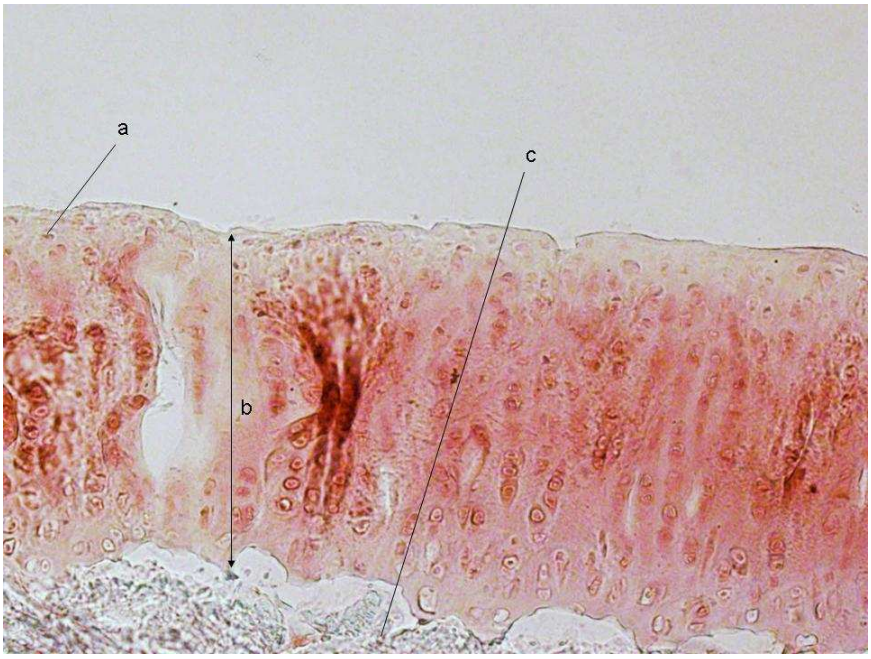

Fig. 3-18: Histological appearance of a full-thickness cartilage of the rat tibia plateau.

Cryosections of osteochondral explants with a full-thickness cartilage defect were stained with hPLAP and fast red for histological analysis. Cell nuclei were stained in brown (a), cartilage, with chondrocytes (b). The subchondral bone in red (c). 0 % serum. This figure showed a complete intact articular cartilage of the tibia plateau with the typical spread distribution of the chondrocytes within the articular cartilage. Magnification: 20-fold.

On the contrary, at 100 % serum **(Fig. 3-19** and **Fig. 3-20)** the MSC attachment within and next to the defect, where cartilage also might be defected, was drastically enhanced. Not only in the defect **(Fig. 3-19)** but also at the intact cartilage surface **(Fig. 3-20)** hPLAP-transgenic MSC could be found to certain extent. These finding were in line with the results obtained

from *ex vivo* and *in vitro* attachment studies (unpublished data). The comparison of the 0 % serum with 100 % serum showed that not only cell nuclei had attached, but also cell clusters were formed. Not only just in the defected areas, but also on the intact surface **(Fig. 3-20)**.

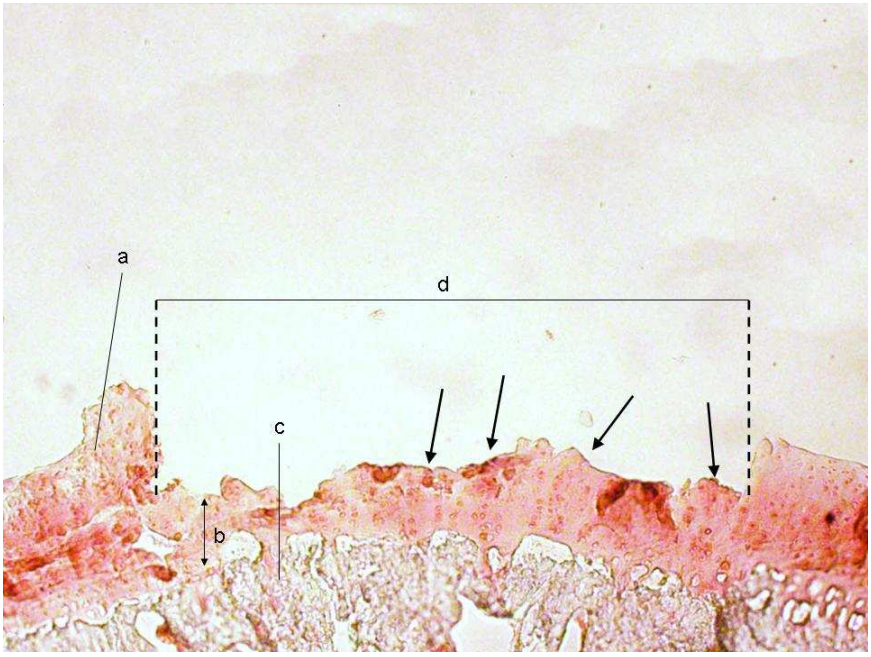

Fig. 3-19: Histological appearance of a full-thickness cartilage defect of the rat tibia plateau.

Cryosections of osteochondral explants with a full-thickness cartilage defect were stained with hPLAP and fast red for histological analysis. Cell nuclei were stained in brown (a), and cartilage, with chondrocytes (b). The subchondral bone in red (c), as well as the defect of the cartilage of the tibia plateau (d, dashed line), were visible. Cell suspensions supplemented with high serum concentrations drastically enhanced the attachment of MSC to full-thickness cartilage defects (arrows). 100 % serum concentration. Magnification: 10-fold.

The hPLAP and fast red staining **(Fig. 3-17** to **Fig. 3-25)** completely approved the results of the former performed stainings **(Fig. 3-2** to **Fig. 3-16)**. hPLAP MSC began to attach on a serum level of 5 % **(Fig. 3-21)**. Also weak cell attachment could be found at 2 % serum at the margin area of the full-thickness cartilage defect.

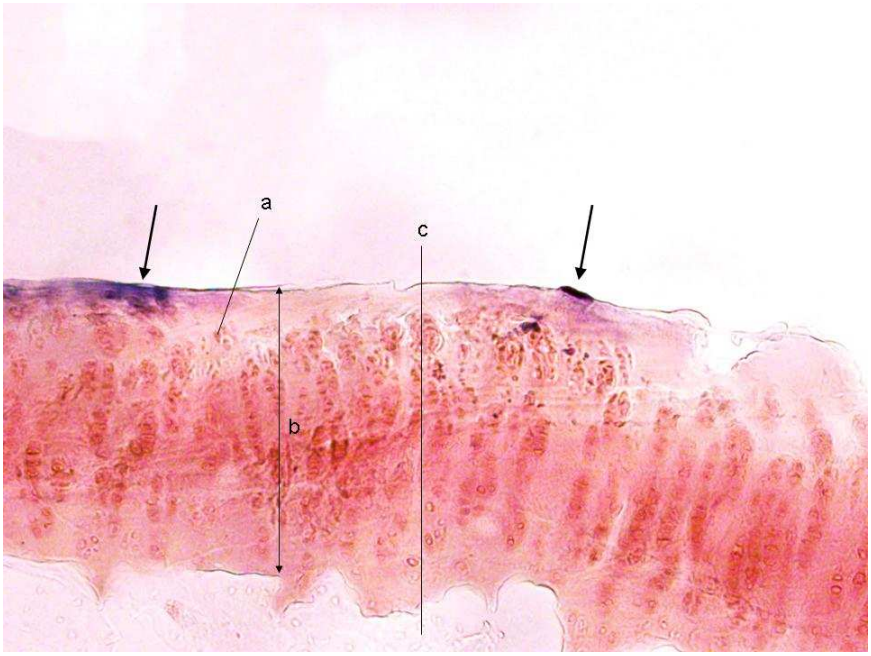

Fig. 3-20: Histological appearance of a full-thickness cartilage defect of the rat tibia plateau.

Cryosections of osteochondral explants with a full-thickness cartilage defect were stained with hPLAP and fast red for histological analysis. Cell nuclei were stained in brown (a), and cartilage, with chondrocytes (b). The subchondral bone in red (c). On the surface of the intact condylus MSC started to attach and enhance the affinity for attachment. Supplementing 100 % serum to MSC the cells were able to attach to the intact cartilage surface (arrows), but to less extend. 100 % serum concentration. Magnification: 20-fold.

The cell attachment increased highly from 5 % to 10 % serum **(Fig. 3-22)**. At 10 % serum cells attached within the defective area, at 20 % serum **(Fig. 3-23)** one cell cluster was observed in the full-thickness cartilage defect and cell attachment could also be found on the intact area. There was a further increase observed in 50 % serum **(Fig. 3-24)** and the highest rates on cell attachment and cell cluster accumulation could be observed in the 100 % serum samples **(Fig. 3-25)**.

In comparison hPLAP/fast red staining to the staining taken before, the blue colored hPLAP cells confirmed the results of the former staining. The increased cell nuclei found in H/E, the enhanced collagen and proteoglycan

concentration according to Weigert's iron haematoxylin/alcian blue and Mayer's haematoxylin/fast green/safranin O staining.

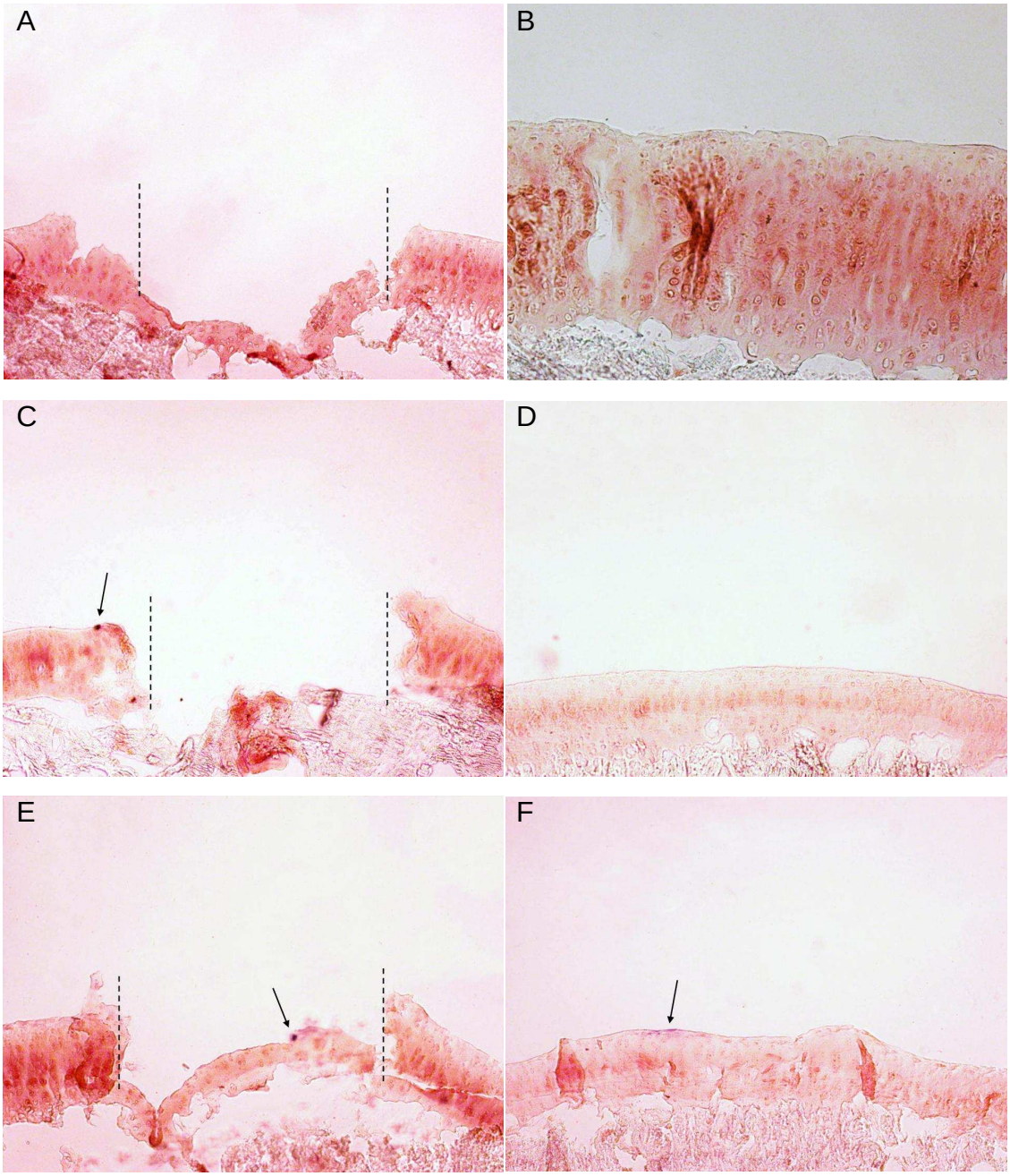

Fig. 3-21: Histological appearance of rat tibia plateaus after MSC attachment with different serum concentrations starting from 0 % to 5 %.

Cells were allowed to attach to the cartilage surface of rat tibia plateaus supplemented with 0 % (A and B), 2 % (C and D), or 5 % serum (E and F). Whereas at 2 % (C) the MSC attached only on the surface, at 5 % (E) cells also attached on the edge of the defect. Magnification: 10-fold.

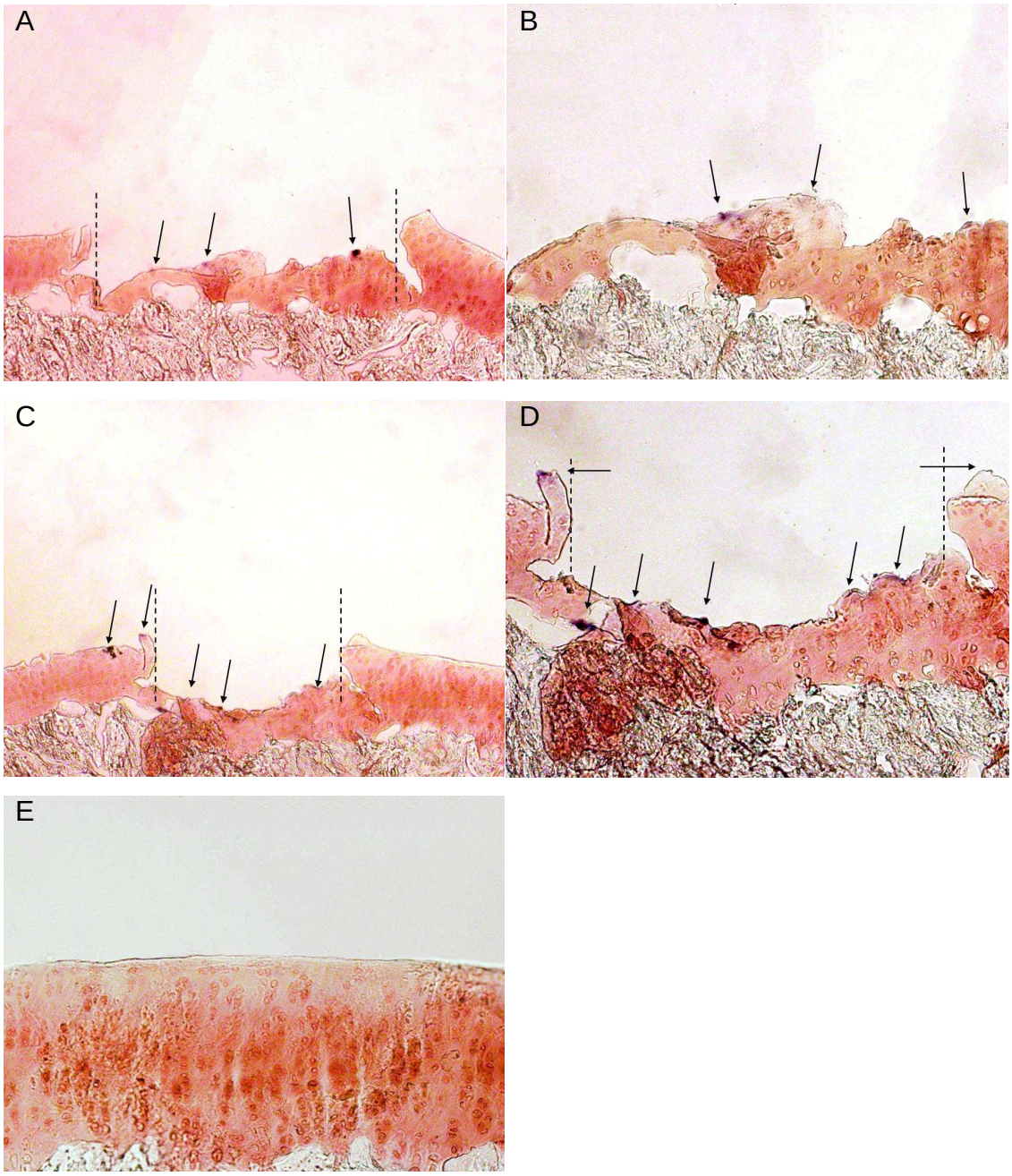

Fig. 3-22: Histological appearance of rat tibia plateaus after MSC attachment with 5 % and 10 % serum concentration.

Cells were allowed to attach to the cartilage surface of rat tibia plateaus supplemented with 10 % serum (A, B, C, D and E). The cell attachment increased rapidly from 5 % to 10 % serum concentration, especially the attachment of MSCs within the defect area (arrows). Magnification: A and C 10-fold, B, D and E 20-fold.

As above, the hPLAP-tg MSC attachment increased with the serum concentration, in 5 % a few cell attached within the defective surface, at 10 % the attachment was further increased **(Fig. 3-22)**.

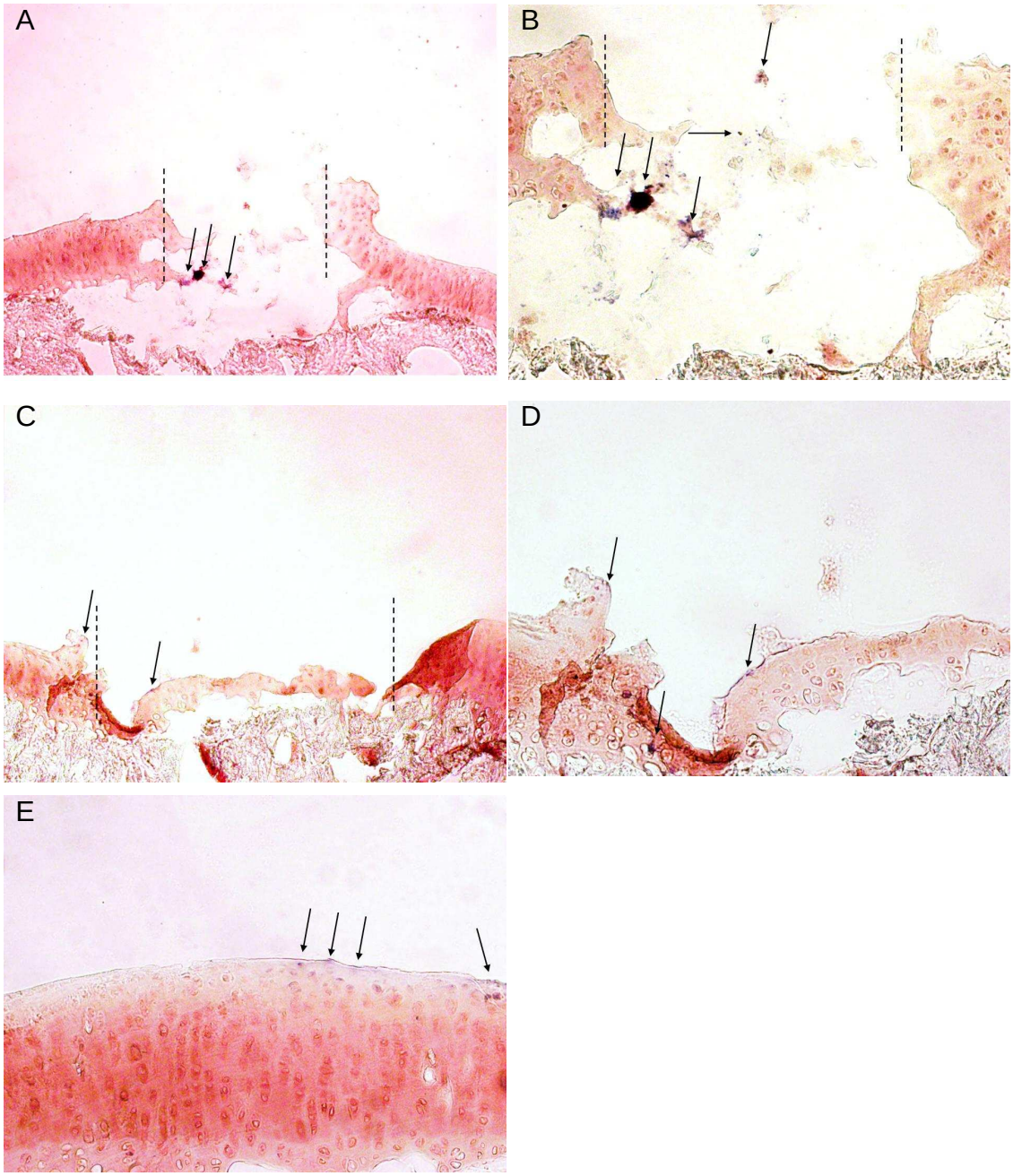

Fig. 3-23: Histological appearance of rat tibia plateaus after MSC attachment with 20 % serum concentration.

Cells were allowed to attach to the cartilage surface of rat tibia plateaus supplemented with 20 % serum (A, B, C, D and E). At a serum level of 20 % not only the cell attachment was enhanced (B), but cells started to increase attachment to the intact surface too. Magnification: A, and C 10-fold, B, D and E 20-fold.

At 20 % serum concentration cell clusters could be observed **(Fig. 3-23)**, as well an increase of cell attachment even on the intact surface was seen.

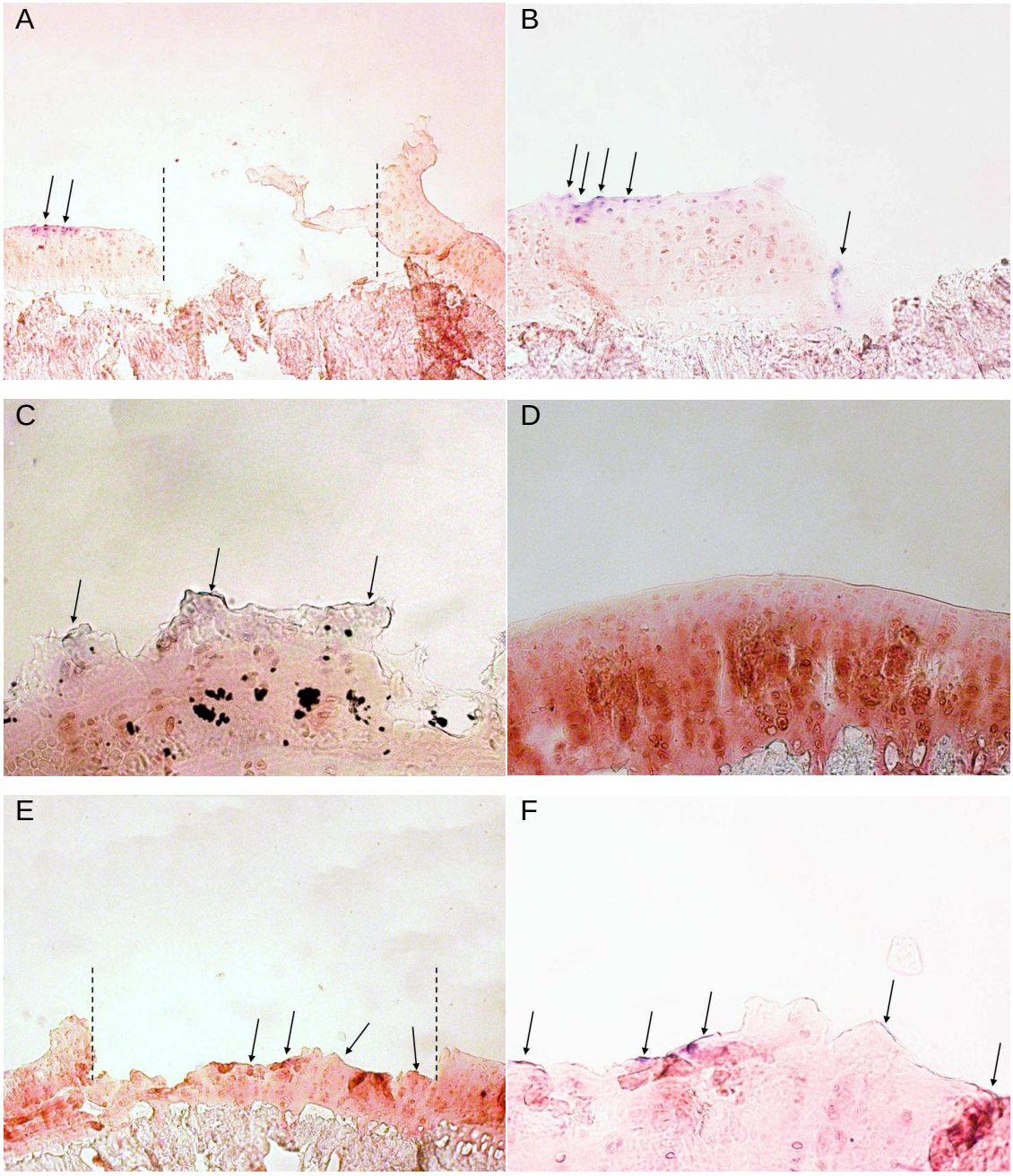

Fig. 3-24: Histological appearance of rat tibia plateaus after MSC attachment with different serum concentrations starting from 50 % to 100 %.

Cells were allowed to attach to the cartilage surface of rat tibia plateaus supplemented with 50 % (A, B, C and D) and 100 % serum (E and F). In both, 50 % and 100 %, the cell attachment was increased and cell clusters could be observed, as the attachment level was drastically enhanced by the increase of the serum concentration. Magnification: A, B and E 10-fold, D 20-fold, C and F 40-fold.

More and more cells attached on the defective osteochondral explants at 50 % **(Fig. 3-24)**. But not only on the full-thickness cartilage defect the hPLAP

MSCs had attached, but also on the intact surface. The highest attachment rate showed the 100 % serum concentration **(Fig. 3-25)**.

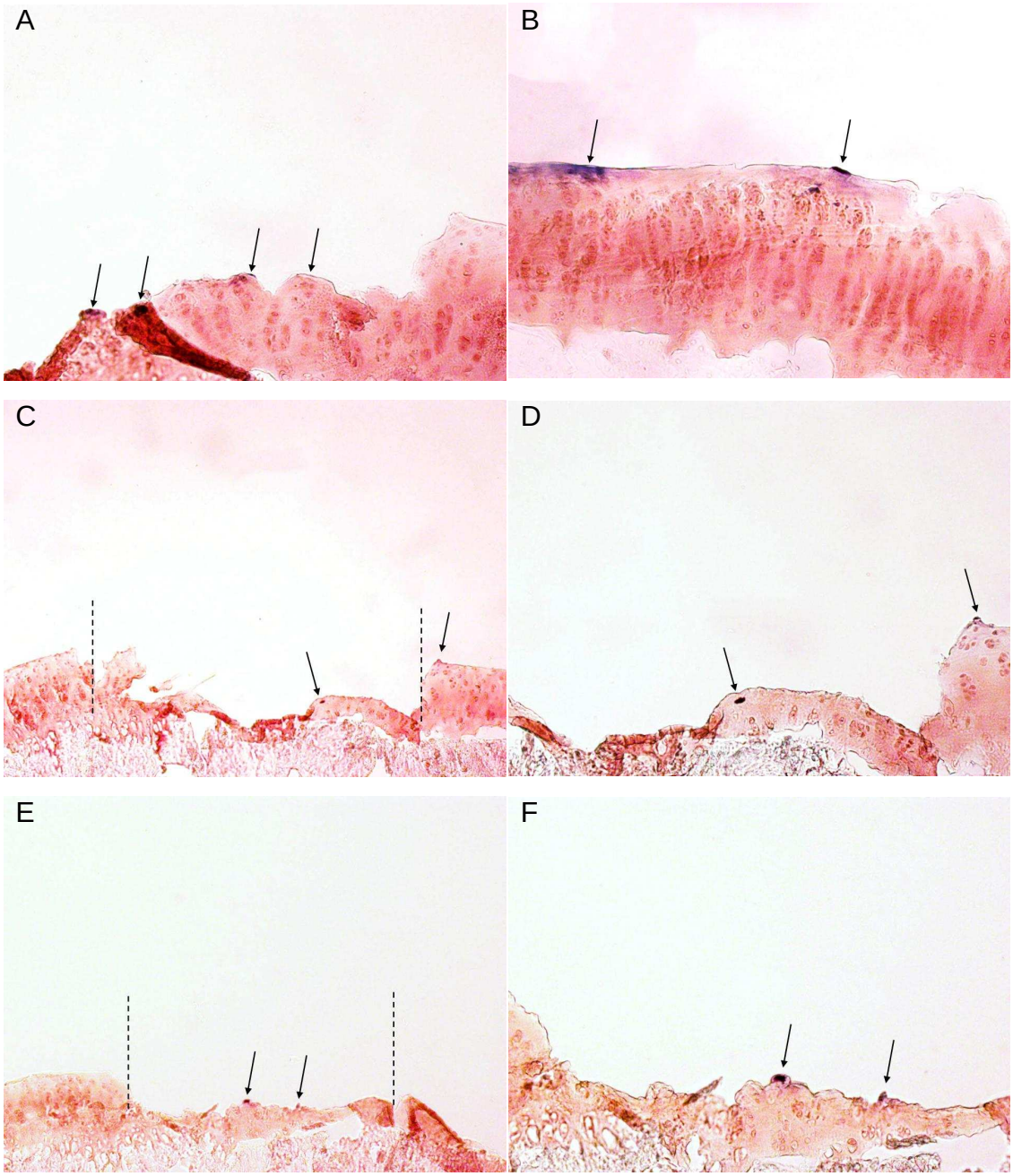

Fig. 3-25: Histological appearance of rat tibia plateaus after MSC attachment with 100 % serum.

Cells were allowed to attach to the cartilage surface of rat tibia plateaus supplemented with 100 % serum (A, B, C, D and E). C and D showed further examples of enhanced cell attachment on a high serum concentration.

Magnification: A, and C 10-fold, B, D, E and F 20-fold.

3.4. Results MSC attachment after divalent ion concentrations

As mentioned in the previous chapter (3.2.2.) divalent ion concentration were tested on their ability the enhance cell attachment. Therefore, the osteochondral explants were processed with the same staining techniques, for better comparison.

3.4.1. Mayer‘s haematoxylin/eosin

3.4.1.1. Calcium

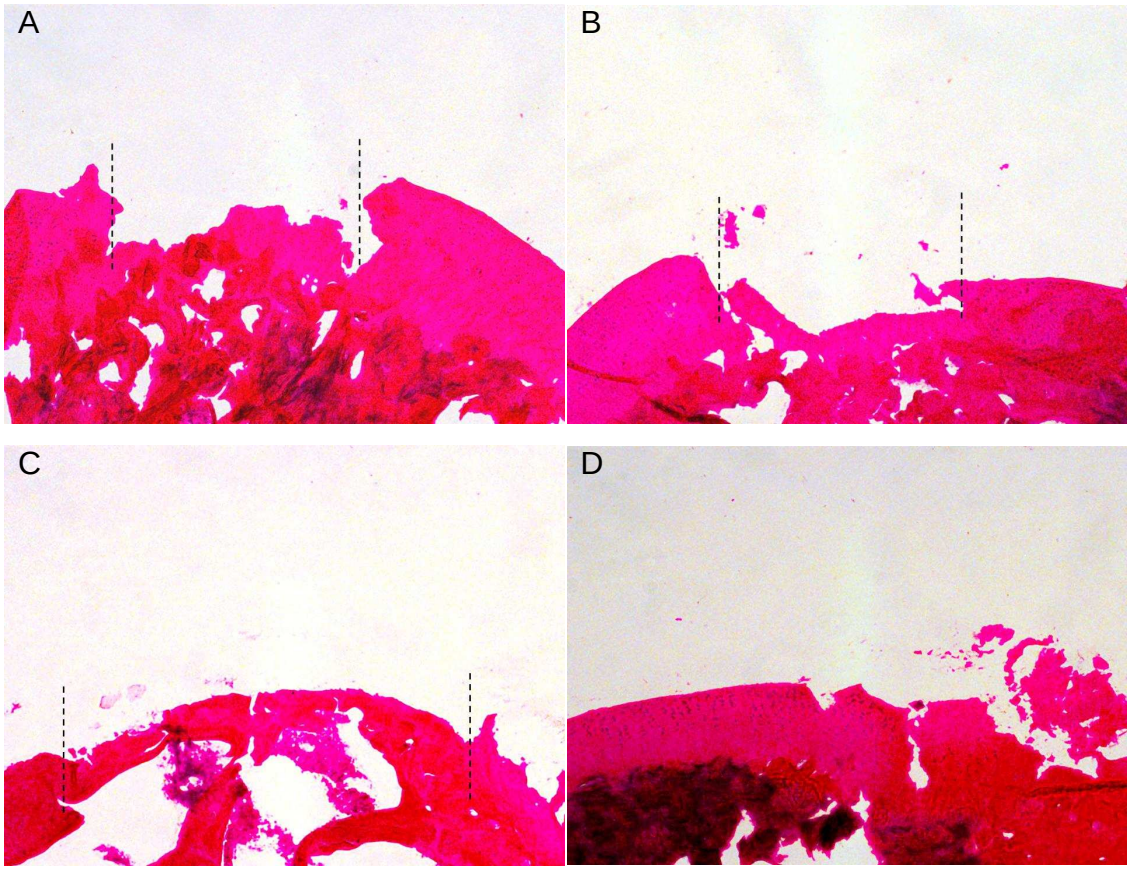

Fig. 3-26: Histological appearance of rat tibia plateaus after MSC attachment with different ion concentrations starting from 1 mM to 10 mM calcium.

Cells were allowed to attach to the cartilage surface of rat tibia plateaus supplemented with 1 mM (A), 2.5 mM (B), 5 mM (C) and 10 mM calcium (D). Only the highest level of calcium (D) showed an increased production of cell nuclei at the edge of the defected area. Magnification: 10-fold.

The osteochondral explants processed with Ca **(Fig. 3-26)** showed the higher the Ca concentration, the more cell nuclei could be found. Compared with the

serum concentration, Ca did not show such dark surfaces within the defective area concluding that even Ca concentrations could not help to increase the attachment.

3.4.1.2. Magnesium

When preincubating MSC with increasing Mg concentrations, the attachment of MSC to defective osteochondral explants could be enhanced. This was indicated by an increasing cell number present within the defects **(Fig. 3-27)**. If compared, the Mg supplemented tibia plateaus showed a higher concentration of cell nuclei than the Ca ones, but not as good attachment as the serum-treated explants.

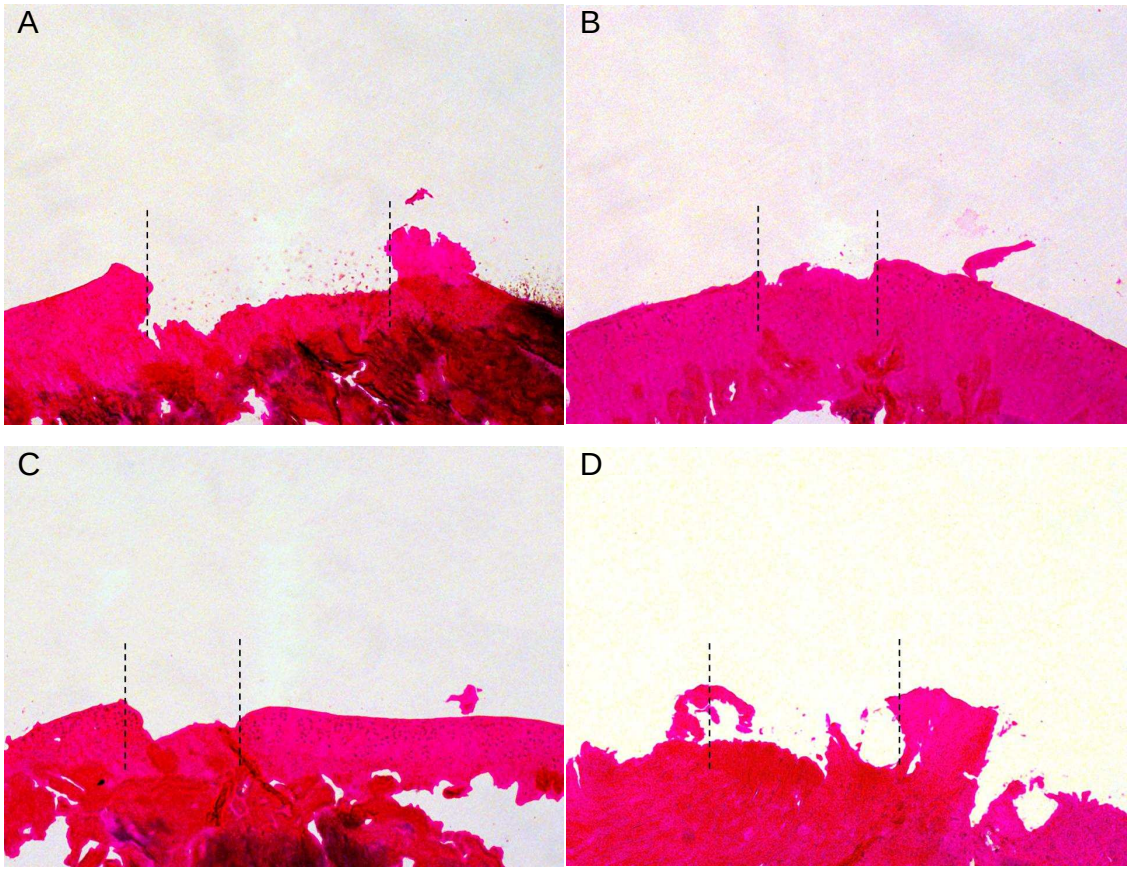

Fig. 3-27: Histological appearance of rat tibia plateaus after MSC attachment with different ion concentrations starting from 1 mM to 10 mM magnesium.

Cells were allowed to attach to the cartilage surface of rat tibia plateaus supplemented with 1 mM (A), 2.5 mM (B), 5 mM (C) and 10 mM magnesium (D). The higher the concentration the more cell nuclei formed at the intact and defect areas of the tibia plateau. Magnification: 10-fold.

3.4.1.3. Magnesium with calcium or manganese

The combination of Mg with Ca showed a darker surface than Mg or Ca concentration alone **(Fig. 3-28)**. Moreover, the solution of Mg with Mn was not that effective than the combination of Mg/Ca. Compared with the serum concentration **(Fig. 3-2** to **Fig. 3-6),** the number of cell nuclei of Mg/Ca was close to the number of cell nuclei in the higher serum concentrations **(Fig. 3-6A and B)**.

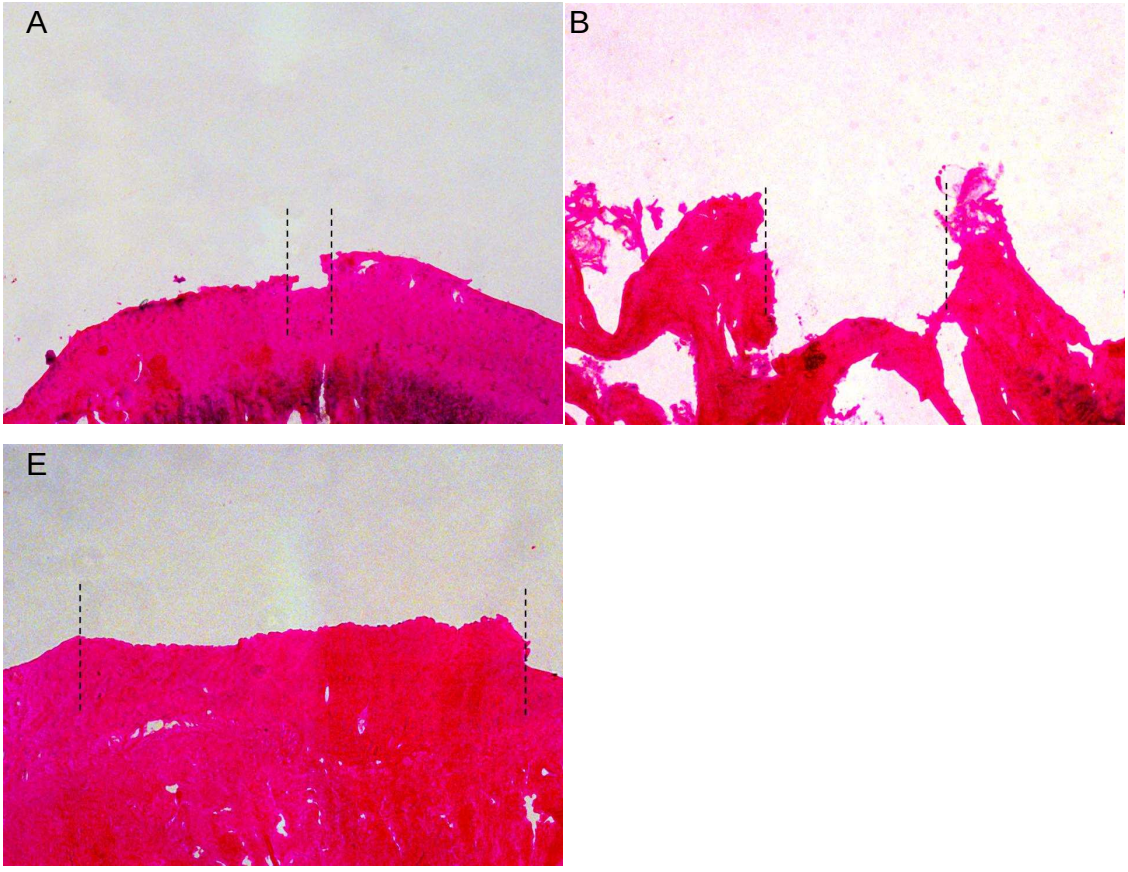

Fig. 3-28: Histological appearance of rat tibia plateaus after MSC attachment with different ion concentrations starting from 1 mM magnesium and 2.5 mM calcium to 2.5 mM magnesium and 1 mM calcium and 1 mM manganese and 2 mM magnesium.

Cells were allowed to attach to the cartilage surface of rat tibia plateaus supplemented with 1 mM magnesium and 2.5 mM calcium (A), 2.5 mM magnesium with 1 mM calcium (B), 1 mM manganese with 2 mM magnesium (C). In C more cells could be seen, because the section was at the beginning of the defect. Magnification: A and B 10-fold, C 20-fold.

3.4.1.4. Manganese, zinc, EDTA

Neither Mn nor Zn showed a significant increase of cell nuclei **(Fig. 3-29)**. Further, EDTA served as negative control **(Fig. 3-29C)**, because it chelated divalent cations. This specific feature allowed EDTA to inhibit the hPLAP-MSC to attach to the full-thickness cartilage defect. Hence, the osteochondral explants did not show an enhanced concentration of cell nuclei. Consequently, EDTA and NaCl as well as the 0 % serum sample were used as negative controls.

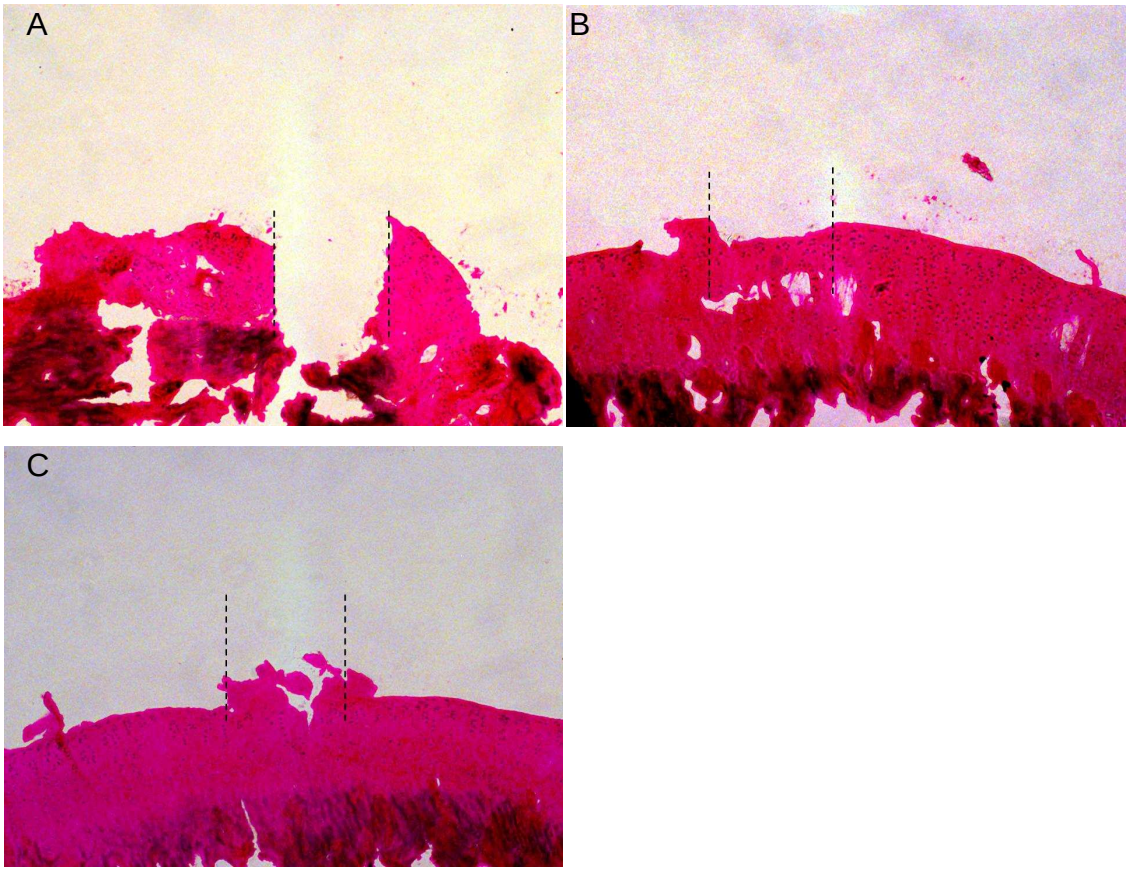

Fig. 3-29: Histological appearance of rat tibia plateaus after MSC attachment with different ion concentrations starting with 1 mM manganese, 1 mM zinc, 10 mM EDTA.

Cells were allowed to attach to the cartilage surface of rat tibia plateaus supplemented with 1 mM manganese (A), 1 mM zinc (B), 10 mM EDTA (C). No significant attachment could be observed. Magnification: 10-fold.

3.4.2. Weigert‘s iron haematoxylin/alcian blue

With the Weigert’s iron haematoxylin/alcian blue staining various divalent ions were tested in their ability to enhance proteoglycans and collagen (both blue) on full-thickness defects. All tibia plateau explants of the ion concentration line were defect full-thickness cartilages. NaCl and EDTA were used as negative controls.

3.4.2.1. Calcium

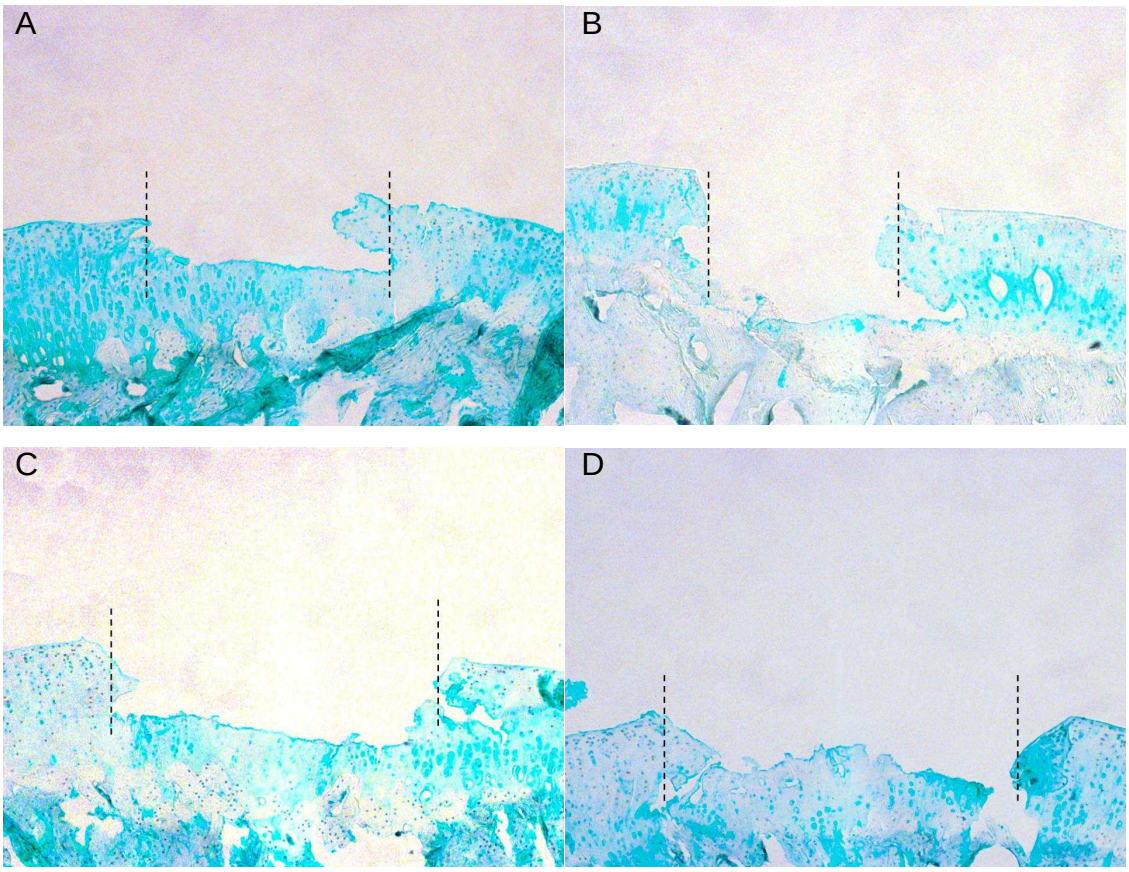

Fig. 3-30: Histological appearance of rat tibia plateaus after MSC attachment with different ion concentrations starting from 1 mM to 10 mM calcium.
Cells were allowed to attach to the cartilage surface of rat tibia plateaus supplemented with 1 mM (A), 2.5 mM (B), 5 mM (C) and 10 mM calcium (D). A weak increase in cell nuclei could be observed within the defect if supplemented with 2.5 mM calcium. Magnification: 10-fold.

The darker surface within the full-thickness cartilage defect indicated that the proteoglycan and collagen concentration in Ca-treated samples was slightly enhanced **(Fig. 3-30)**. The same could be observed for the Mg-treated samples **(Fig. 3-31)**. If compared with the same staining of the serum-treated explants, neither Ca nor Mg showed a higher enhancement than the explants supplemented with 100 % serum. By contrast, with the H/E staining **(Fig. 3-26** and **Fig. 3-27)** Weigert's haematoxylin and alcian blue staining confirmed an increased number of cell nuclei.

3.4.2.2. Magnesium

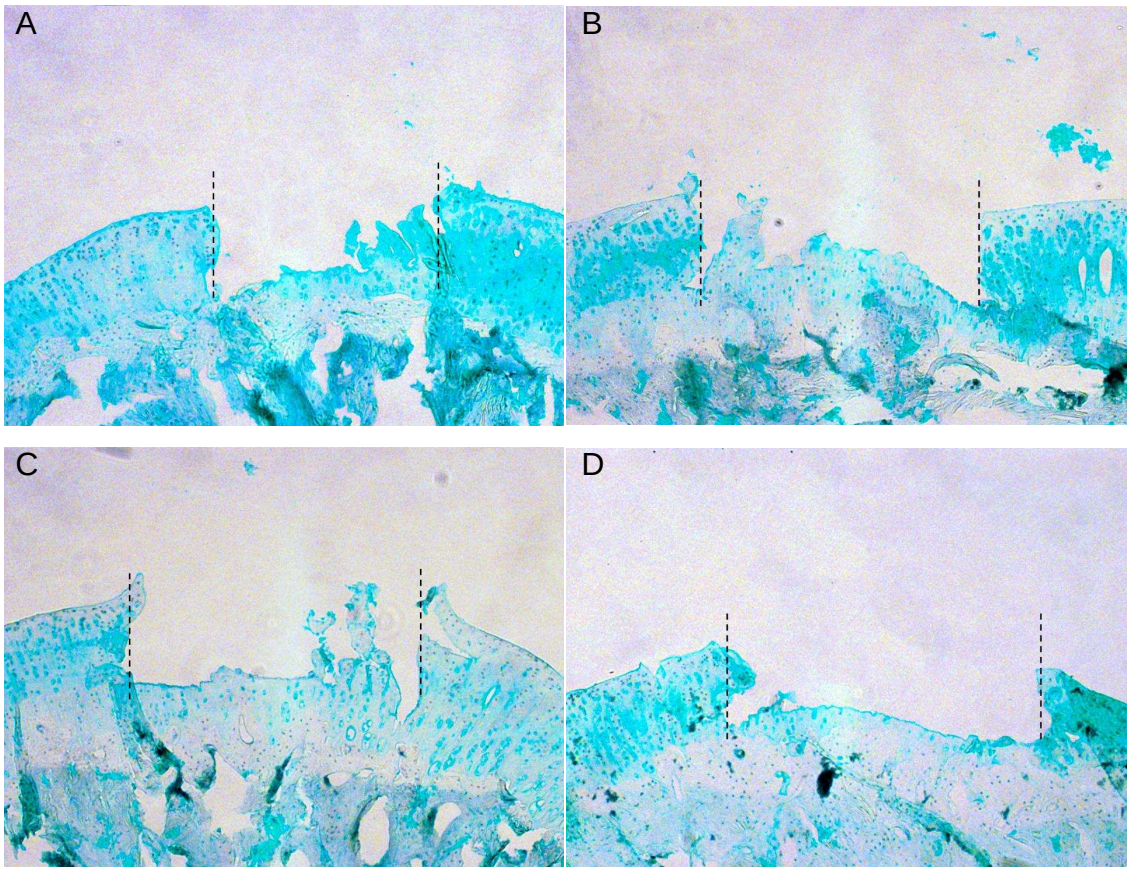

Fig. 3-31: Histological appearance of rat tibia plateaus after MSC attachment with different ion concentrations starting from 1 mM to 10 mM magnesium.
Cells were allowed to attach to the cartilage surface of rat tibia plateaus supplemented with 1 mM (A), 2.5mM (B), 5 mM (C) and 10 mM magnesium (D). A comparison between the margins processed with magnesium and the ones with calcium showed that the magnesium ones were darker, which indicated that there were more cells attached than to those processed with calcium. Magnification: 10-fold.

3.4.2.3. Magnesium with calcium or manganese

The divalent ions Mg and Ca in combination made up the best combination in respective of divalent ions **(Fig. 3-32)**, but not compared to the serum-treated samples Interestingly, proteoglycans and collagens (darker blue) were more enhanced than in the Mg or Ca single samples **(Fig. 3-30** and **Fig. 3-31)**. Further, the combination of Mg with Mn showed an increased collagen and proteoglycan concentration **(Fig. 3-32C)**, however not as significant as the other combinations.

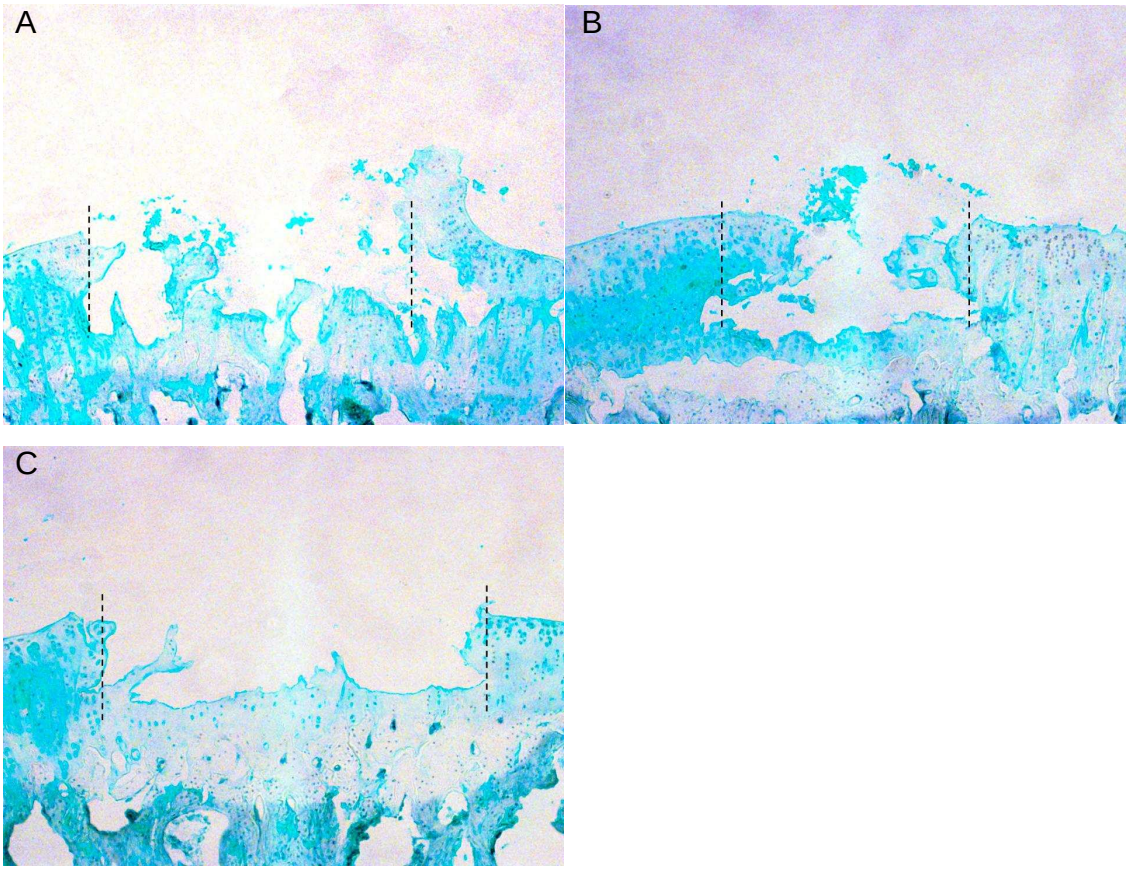

Fig. 3-32: Histological appearance of rat tibia plateaus after MSC attachment with different ion concentrations starting from 1 mM magnesium with 2.5 mM calcium to 2.5 mM magnesium and 1 mM calcium and 1 mM manganese and 2 mM magnesium.

Cells were allowed to attach to the cartilage surface of rat tibia plateaus supplemented with 1 mM magnesium and 2.5 mM calcium (A), 2.5 mM magnesium and 1 mM calcium (B), 1 mM manganese and 2 mM magnesium (C). Nothing significant could be observed in this staining. Magnification: 10-fold.

3.4.2.4. Manganese, zinc, EDTA and NaCl

Mn and Zn showed a slightly increased cell attachment **(Fig. 3-33A and B)**. NaCl could be triggered through the ability of fiber conservation and not caused by the cell attachment **(Fig. 3-33D)**. Since both, NaCl and EDTA, served as negative controls and EDTA did not show significant enhancement, the increased proteoglycan and collagen resulted of preservation of the osteochondral explant. Further, the increase of Mn or Zn was not as high as the increase of the 100 % serum **(Fig. 3-11)**.

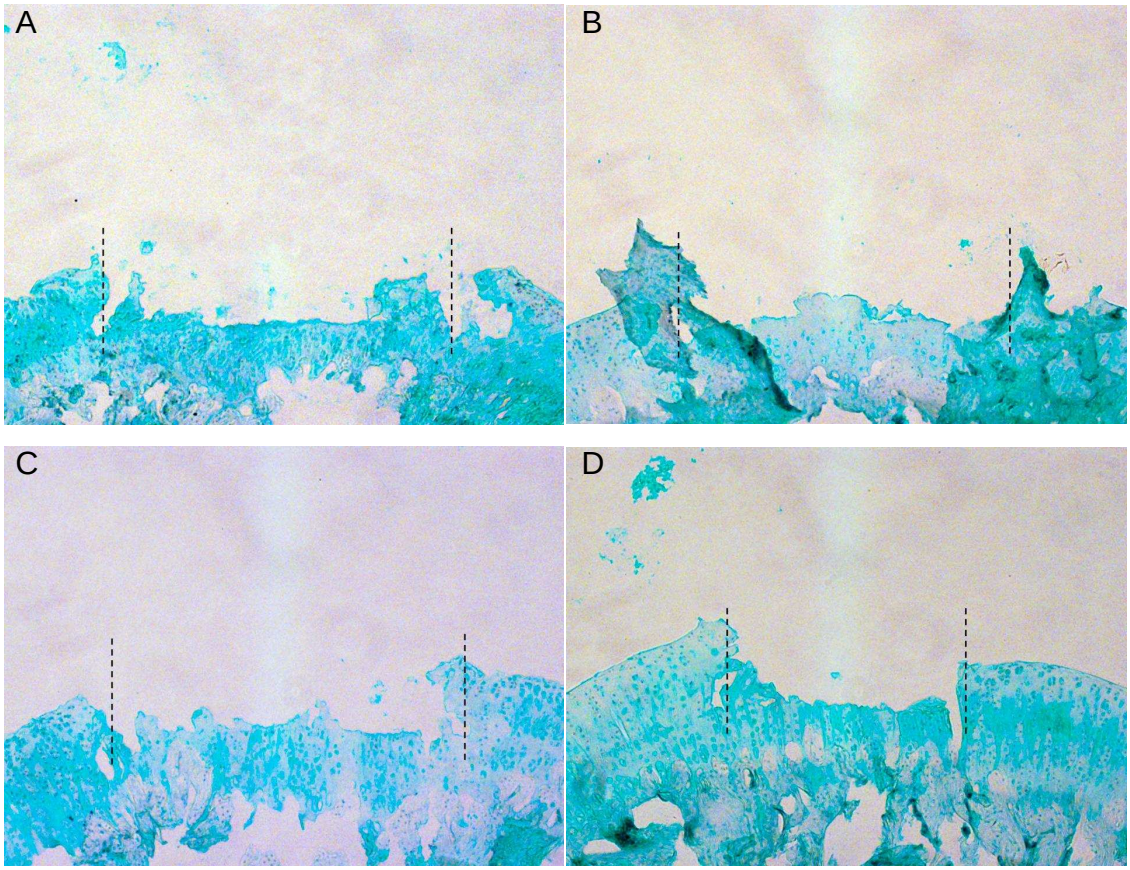

Fig. 3-33: Histological appearance of rat tibia plateaus after MSC attachment with different ion concentrations starting with 1 mM manganese, 1 mM zinc, 10 mM EDTA and NaCl.

Cells were allowed to attach to the cartilage surface of rat tibia plateaus supplemented with 1 mM manganese (A), 1 mM zinc (B), 10 mM EDTA (C) and NaCl (D). Mn and Zn showed a slightly darker surface of the defect, which indicated a higher level of cell nuclei. EDTA and NaCl showed no increase in cell nuclei. Magnification: 10-fold.

3.4.3. Mayer‘s haematoxylin/fast green/ safranin O

As mentioned before the osteochondral explants were tested on divalent ion concentrations. Therefore, the Mayer’s haematoxylin/fast green/safranin O staining had taken place to get a more detailed perspective of proteoglycans (red) and collagens (green) on full-thickness defects. Like for the testing of divalent ion concentrations, all tibia explants had full-thickness cartilage defects.

3.4.3.1. Calcium

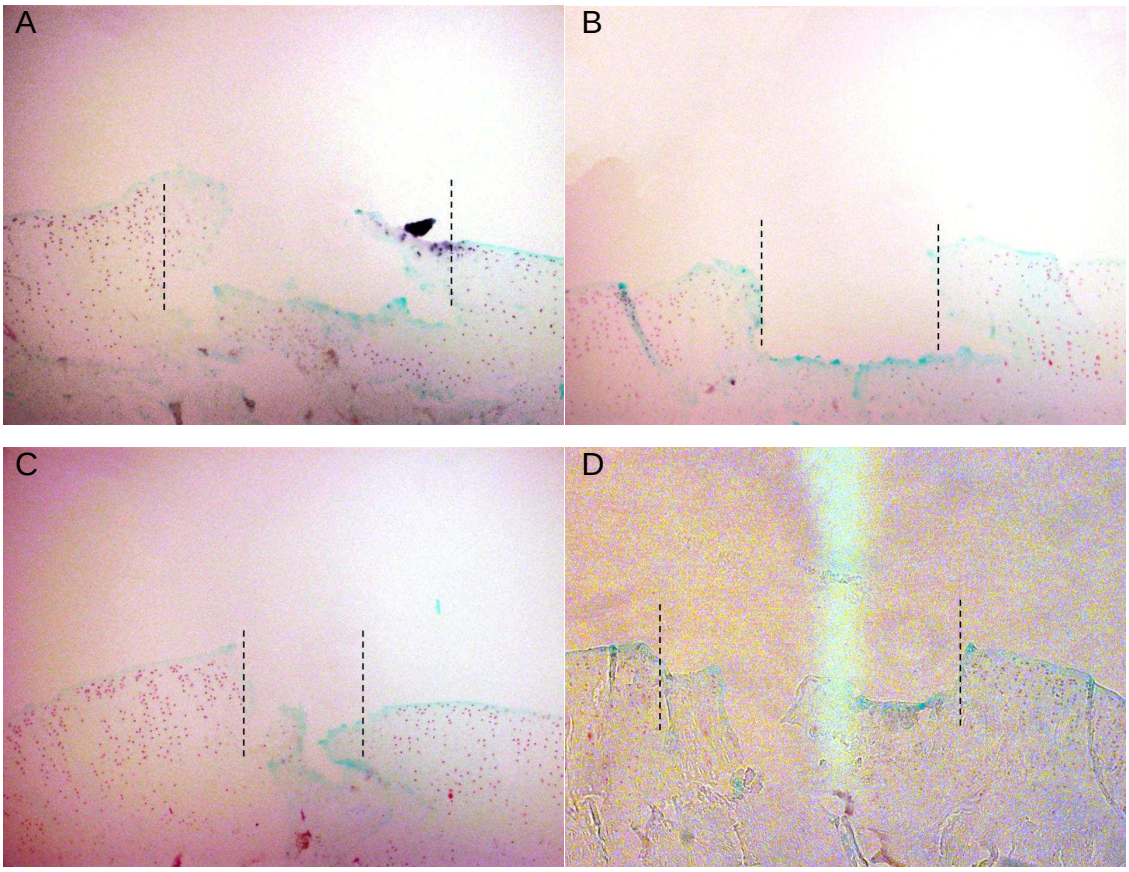

Fig. 3-34: Histological appearance of rat tibia plateaus after MSC attachment with different ion concentrations starting from 1 mM to 10 mM calcium.
Cells were allowed to attach to the cartilage surface of rat tibia plateaus supplemented with 1 mM (A), 2.5 mM (B), 5 mM (C) and 10 mM calcium (D). The margins of the defects showed a green staining. This could be a sign that collagens were now easier accessible for binding than in the enclosed intact status. Magnification: 10-fold.

Within the defective area the green colored collagen showed that it is enhanced, as well as the proteoglycans (red) **(Fig. 3-34** and **Fig. 3-35)**. Both figures demonstrated how collagens and proteoglycans were distributed; the collagens were more enhanced on the surface and the proteoglycans within the cartilage. Compared to the results of the Weigert's haematoxylin and alcian blue **(Fig. 3-30 and Fig. 3-31)**, the staining approved the former data.

3.4.3.2. Magnesium

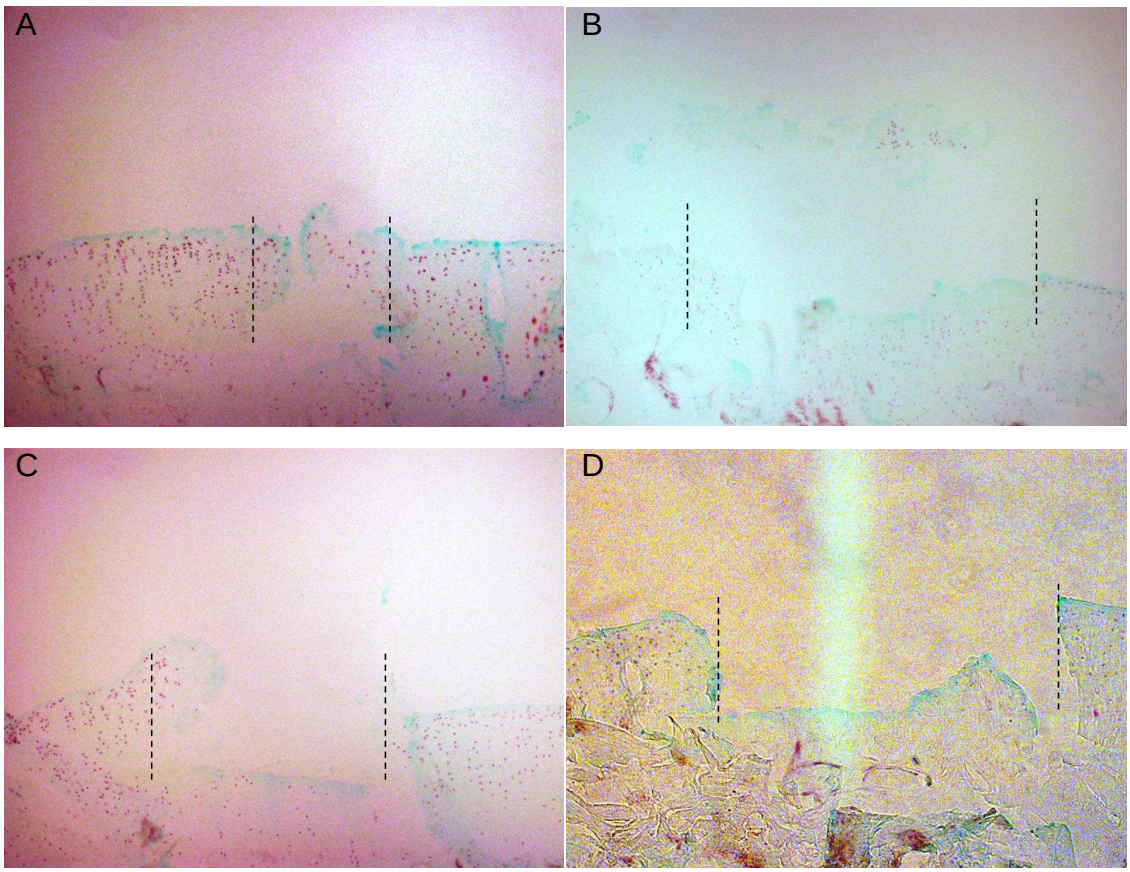

Fig. 3-35: Histological appearance of rat tibia plateaus after MSC attachment with different ion concentrations starting from 1 mM to 10 mM magnesium.
Cells were allowed to attach to the cartilage surface of rat tibia plateaus supplemented with 1 mM (A), 2.5 mM (B), 5 mM (C) and 10 mM magnesium (D). The magnesium processed tibia plateaus show an enhanced value of collagen, cell nuclei and cartilage. Magnification: 10-fold.

3.4.3.3. Magnesium with calcium or manganese

The combinations with Mg and Ca or Mn showed, that the higher the Mg concentration the higher the collagen and proteoglycan concentration got within the full-thickness cartilage defect **(Fig. 3-36)**. Further, the 2.5 mM Mg/1 mM Ca showed the best outcome of all combinations with Mg. However, the enhanced proteoglycans and collagens were not as high as in the 100 % serum explant **(Fig. 3-16)**.

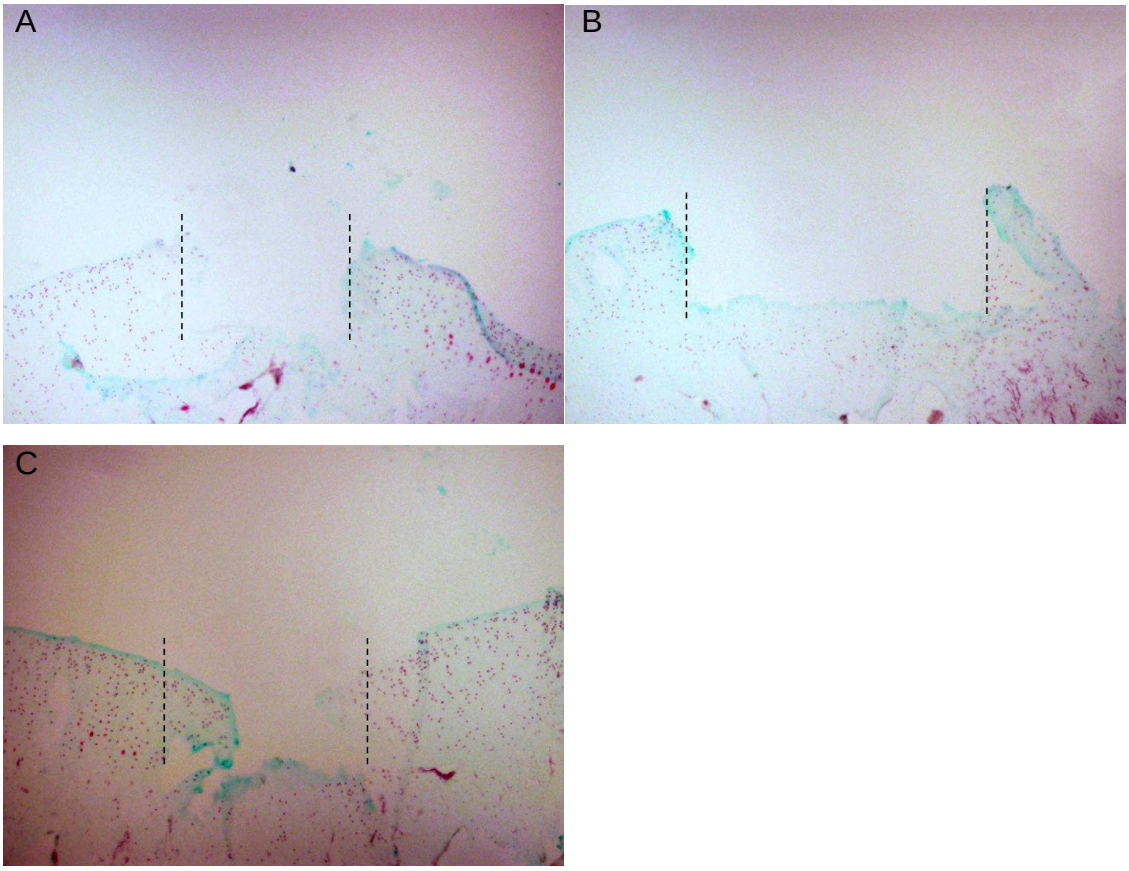

Fig. 3-36: Histological appearance of rat tibia plateaus after MSC attachment with different ion concentrations starting from 1 mM magnesium and 2.5 mM calcium to 2.5 mM magnesium and 1 mM calcium and 1 mM manganese with 2 mM magnesium.

Cells were allowed to attach to the cartilage surface of rat tibia plateaus supplemented with 1 mM magnesium and 2.5 mM calcium (A), 2.5 mM magnesium and 1 mM calcium (B), 1 mM manganese and 2 mM magnesium (C). Tibia plateaus processed with manganese and magnesium showed an enhanced ratio of collagens and cell nuclei. Magnification: A and B 10-fold, C 20-fold.

3.4.3.4. Manganese, zinc, EDTA, NaCl

The divalent ion Zn showed a better outcome in enhancing collagens and proteoglycans than Mn **(Fig. 3-37)**. Yet, Zn was not as effective as Mg or Ca **(Fig. 3-37B)**. EDTA and NaCl, which served as negative controls, showed a rise in the proteoglycan or the collagen **(Fig. 3-37C and D)**.

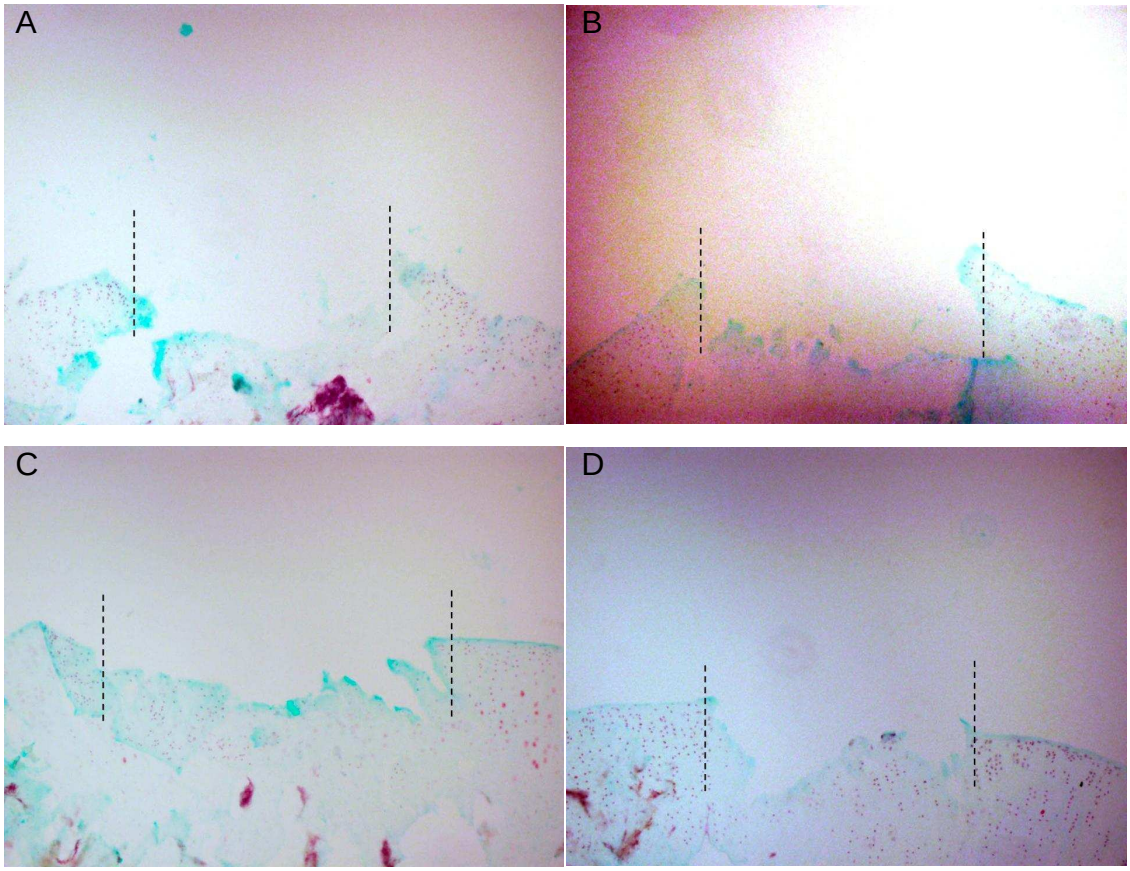

Fig. 3-37: Histological appearance of rat tibia plateaus after MSC attachment with different ion concentrations starting with 1 mM manganese, 1 mM zinc, 10 mM EDTA, NaCl.

Cells were allowed to attach to the cartilage surface of rat tibia plateaus supplemented with 1mM manganese (A), 1mM zinc (B), 10 mM EDTA (C), NaCl (D). The tibia plateau processed with manganese (A) shows less cell nuclei and collagen, than those processed with zinc (B). EDTA (C) and NaCl (D), which served as negative control, show the same result. Magnification: 10-fold.

3.4.4. hPLAP/fast red

The tibia plateaus were supplemented with hPLAP-MSC at the diverse divalent ion concentrations. As well as in the serum experiment the hPAP/fast red was performed after a positive testing of the prior staining solutions. The hPLAP staining showed if cells had attached on the defective surface and which divalent ion concentration was the most effective.

3.4.4.1. Calcium

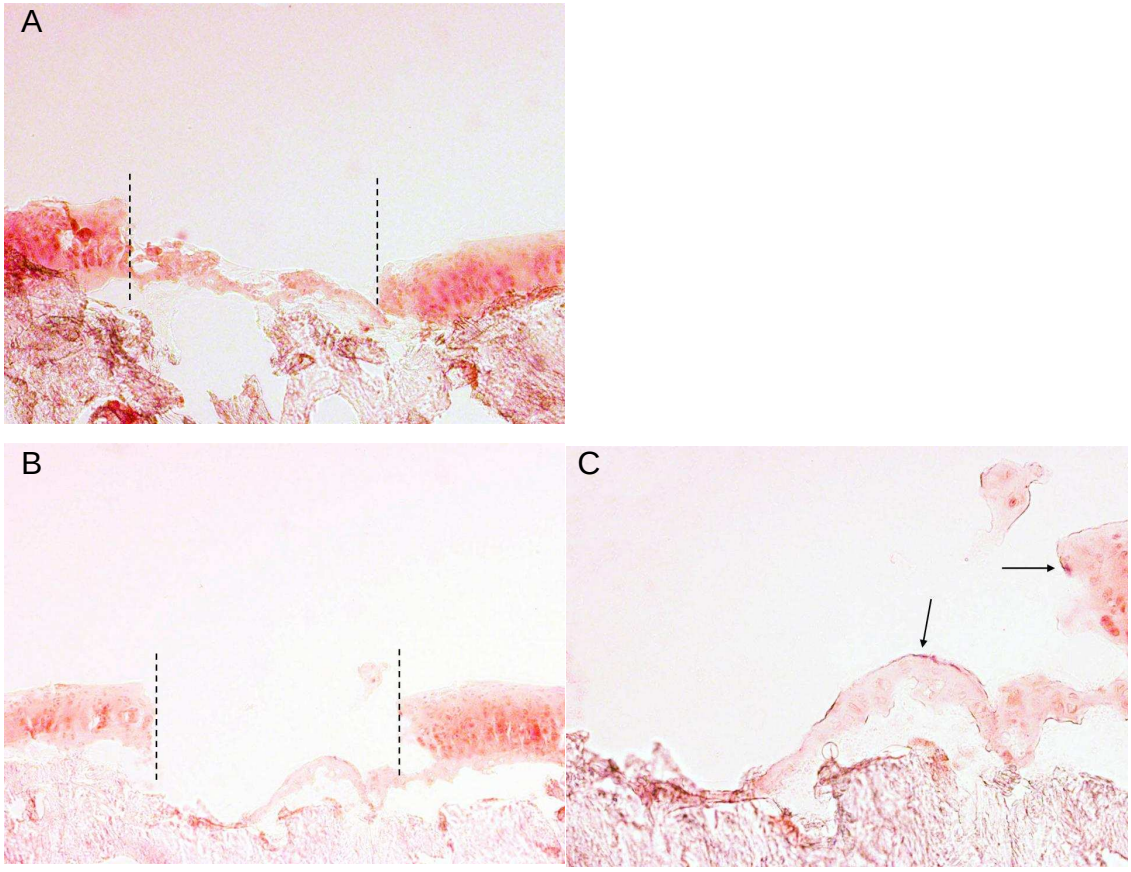

Fig. 3-38: Histological appearance of rat tibia plateaus after MSC attachment with different ion concentrations starting from 1 mM to 2.5 mM calcium.

Cells were allowed to attach to the cartilage surface of rat tibia plateaus supplemented with 1 mM (A) and 2.5 mM Ca (B, C).The higher the Ca concentration, the more hPLAP MSC attached to the defective surface. Magnification: A, B and C 10-fold.

The hPLAP-MSC started to attach on 2.5 mM Ca level within the full-thickness cartilage defect **(Fig. 3-38)**. Due to the observation of the former stainings, hPLAP and fast red staining confirmed the data of the enhanced

cell nuclei, collagen and proteoglycan levels. The higher the Ca level the more hPLAP-MSC attached **(Fig. 3-39)**.

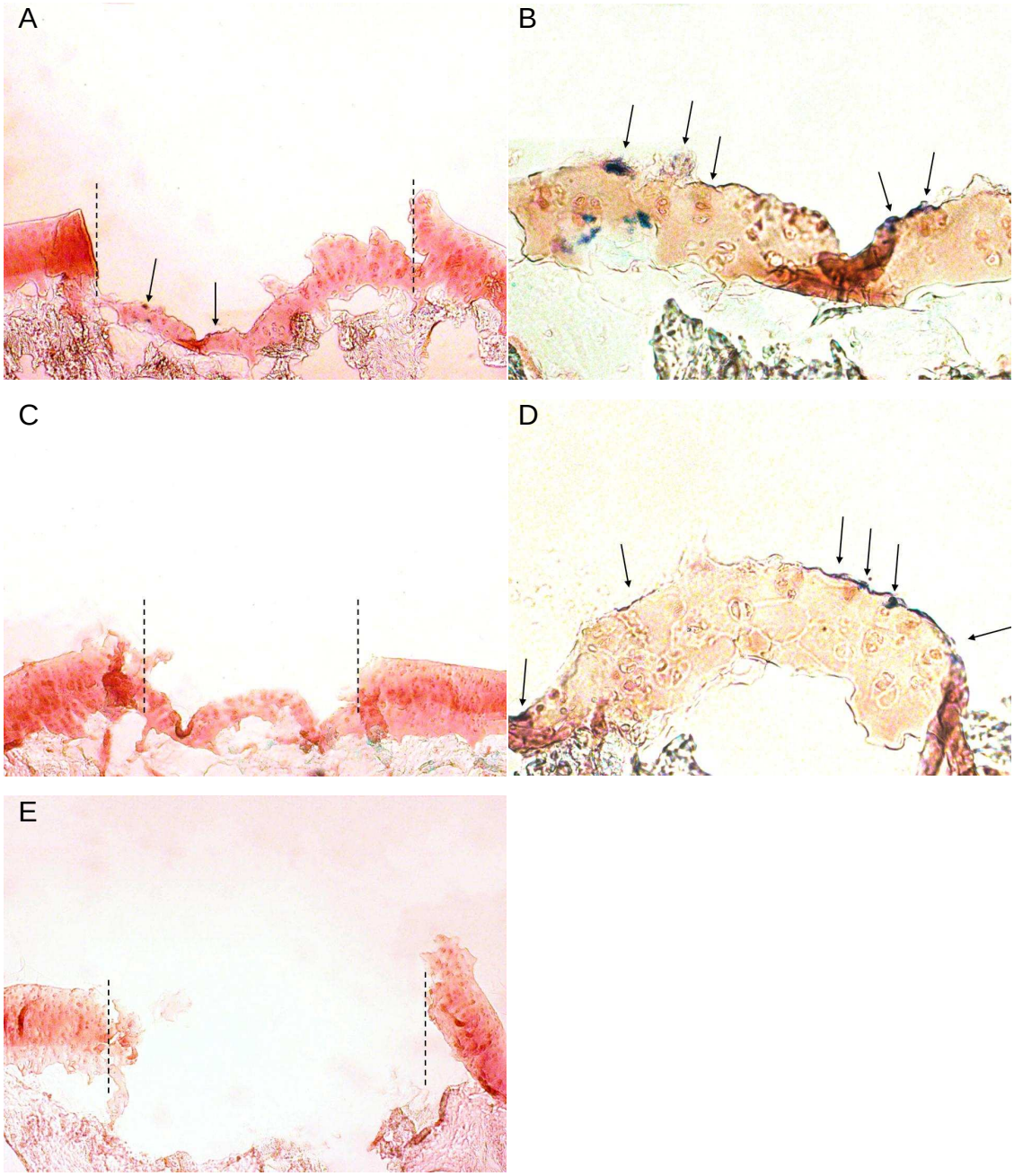

Fig. 3-39: Histological appearance of rat tibia plateaus after MSC attachment with different ion concentrations starting from 5 mM to 10 mM calcium.

Cells were allowed to attach to the cartilage surface of rat tibia plateaus supplemented with 5 mM (A, B, C, D) and 10 mM Ca (E). B showed that on 5 mM calcium level the attached cells increased. Magnification: A, C and E 10-fold, B and D 40-fold.

3.4.4.2. Magnesium

Comparing the cell attachment of the diverse Ca levels, Mg showed an increased hPLAP-MSC attachment **(Fig. 3-40).**

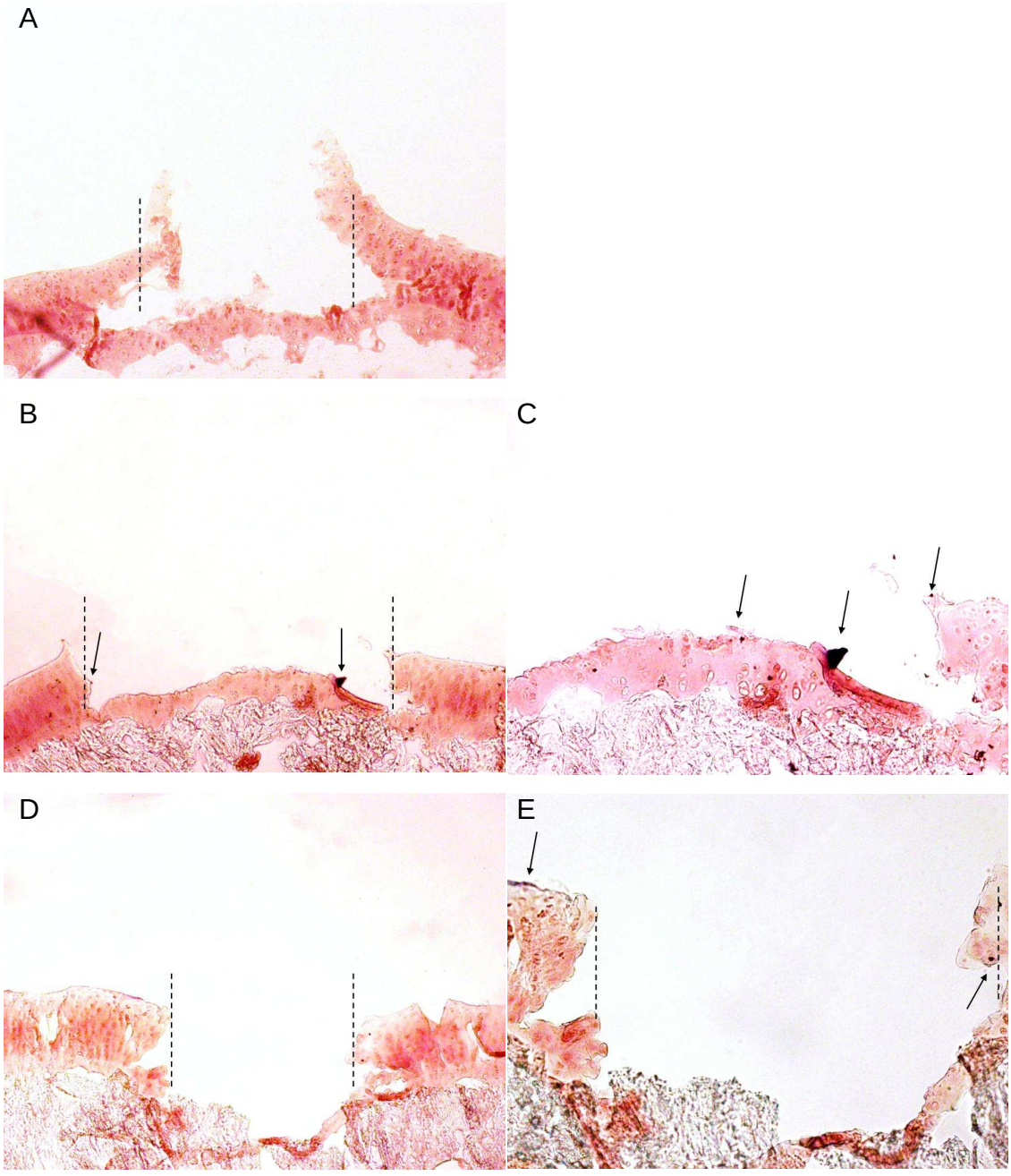

Fig. 3-40: Histological appearance of rat tibia plateaus after MSC attachment with different ion concentrations starting from 2.5 mM to 10 mM magnesium.

Cells were allowed to attach to the cartilage surface of rat tibia plateaus supplemented with 2.5 mM (A), 5 mM (B and C) and 10 mM magnesium (D and E). On a 5 mM magnesium level cells began to attach to the surface of the defect. Magnification: A, B and D 10-fold, C and E 20-fold.

At 5 mM Mg a cell cluster at the edge of the defect could be observed.

3.4.4.3. Magnesium and calcium

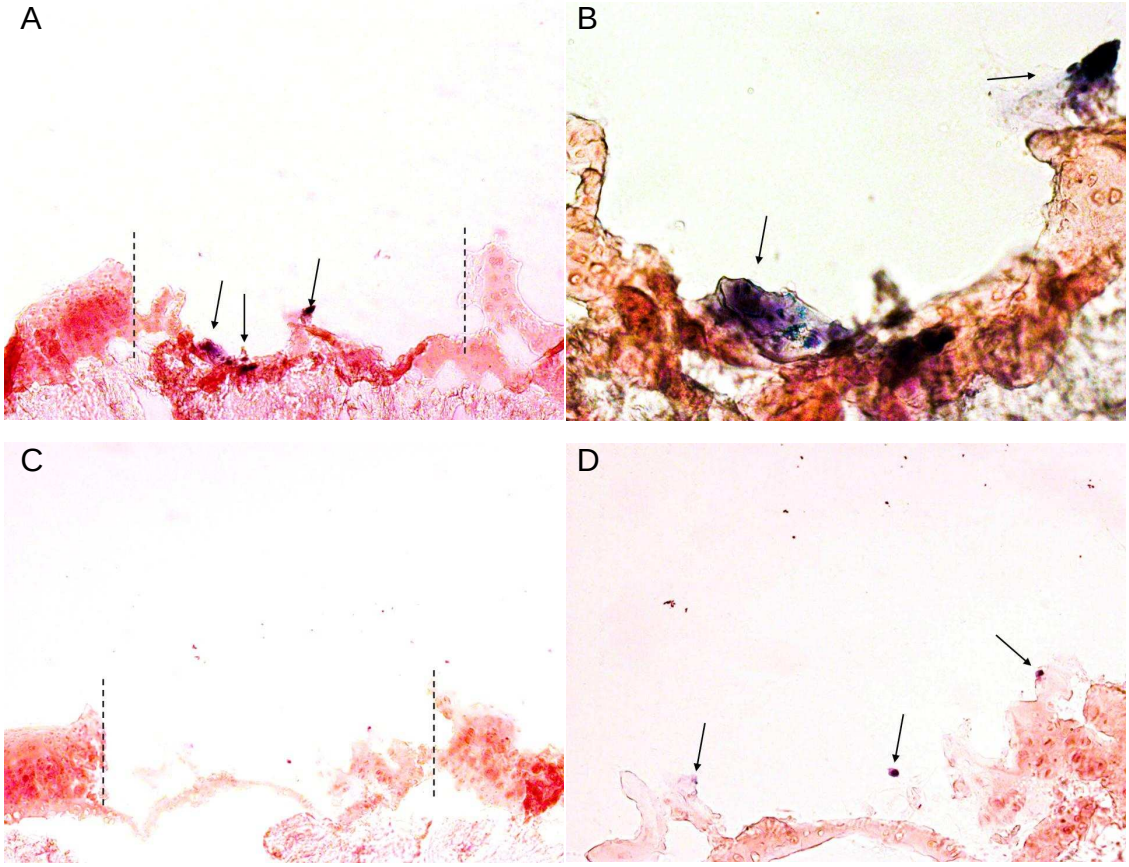

Fig. 3-41: Histological appearance of rat tibia plateaus after MSC attachment with different ion concentrations starting from 1 mM magnesium and 2.5 mM calcium to 2.5 mM magnesium and 1 mM calcium.

Cells were allowed to attach to the cartilage surface of rat tibia plateaus supplemented with 1 mM magnesium and 2.5 mM calcium (A, B), 1 mM magnesium and 2.5 mM calcium (C and D). Magnesium and calcium in combination were more effective in enhancing MSC attachment to the defect surface than each cation alone. Magnification: A, and C 10-fold, D 20-fold, B 40-fold.

Cell clusters were formed with the combination Mg and Ca within the defective area of the tibia plateau **(Fig. 3-41)**. This effect could also be observed with 20 %, 50 % and 100 % serum and with the combination Mg and Mn **(Fig. 3-23, Fig. 3-24, Fig. 3-25** and **Fig. 3-42)**. Compared to the data of the former performed stainings, the rise of the cell nuclei, collagens and

proteoglycans could now be credited to the fact that hPLAP cells attached to the defective surface.

3.4.4.4. Manganese and magnesium

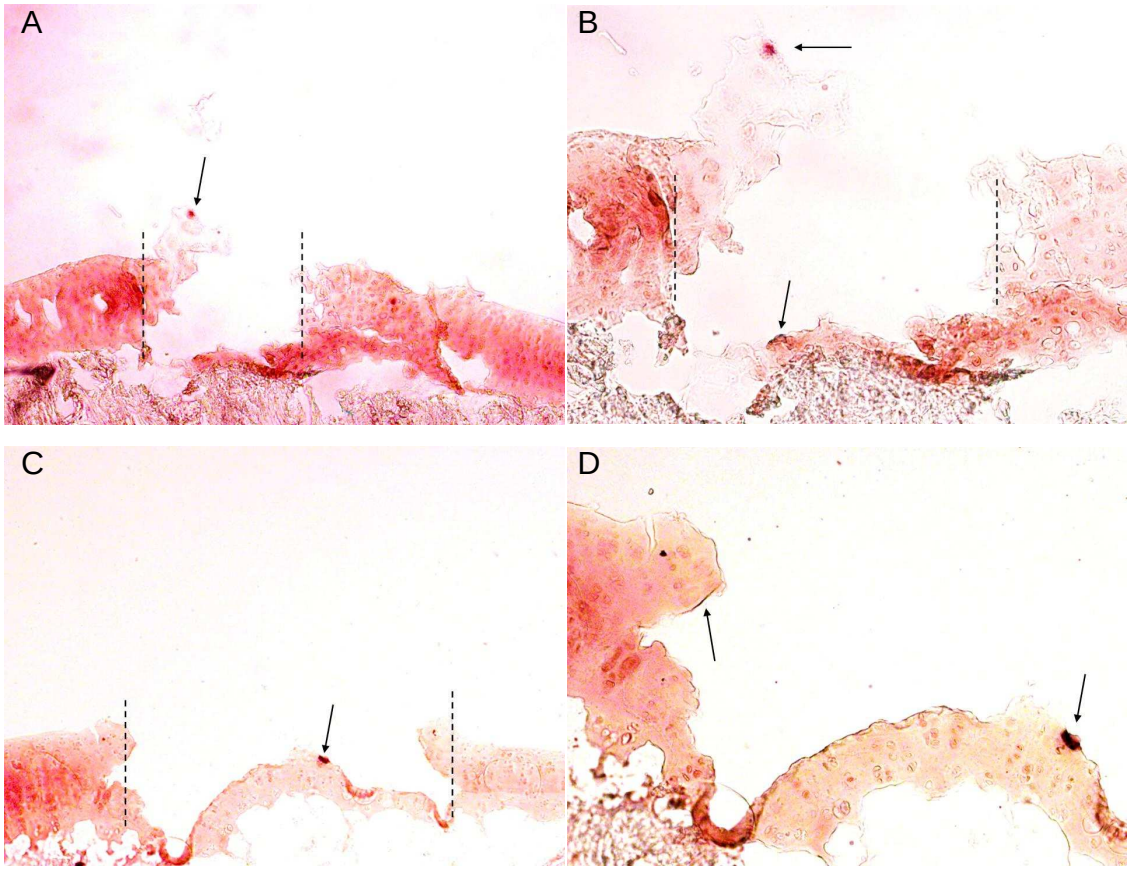

Fig. 3-42: Histological appearance of rat tibia plateaus after MSC attachment with different ion concentrations starting with 1 mM manganese and 1 mM manganese and 2 mM magnesium in combination.

Cells were allowed to attach to the cartilage surface of rat tibia plateaus supplemented with 1 mM manganese (A, B), 1 mM manganese and 2 mM magnesium (C and D). Manganese in combination with magnesium showed a higher ability for MSC to attach and build cell clusters. Magnification: A, and C 10-fold, B and D 20-fold.

3.4.4.5. Zinc, EDTA and NaCl

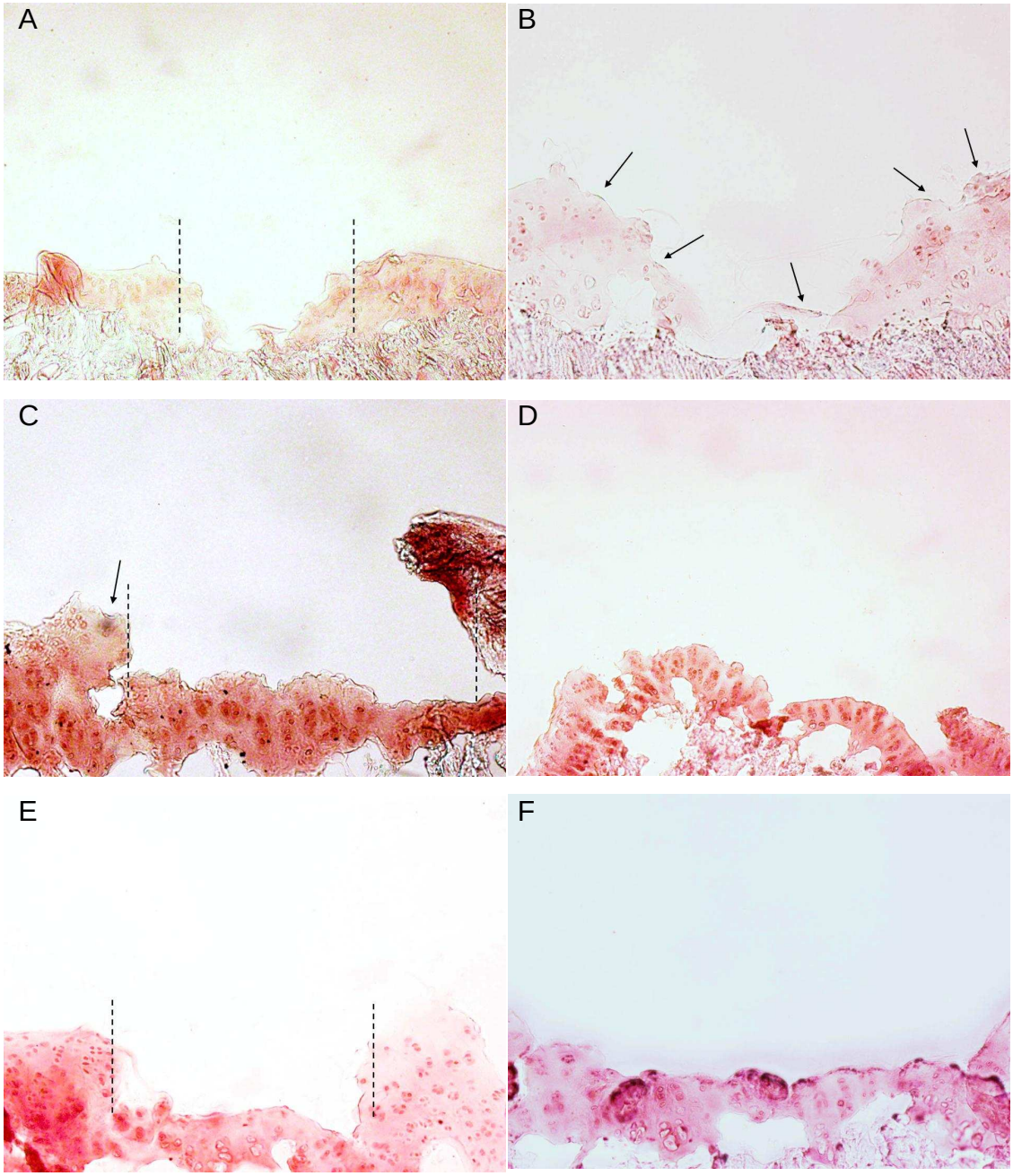

Fig. 3-43: Histological appearance of rat tibia plateaus after MSC attachment with different ion concentrations starting with 1 mM zinc, 10 mM EDTA and NaCl.

Cells were allowed to attach to the cartilage surface of rat tibia plateaus supplemented with 1 mM zinc (A, B), 10 mM EDTA (C, D) and NaCl (E and F). 1 mM Zn (A) showed a low cell attachment rate. NaCl (E and F) served as negative control and was comparable to 10 mM EDTA (C and D) Magnification: A 10-fold, B, C, D, and E 20-fold, F 40-fold.

1 mM Zn enhanced the hPLAP-MSC attachment slightly **(Fig. 3-43)**. Further, EDTA showed only one attached cell on the defective surface. This effect was caused by the ability of EDTA to chalet divalent ions, which were important for the enhancement of the MSC attachment. Further, no cell attachment could be observed with NaCl, which served as negative control of this study. Hence, it confirmed that NaCl had only shown the increase of collagen and proteoglycan **(Fig. 33** and **Fig. 37)**, because of its conserving ability.

4. Discussion

4.1. Establish protocols for the histochemical staining of osteochondral explants

The experiment took place from September 2012 to April 2013. First the rat tibia had to be extracted, without injuring the cartilage. Afterwards, a round defect was established on 95 of the 142 rat tibias, the other 47 stayed intact. This procedure was performed to find out, if there was a difference in MSC attachment between defective and intact cartilage. All explants were used to investigate the hPLAP-tg MSC attachment supplemented with serum or divalent cations as vehicle. The hPLAP-MSCs were used to identify attached MSC on wild type osteochondral explants. Serum concentrations of 0 %, 2 %, 5 %, 10 %, 20 %, 50 % and 100 % and the divalent ion concentrations of 1 mM, 2.5 mM, 5 mM and 10 mM magnesium or calcium, 1 mM manganese or zinc, 1 mM magnesium with 2.5 mM calcium, 2.5 mM magnesium with 1 mM calcium, 1 mM manganese with 2 mM magnesium, 10 mM ETDA and NaCl were investigated. In this study 0 % serum, 10 mM ETDA and NaCl were taken as a negative control. EDTA chelates divalent cations and therefore, served as control to identify the possible influence of divalent cations supplemented to MSC prior to their attachment.

To section the explants they needed to be embedded. The choice of the embedding procedure was quite difficult, because the β1 subunit of integrins, where collagen I and II bind to, needed to be accessible, to show that they are the key mediator for the MSC attachment to defective cartilage. After intense research on embedding techniques, Tissue-Tek® for cryo sectioning was chosen. MMA or paraffin embedding techniques would have made it impossible to perform immunofluorescence stainings, which had to be avoided. To embed in Tissue-Tek® also meant that the explants had to be processed with the cryostat. Because a knife with a tungsten-carbide coating

was not available at that time the explants needed to be cut with a common steel knife. To get sections which were suitable for staining, the explants needed to be decalcified. The calcification took four weeks although only explants were used and not whole long bones. To find out if the explants were ready to cut, a trial cut had taken place after two weeks of decalcification. After four weeks all explants were suitable for sectioning. In the next step cryo sections for the staining trial were produced, to figure out how the sections could be stained the best way. Thus, the cryo sections were stained with Mayer's haematoxylin and eosin. Despite the fact that the staining worked quite well, unfortunately most of the sections floated away. To overcome that problem, the slides were APES coated. After a series of testing, the slides with the cryo sections could be taken properly and stained after three different protocols. Mayer's haematoxylin and eosin, Mayer's haematoxylin, fast green and safranin O, and Weigert's haematoxylin and alcian blue showed that with increased serum levels more cells could be found at the defective surface compared to the intact cartilage. This gives evidence that the additional nuclei belong to the attached MSC. Therefore, the hPLAP and fast red staining was performed to specifically stain the hPLAP-MSC attached to the explants.

4.2. Serum drastically increases the MSC attachment to defective cartilage

A positive effect of serum as vehicle for the MSC-based therapy was shown in several studies (Giordano, et. al.; 2007, Lepperdinger, et. al.; 2008, Murphy, et. al.; 2003). To prove that the MSC attachment on defective cartilage was true, MSC were pre-incubated with increasing serum concentrations and allowed to attach to intact and defective osteochondral explants. Adding 0 % to 5 % serum as vehicle to MSC, increased the cell attachment within the defect (Weigert's haematoxylin/alcian blue). Moreover, MSC supplemented with 10 % to 50 % enhanced the attachment further, even on intact sides of the tibia plateaus. The best results could be observed

when adding 100 % serum. The highest rate of cell nuclei was detected on the surface of both full-thickness cartilage defects and intact explants. Within the Mayer's haematoxylin/eosin staining the defects of the tibia plateau showed the heterogeneity of this experiment, because some sections showed the remaining cartilage after abrasion process. Further, some sections showed a smaller defect, implicating that the section was not exactly in the middle of the defect. Nevertheless, the obtained results represented the *in vitro* results.

The defect surface, where higher serum concentrations were used, appeared to be darker, which is caused by the enhanced cell attachment rate. Therefore, the darkest surface and hence the highest density of cell nuclei could be found on the full-thickness cartilage defects supplemented with 100 % serum. Mayer's haematoxylin/fast green/safranin O staining showed that the density of cartilage was depressed at low serum levels. If the serum concentration rate was increased from 10 % to 50 %, more cells attached within the defect and even started to attach on the intact sides. 100 % of serum supplemented to attaching MSC showed the best results, where the highest level of cell attachment was observed within the defect and weakly on the intact sides of the tibia plateau.

The hPLAP/fast red staining pointed out, that at low serum levels (2 %), MSC started to attach within the defective area. Further, there was a rapid increase in cell attachment between 5 % and 10 %. At a serum level of 20 % cells also started to attach on the intact sides of the tibia plateau. Hence, at a supplementation of 50 % to 100 % of serum cell clusters were found within the full-thickness cartilage defect. Finally, using 100 % serum cell clusters were also seen on the intact cartilage.

The tibia plateaus supplemented with 0 % serum were used as the negative control of the experiment showing that there was hardly any attachment of MSC to the defective or intact cartilage surface. These experiments proved the impact of serum having a very positive effect on the attachment of MSC

to osteochondral explants, even more if MSC should attach to defective cartilage. This fact should be taken into consideration when thinking of a MSC-based therapy for successfully treatment of OA.

4.3. Influence of divalent cations on the attachment of MSC to osteochondral explants

The tibia plateaus were processed with different concentrations of magnesium, calcium, manganese and zinc or combinations of the mentioned ions. When supplementing magnesium to attaching MSC, darker margins within the defect were observed with the Weigert's haematoxylin/alcian blue staining. This could be an indicator of the enhancement of cell nuclei in that region. On the other hand, addition of calcium, manganese and zinc did not show any improvement of cell nuclei, implying no positive influence on the MSC attachment to explants supplemented with 1 mM calcium, manganese or zinc. Mayer's haematoxylin and eosin staining showed that at 2.5 mM of calcium cell nuclei and cytoplasm within the defect were increased. The same effect could be observed when using 1 mM manganese with 2 mM magnesium. Further, the sections processed with calcium showed that collagens appeared to be easier accessible for binding within the full-thickness cartilage defects (Mayer's haematoxylin/fast green/safranin O). Therefore, the rate of cell nuclei and collagens seemed to be enhanced when using high levels of magnesium or 1 mM magnesium with 2.5 mM calcium, whereas high magnesium levels were no longer physiological.

The hPLAP/fast red staining showed that the higher the magnesium concentration the more cells attached within the defect. Increasing magnesium levels had the ability to advance the MSC attachment, because cell nuclei started to attach even on the intact sides of the tibia plateau.

Supplementing 10 mM EDTA to the attaching MSC had a negative effect on the attachment to defective cartilage, comparable to the negative control NaCl. EDTA chelated divalent cations like magnesium, calcium, manganese or zinc. These results indicated that EDTA not only was chelating supplemented cations, but also the ions present in the matrix of the defective cartilage. To conclude, the explants processed with magnesium and calcium showed cell clusters within the defect making the combination the most effective one among the tested divalent cations.

4.4. Implications on the MSC-based treatment of OA

Osteoarthritis concerns millions of people and is one of the most wide spread diseases of the articular joint (Matsumoto, et. al.; 2009). The articular cartilage is not supplied by nerves, blood vessels and the lymphatic system, so its ability for self-repair is very limited. Therefore, the transplantation of chondrocytes had been analyzed and performed *in vivo* already. Thus, autologous chondrocytes were cultured and transplanted through injection under a periosteal flap, which was sutured over the defect (Brittberg, et. al.; 1994). Out of 16 patients 81 % had an excellent or good recovery, because the transplanted chondrocytes repopulated the defective area.

Further methods are the transplantation of an autologous osteochondral cylinder, resurfacing with perichondrium, periosteum, allografts and osteochondral plugs, arthroscopic lavage or debridement, or marrow-stimulation techniques (Horas, et. al.; 2003, Knutsen, et. al.; 2004, Veronesi, et. al.; 2013, Yen, et. al.; 2008). The transplantation of multiple, tiny, autologous grafts had a huge disadvantage; the limited donor-site morbidity and the availableness of said tissue (Veronesi, et. al.; 2013). Further, long term surveys did not show significant data, because the quality and consistency of the fibro cartilage was questionable. Horas, et. al. (2003) compared the autologous chondrocytes transplantation with the

osteochondral cylinder transplantation method and discovered, that after a two year follow up the osteochondral cylinder transplantation led to a better recovery of original cartilage. In contrast, the autologous chondrocyte transplantation started to build fibro-cartilage, which just improved the condition of OA.

Microfracture was also a very promising treatment belonging to the *"bone marrow stimulation techniques"* like abrasion arthroplasty (Vijayan, et. al.; 2010, Yen, et. al.; 2008). Through penetrating the osteochondral bone the articular surface got stimulated and the increased marrow elements helped to heal the full-thickness cartilage defect (Yen, et. al.; 2008). Because the subchondral bone got penetrated, blood vessels could help to foster fibrin clot formation. Hence, MSC were allowed to migrate into the clot and responsible of forming a fibro-cartilaginous surface, with a type I and II cartilage. In the abrasion arthroplasty the surgical success was a short one, after 5 years post-treatment of OA, OA recured (Vijayan, et. al; 2010). Therefore, it is recommended that the abrasion arthroplasty was combined with joint debridement or micro-fracturing to reestablish the surface tissue.

Due to the fact, that in adults the chondrocytes do not show mitotic activity anymore, the potential for regeneration of OA is low (Steinwachs, et. al.; 2008, Veronesi, et. al.; 2013). Hence, the chondrocytes encapsulated within the matrix are not able to continue to implement their repair process (Steinwachs, et. al; 2008). Further, the intrinsic activity is very low, which leads to the fact that chondral and osteochondral defects of full-thickness cartilage cannot heal anymore. Therefore, the technique of an autologous matrix induced chondrogenesis (AMIC®) was invented. This technique made it able to treat bigger defective areas by using collagen I and III membranes. First, the destroyed or affected area was removed. Second, microfractures had to be established. Third, the AMIC® membrane was implemented on the defects. Because of its ability to stabilize the blood clot, through the bilayer matrix, which hosted the MSC and the porcine collagen type I and III, in

combination with the technique of microfracturing, which guaranteed the nutrition of the MSC, the AMIC® represented a real alternative.

However, injuries caused by OA harm the subchondral bone, which leads to an immune reaction with fibrin clots, hematoma and an increase of the MSC production in the bone marrow (Veronesi, et. al.; 2013). Yet, a new cartilage with its natural functions can be restored. Hence, a further approach of a surgical OA treatment was implemented; the autologous chondrocyte implantation (ACI). First, autologous chondrocytes were harvested and augmented in cell culture. Second, the augmented chondrocytes got implanted onto the defect area of the osteochondral bone. The next step was the matrix guided autologous chondrocyte implantation (MACI). MACI derived from the ACI technique and increased the practicality of ACI. But still, both techniques require a surgical operation and because the chondrocytes of OA patients are not in the best condition, the chondrogenesis is limited. Therefore, an autologous transplantation of chondrocytes is difficult, given that an adequate number of chondrocytes is hard to produce effectively, because of the morbidity of the donor site.

In OA many factors play a critical role, like the catabolism and the inflammatory process (van Buul G.M., et. al.; 2012). MSC can act immunomodulationary and have the ability of regeneration of tissue and may reduce the inflammatory response and decrease matrix degradation.

4.5. Future prospect

This study has shown that the best MSC attachment could be achieved, if high serum levels or 1 mM magnesium and 2.5 mM calcium, but not to that extent as 100 % serum, were supplemented. The experiment was held under *ex vivo* conditions and only full-thickness cartilage defects were performed resembling the defects resulting during OA. Therefore, no immune cells could have interfered with the foreign cell attachment which could be the case in an

in vivo situation. The building of cell clusters is a prosper start for gaining full recovery within the full-thickness cartilage defects. The next steps to prove a full recovery of a defect tibia plateau, should be a longer culture phase after attachment and supplementing the MSC with 100 % serum and the most promising divalent ion concentrations, e.g. 1 mM magnesium and 2.5 mM calcium. With that the following questions should be answered:

- Do the attached cells within the defect start to differentiate into chondrocytes?
- Does the newly built cartilage have the same characteristics and properties as normal/healthy cartilage?

These questions have to be answered in *in vivo* experiments, which are ongoing studies in the group of Reinhold Erben.

- First, the existing *in vitro* and *ex vivo* data need to be reproduced in the *in vivo* system. If possible, a long-term experiment to analyze the recovery potential of defective cartilage after MSC attachment should be started.
- Does the living organism immunologically react to the MSC therapy?

Still, there are lots of questions which have to be answered prior of thinking of an available MSC-based therapy, but research is going on with great progress.

5. Zusammenfassung and Abstract

5.1. Zusammenfassung

Osteoarthrose (OA) wird verursacht durch das Verkleinern und den Verlust der Knorpelschicht der Gelenksflächen. Dies verursacht, dass der Gelenksspalt sich verkleinert und eine Reibung der Gelenksflächen zulässt. Diese Verkleinerung führt in weiterer Folge zur Entzündung des Gelenkes und auch zu Veränderungen am Gelenk selbst. Derzeit leiden Millionen von Menschen auf der ganzen Welt an OA. Da es bisher keine medizinische Behandlung für OA-Patienten gibt, die zur vollständigen Heilung führen würde, würde eine mesenchymale Stammzell-Therapie eine neue Form der Heilungsmethoden darstellen. Mesenchymale Stammzellen (MSC) sind multipotente Zellen, die in verschiedene Zelllinien differenzieren können, wie z.B. Knochen-, Knorpel- und Fettzellen. Da bisher wenig über die biochemischen Mechanismen einer möglichen MSC-Therapie für OA bekannt ist, sollte dies im Rahmen dieser Arbeit untersucht werden. Zum jetzigen Zeitpunkt gibt es Hinweise auf eine Integrin-vermittelte Adhäsion von MSC zu extrazellulären Matrix (ECM) Proteinen des artikulären Knorpels und Knochen.

Im Rahmen dieser Arbeit sollte die MSC-Adhäsion an defekte osteochondrale Explantate aus Fischer 344 Wildtyp Ratten histologisch untersucht werden. Zuvor wurden MSC von hPLAP (humane plazentäre Alkalische Phosphatase)-transgenen Ratten mit verschiedenen Serum- und Kationenkonzentrationen präinkubiert und deren Adhäsion am Explantat, mit dem induzierten Defekt, bestimmt. Die verschiedenen Serum- und Kationenkonzentrationen wurden als Vehikel verwendet, um heraus zu finden, welcher dieser Stoffe eine höhere Adhäsion von MSC an defekten Gelenksflächen, hervorruft. Die Explantate sollten histologisch analysiert werden, wofür diese zunächst dekalzifiziert und dann in Tissue-Tek® eingebettet wurden um später Kryoschnitte herstellen zu können. Anhand

von histochemischen Analysetechniken wurde die MSC-Adhäsion unter verschiedenen Bedingungen ermittelt. Ab einer Serumkonzentration von 2 % oder konzentrationsabhängig von Kalzium (Ca) oder Magnesium (Mg) fingen hPLAP-tg (transgene) MSC an, sich an der defekten Oberfläche anzusiedeln. Ab einer Serumkonzentration von 20 % oder einer Kationenkonzentration von 1 mM Mg/2,5 mM Ca konnte die Bildung von Zellansammlungen beobachtet werden. Die beste Zelladhäsion konnte jedoch bei einer Serumkonzentration von 100 % erzielt werden, wobei hier nicht nur die Bildung von Zellansammlungen im defekten Gelenksknorpel, sondern auch am intakten Gelenksknorpel zu beobachten war. Diese Studie konnte beweisen, dass die MSC-Adhäsion unter *ex vivo* Bedingungen am defekten Gelenksknorpel durch hohe Serumkonzentration und einer Kombination aus den Kationen Mg und Ca verstärkt werden kann. Es müssen jedoch noch weitere Studien durchgeführt werden um die genauen biochemischen Mechanismen, die die MSC-Adhäsion zu defekten Knorpel vermitteln, exakt zu verstehen. Dies würde als Grundlage für die Etablierung einer erfolgreichen MSC-basierenden Therapie für OA-Patienten dienen.

5.2. Abstract

Osteoarthritis (OA) is caused by the thinning and loss of articular cartilage. This reduces the synovial joint space, which induces that the articular cartilage grinds together. That effect causes synovitis and leads to the building of bone spurs. Currently, there are millions of people all over the world who suffer from OA. Since there is no treatment available to recover the defective articular cartilage, a mesenchymal stem cell (MSC)-based therapy would represent a future cure. MSC are multipotent cells that can differentiate into chondrocytes, adipocytes or. Up to date, little is known about the biochemical mechanisms of a potential MSC-based therapy. Until now, there are hints for an integrin-mediated adhesion of MSC to extracellular matrix (ECM) proteins of defective articular cartilage and bone.

The goal of this study was to histochemically analyze the MSC adhesion to defective osteochondral explants of Fischer 344 wild type rats. The adhesion of hPLAP (human placental alkaline phosphatase)-transgenic MSC preincubated with various serum or cation concentrations explants, with an induced defect, was already determined. Various serum and/or divalent ions were used to investigate a positive effect on the MSC attachment on full-thickness cartilage defects. To analyze the explants histochemically they had to be decalcified and afterwards embedded in Tissue-Tek® for cryo sectioning. To investigate the attachment of hPLAP-tg (transgenic) MSC under different conditions all explants were stained in four different ways hPLAP-tg MSC started to attach with 2 % serum or calcium (Ca) and magnesium (Mg) concentration dependent. At a serum level of 20 % or 1 mM Mg and 2.5 mM Ca as vehicle cell clusters appeared. The highest cell attachment was found with 100 % serum, where cell clusters were present within the defective area but also on the intact surface. Hence, this study has proven that the MSC attachment on full-thickness cartilage defects under *ex vivo* conditions could be enhanced by high serum levels and a combination of Mg and Ca. Thus, further studies have to exactly identify the biochemical

mechanisms driving the MSC attachment to defective cartilage, which is needed to establish a MSC-based therapy to successfully treat OA patients.

6. Literature

Agung M., Ochi M., Yanada S., Adachi N., Izuta Y., Yamasaki T., Toda K., 2006, Mobilization of bone marrow-derived mesenchymal stem cells into the injured tissues after intraarticular injection and their contribution to tissue regeneration, © Springer-Verlag 2006, Experimental Study, Knee Surg Sports Traumatol Arthrosc (2006) 14:1307-1314, DOI 10.1007/s00167-006-0124-8

Arden E., Arden N., Hunter D., 2008, Osteoarthritis, (c) 2008 Oxford University Press

Augello A., Tasso R., Negrini S.M., Cancedda R., Pennesi G., 2007, Cell Therapy Using Allogeneic Bone Marrow Mesenchymal Stem Cells Prevents Tissue Damage in Collagen-Induced Arthritis, © 2007, American College of Rheumatology, ARTHRITIS & RHEUMATISM, Vol. 56, No. 4, April 2007, pp 1175-1186

Avwioro G., 2011, Histochemical uses of haematoxylin – a review, JPCS Vol (1), April-June 2011, www.arpapress.com/Volumes/JPCS/Vol1/JPCS_1_05.pdf

Bond M., Davis A., Lohmander S., Hawker G., 2012, Responsiveness of the OARSI-OMERACT osteoarthritis pain and function measures, © 2012 Osteoarthritis Research Society International, Elsevier Ltd

Brittberg M., Lindahl A., Nilsson A., Ohlsson C., Isaksson O., Peterson L., 1994, Treatment of deep cartilage defects in the knee with autologous chondrocyte transplantation, © 1994 by the Massachusetts Medical Society, The New England Journal of Medicine, Vol. 331, No. 14

Buckwalter J.A., Mankin H.J., Grodzinsky A.J., 2005, Articular Cartilage and Osteoarthritis, AAOS Instructional Course Lectures, Volume 54, 2005

Bulman S.E., Barron V., Coleman C.M., Barry F., 2012, Enhancing the

Mesenchymal Stem Cell Therapeutic Response: Cell Localization and Support for Cartilage Repair, © Mary Ann Liebert, Inc., TISSUE ENGINEERING: Part B, Review Article

Caplan A.I., Bruder S.P, 2001, Mesenchymal stem cells: building blocks for molecular medicine in the 21st century, © 2001 Elsevier Science Ltd, TRENDS in Molecular Medicine Vol. 7, No. 6, June 2001

Choi Y.H., Gu Y-M., Oh J-W, Lee K-Y., 2011, Osterix is regulated by Erk1/2 during osteoblast differentiation, © 2011 Elsevier Inc., Biochemical and Biophysical Research Communivatins 415 (2011) 472-478

Conaghan P., Birrell M., Cumming J., Dickson J., Dieppe P., Doherty M., Dziedzic K., Francis R., Grant R., Kell C., Latimer N., MacGregor A., Naisby C., O'Mahony R., Oliver S., Richards A., Underwood M., 2008, Osteoarthritis National clinical guideline for care and management in adults, The National Collaborating Centre for Chronic Conditions, © 2008 Royal College of Physicians, ISBN 9781860163296

Docheva D., Haasters F., Schieker M., 2008, Mesenchymal Stem Cells and Their Cell Surface Receptors, © 2008 Bentham Science Publishers Ltd., Current Rheumatology Reviews, 2008, 4, 000-000

Efpia-Lander Loeckx, 2012, http://www.medicinesformankind.eu/de/krankheiten/osteoarthritis/2986/ .12.2012 (11:36 h)

Erben R., 2007, APES-Coating, staining: Mayer's haematoxylin, eosin; Mayer's haematoxylin, fast green, safranin O; Weigert's haematoxylin, alcian blue; hPLAP, fast red; staining solutions: 1% eosin, 0,001% fast green, fast red, Mayer's haematoxylin, 0,1% safranin O, Weigert's haematoxylin, BCIP, NBT, Buffer: TNM, 1x BPS, 1% Magnesium chloride in 100mM tris-maleat, SOPs of the Institute of Pathophysiology of the University of Veterinary Medicine, Vienna

Faller A., Schünke M., 1996, Der Körper des Menschen, 16. Auflage, © 1966, 2012 Georg Thieme Verlag KG, ISBN: 9783131519565

Ferrera D., Poggi S., Biassoni C., Dickson G.R., Astigiano S., Barbieri O., Favre A., Franzi A.T., Strangio A., Federici A., Manduca P., 2002, three-dimensional Cultures of Normal Human Osteoblasts: Proliferation and Differentiation Potential In Vitro and Upon Ectopic Implantation in Nude Mice, © 2002 by Elsevier Science Inc., Bone Vol. 30, No. 5, May 2002:718-725

Giordano A., Galderisi U., Marino I.R., 2007, From the Laboratory Bench to the Patient's Bedside: An Update on Clinical Trials With Mesenchymal Stem Cells, © 2007 Wiley-Liss. Inc., Journal of Cellular Physiology, 211:27-35

Goldring M.B., Goldring S.R., 2010, Articular cartilage and subchondral bone in the pathogenesis of osteoarthritis, © 2010, New York Academy of Sciences, Issue: Skeletal Biology and Medicine, Ann. N.Y. Acad. Sci. 1192 (2010) 230-237

Gronthos S., Graves S.E., Ohta S., Simmons P.J., 1994, The STRO-1+ Fraction of Adult Human Bone Marrow Contains the Osteogenic Precursors, (c) 1994 The American Society of Hematology, Blood, Vol 84, No 12 (December 15), 1994: pp 4164-4173

Gruber H.E., Ingram J., Hanley Jr. E.N., 2001, An improved staining method for intervertebral disc tissue, © Biological Stain Commission, Biotechnic & Histochemistry 2002, 77(2):81-83

Hayami T., Pickarski M., Wesolowski G.A., Mclane J., Bone A., Destefano J., Rodan G.A., Duong L.T., 2003, The Role of Subchondral Bone Remodeling in Osteoarthritis, © 2004, American college of Rheumatology, Arthritis & Rheumatism, Vol. 50, No.4, April 2004, pp 1193-1206, DOI 10.1002/art.20124

Hochberg M.C., McAlindon T., Felson D.T., 2000, Systemic and topical treatments. In: Felson D.T, conference chair, Osteoarthritis: new insights. Part 2: Treatment

approchaches. Ann Intern Med. 2000;133:726-729

Horas U., Pelinkovic D., Herr G., Aigner T., Schnettler R., 2003, Autologous Chondrocyte Implantation and Osteochondral Cylinder Transplantation in Cartilage Repair of the Knee Joint: A Prospective, Comparative Trail, The Jounal of Bone & Joint Surgery, Vol. 85, Issue 2, 2003 Feb 01, 85(2):185-192

http://bp2.blogger.com/_UMzm3PF6N5M/Rjkp2RF-1xI/AAAAAAAAACE/GOC_5Zkn6BQ/s1600-h/normal.bmp, 17.10.2012 (13:19 h)

http://www.medicinenet.com/osteoarthritis_overview_pictures_slideshow/article.htm **Medicinenet**, 2012, http://www.medicinenet.com/osteoarthritis_overview_pictures_slideshow/article.htm, 17.12.2012 (12:46 h)

Jones G., Changhai Ding, Scott F., Glisson M., Cicuttini F., 2003, Early radiographic osteoarthritis is associated with substantial changes in cartilage volume and tibial bone surface area in both males and females, © 2003 OsteoArthritis Research Society International. Published by Elsevier Ltd., OsteoArthritis and Cartilage (2004), 12, 169-174, soi:10.1016/j.joca.2003.08.010

Jordan J.M., Kington R.S., Lane N.E., Nevitt M.C., Zhang Y., Sowers M.F., et.al., 2000, Systemic risk factors for osteoarthritis. In Felson DT, conference chair. Osteoarthritic: new insights. Part 1: The disease and its risk factors. Ann Intern Med. 2000;133:637-639

Josephy P.D., 2000, The Escherichia coli lacZ reversion mutagenicity assay, © 2000 Elsevier Science B.V., Mutation Research 455 (2000) 71-80

Kanczler J.M., Ginty P.J., Barry J.J.A., Clarke N.M.P, Howdle S.M., Shakesheff K.M., oreffo R.O.C., 2008, The effect of mesenchymal populations and vascular endothelial growth factor delivered from biodegradable polymer scaffolds on bone formation, © 2008 Elsevier Ltd., Biomaterials 29 (2008) 1892e 1900

Kerkhof H.J.M., Doherty M., Arden N.K., Abramson S.B., Attur M., Bos S.D., Cooper C., Dennison E.M., Doherty S.A., Evangelou E., Hart D.J., Hofman A., Javaid K., Kerna I., Kisand K., Kloppenburg M., Krasnokutsky S., Maciewicz R.A., Meulenbelt I., Muir K.R., Rivadeneira F., Samuels J., Sezgin M., Slagboom E., Smith A.J.P., Spector T.D., Tamm A., Tamm A., Uitterlinden A.G., Wheeler M., Zhai G., Zhang W., van Meurs J.B.J., Valdes A.M., 2011, Large-scale meta-analysis of interleukin-1 beta and interleukin-1 receptor antagonist polymorphisms on risk of radiographic hip and knee osteoarthritis and severity of knee osteoarthritis, OARSI Osteoarthritis Research Society International, Osteoarthritis and Cartilage 19 (2011) 265 271

Kieman J.A., 2008, Nuclear Stains, © 2008 Cold Spring Harbor Laboratory Press, Vol. 3, Issue 7, July 2008

Knutsen G., Engebertsen L., Ludvigsen T.C., Drogset J.O., Grøntvedt L., Solheim E., Strand T., Roberts S., Isaksen V., Johansen O., 2004, Autologous Chondrocyte Implantation Compared with Microfracture in the Knee, © 2004 by the Journal of Bone and Joint Surgery, Incorporated, JBJS.ORG, Vol. 86-A, No.3, March 2004

Kurita H., Sakai H., Kamata T., Koike T., Kobayashi H., Kurashina K., 2008, Accuracy of intraoperative tissue staining in delineating deep surgical margins in oral carcinoma surgery, © 2007 Elsevier Ltd., Oral Oncology (2008) 44, 935-940

Kwan Tat S., Pelletier J-P, Amiable N., Boileau C., Lavigne M., Martel_Pelletier J., 2009, Treatment with ephrin B2 positively impacts the abnormal metabolism of human osteoarthritic chondrocytes, © 2009 Kwan Tat et.a.:, licensee BioMed Central Ltd., Arthritis Research & Therapy 2009, 11:R119

Lepperdinger G., Brunauer R., Jamnig A., Laschober G., Kassem M., 2008, Controversial issue: Is it safe to emplay mesenchymal stem cells in cell-based therapies?, © 2008 Elsevier Inc., Experimental Gerontology 43 (2008) 1018-1023

Lorenz H., Richter W., 2006, Osteoarthritis: Cellular and molecular changes in

degenerating cartilage, © 2006 Elsevier GmbH, Progress in Histochemistry and Cytochemistry 40 (2006) 135 163

Mackay A.M., Beck S.C., Murphy J.M., Barry F., Chichester C.O., Pittenger M., 1998, Chondrogenic Differentiation of Cultured Human Mesenchymal Stem Cells from Marrow, Mary Ann Liebert, Inc., Tissue Engineering, Vol. 4, No. 4, 1998

Matsumoto T., Cooper G.M., Gharaibeh B., Meszaros L.B., Li G., Usas A., Fu F.H., Huard J., 2009, Cartilage Repair in a Rat Model of Osteoarthritis Through Intraarticular Transplantation of Muscle-Derived Stem Cells Expressing Bone Morphogenetic Protein 4 Soluble Flt-1, © 2009, American College of Rheumatology, Arthritis & Rheumatism, Vol. 60, No. 5, May 2009, pp 1390-1405

McGonagle D., Gibbon W., Emery P., 1998, Classification of inflammatory arthritis by enthesitis, The Lancet, Col 352, October 3, 1998

Murphy J.M., Fink D.J., Hunziker E.B., Barry F.P., 2003, Stem Cell Therapy in a Caprine Model of Osteoarthritis, (c) 2003, American college of Rheumatology, Arthritis & Rheumatism, Vol. 48, No. 12, December 2003, pp 3464-3474

Mutschler E., Schaible H-G., Vaupel P., 2007, Anatomie, Physiologie, Pathophysiologie des Menschen, 6., völlig überarbeitete und erweiterte Auflage, © 2007 Wissenschaftliche Verlagsgesellschaft mbH, ISBN: 9783804723429

Odörfer K.I., Walter I., Kleiter M., Sandgren E.P., Erben R.G., 2008, Role of endogenous bone marrow cells in long-term repair mechanisms after myocardial infarction, © The Authors, Journal compilation © 2008 Foundation for Cellular and Molecular Medicine/Blackwell Publishing Ltd., J. Cell. Mol. Med. Vol. 12., No. 6B, 2008 pp. 2867-2874

Paul S., 2012, Functional Anatomy of the Knee: Movement and Stability, Interactive Biology, http://www.interactive-biology.com/3992/functional-anatomy-of-the-knee-movement-and-stability/ (2013-06-19, 11:46h)

Pittenger M.F., Mackay A.M., Beck S.C., Jaiswal R.K., Douglas R., Mosca J.D., Moorman M.A., Simonetti D.W., Craig S., Marshak D.R., 1999, Multilineage Potential of Adult Human Mesenchymal Stem Cells, Science 2 April 1999, Vol. 284, no.5411, pp. 143-147

Porcellini A., 2009, Regenerative medicine: A review, Rev. Bras. Hematol., Hemoter. 2009, 31(Supl. 2):63-66

Pottek T.S., Büttner H., Hartmann M., 1997, 181 – Testicular Cancer: Human Placental Alkaline Phosphatase (hPLAP), Renal and Testicular Cancer, Monday 15 September 1997, S 43

Richardson S.M., Curran J.M., Chen R., Vaughan-Thomas A., Hunt J.A., Freemont A.J., Hoyland J.A., 2006, The differentiation of bone marrow mesenchymal stem cells into chondrocytes-like cells on poly-L-lactic acid (PLLA) scaffolds, © 2006 Elsevier Ltd., Biometerials 27 (2006) 4069-4078

Sagar D.R., Ashraf S., Xu L., Burston J.J., Menhinick M.R., Poulter C.L., Bennett A.J., Walsh D.A., Chapman V., 2013, Osteoprotegerin reduces the development of pain behaviour and joint pathology in a model of osteoarthritis, © Article author 2013, BMJ Publishing Group Ltd (&EULAR), ARD Online First, 10.1136/annrheumdis-2013-203260

Schmidt A., Tief K., Foletti A., Hunziker A., Penna D., Hummler E., Beermann F., 1998, lacZ Transgenic mice to monitor gene expression in embryo and adult, © 1998 Elsevier Science B.V., Brain Research Protocols 3 (1998) 54-60

Schünke M., Schulte E, Schumacher U., 2009, Prometheus, LernAtlas der Anatomie, Allgemeine Anatomie und Bewegungssystem, © 2005, 2007 Georg Thieme Verlag, ISBN: 9783131395221

Seijffers R., Woolf C.J., 2004, Utilization of an HSV-based amplicon vector encoding

the axonal marker hPLAP to follow neurite outgrowth in cultured DRG neurons, © 2003 Elsevier B.V., Journal of Neuroscience Methods 132 (2004) 169-176

Sirerol-Piquer M.S., Cebrián-Silla A., Alfaro-Cervelló C., Gomez-Pinedo U., Soriano-Navarro M., Verdugo J-M.G., 2012, GFP immunogold staining, from light to electron microscope, in mammalian cells, © 2011 Elsevier Ltd., Micron 43 (2012) 589-599

Steinwachs M.R., Guggi T., Kreuz P.C., 2008, Marrow stimulation techniques, © 2008 Elsevier Ltd., Injury, Int. J. Care Injured (2008) 39S1, S26-S31

Van Buul G.M., Villafuertes E., Bos P.K., Waarsing J.H. Kops N., Narcisi R., Weinans H., Verhaar J.A.N., Bernsen M.R., von Osch G.J.V.M., 2012, Mesenchymal stem cells secrete factors that inhibit inflammatory processes in short-term osteoarthritic synovium and cartilage explant culture, © 2012 OsteoArthritis Society International, by Elsevier Ltd., Osteoarthritis and Cartilage 20 (2012) 1186-1196

Veje K., Hyllested-Winge J.L., Ostergaard K., 2003, Topographic and zonal distribution of tenascin in human articular cartilage from femoral heads: normal versus mild and severe osteoarthritis, © 2003 OsteoArthritis Research Society International, Elsevier Science Ltd., OsteoArthritis and Cartilage (2003) 11, 217-227

Veronesi F., Giavaresi G., Tschon M., Borsari V., Aldini N.N., Fini M., 2013, Clinical Use of Bone Marrow, Bone Marrow Concentrate, and Expanded Bone Marrow Msenchymal Stem Cells in Cartilage Disease, © Mary Ann Liebert, Inc., Stem Cells and Development, Vol. 22, No. 2, 2013

Vijayan S., Bentley G., Briggs T.W.R., Skinner J.A., Carrington R.W.J., Pollock R., Flanagan A.M., 2010, Cartilage repair: A review of Stanmore experience in the treatment of osteochondral defects in the knee with various surgical techniques, Indian Journal of Orthopaedics 2010 Jul-Sep; 44(3): 238-245

Waldeyer A., 2003, Anatomie des Menschen, 17. Auflage, Herausgeber J. Fanghänel, F. Pera, F. Anderhuber, R. Nitsch, © Copyright 2003 by Walter de

Gruyter GmbH & Co. KG, 10785 Berlin, ISBN: 9783110165619

Weitzer G., 2006, Embryonic Stem Cell-Derived Embryoid Bodies: An In Vitro Model of Eutherian Pregastrulation Development and Early Gastrulation, (c) Springer-Verlag Berlin Heidelberg 2006, HEP (2006) 174:21-51

Yen Y.-M., Cascio B., O'Brien L., Stalzer S., Millett P.J., Steadman J.R., Treatment of Osteoarthritis of the Knee with Microfracture and Rehabilitation, © 2008 by the American College of Sports Medicine, Medicine & Science in Sports & Exercise, Vol. 40, No. 2, pp. 200-205, 2008

Zwolanek D., Flicker M., Balmayor E.R., Lepperdinger G., van Osch G.JVM, Erben R.G., 2013, beta1 integriin mediates attachment of MSC to cartilage and bone in vitro, Poster, Department of Biomedical Science, University of Veterinary Meicine, Vienna.

7. Figures

haematoxylin/eosin, cation concentrations

Fig. 3-30 to Fig. 3-33 Weigert's haematoxylin/alcian blue, cation concentrations — See **Fig. 3-2 to Fig. 3-6**

Fig. 3-34 to Fig. 3-37 Mayer's haematoxylin/fast green/safranin O, cation concentrations — See **Fig. 3-2 to Fig. 3-6**

Fig. 3-38 to Fig. 3-43 hPLAP/fast red, cation concentrations — See **Fig. 3-2 to Fig. 3-6**

Curriculum vitae

Name: Elisabeth Richl

Internships

Aug 12 – Apr 13	Analyze techniques in immunohistochemistry, Institute of Pathophysiology, University of Veterinary Medicine, Vienna
Oct 11 – Jan 12	Training in forensic medicine, Institute of Forensic Medicine, University of Medicine, Vienna
Mar – Jun 10	Multivariate biostatistics, Technical University of Vienna
Mar – Jun 09	Training in human ecological methods, Institute of Human Ecology, University Vienna
Mar – Sept 08	Behavior analyses, Institute of Human Ethology, University Vienna
Oct 07 – Jan 08	Practical training in the field of research: osteoporosis, Institute of Social Anthropology, University Vienna
Oct 06 – Jan 07	Training in biological physics, University Vienna
Mar – Jun 06	Training in organic and inorganic chemistry, Technical University of Vienna
Sept 04 – Jun 13	University studies: Biology, University of Vienna

School

June 04	General qualification for university entrance, German, English, Mathematic, National Economics, Accounting, Business Economics, Business Informatics and Organization